Mean Field Game Modeling of Overconfidence in Financial Markets

Lucas Sneller

Miami University, Oxford, OH 45056, USA

WORKING PAPER • v0.9.0 • 2026-02-14

Abstract

This paper develops a mean field model of overconfidence in a market with flow-driven price impact and inventory carryover. A continuum of investors filters an unobserved fundamental from noisy private signals and trades against an endogenous price that mean-reverts toward fundamentals and responds to aggregate order flow; overconfidence enters as misperceived private-signal precision, generating heterogeneous filtered beliefs. The main equilibrium object is a *discrete-time myopic mean-field equilibrium*: given a conjectured mean trading rate, each agent chooses next-step inventory to maximize one-step CARAutility under conditionally Gaussian price increments. This yields a linear feedback rule and reduces mean-field consistency to a scalar stock–flow fixed point at each time step. A theorem gives per-step well-posedness of this discrete-time closure under the checkable condition $0 \leq B_t^{\mathrm{sf}} < \Delta t$ (with B_t^{sf} the stock–flow closure coefficient; Theorem 4.6). In simulations across bull/bear regimes and a targeted joint grid over anchoring, impact, and noise trading, microstructure parameters govern mispricing levels, whereas overconfidence primarily increases disagreement and trading intensity with limited effect on price-level mispricing in the baseline anchored-impact regime. As a benchmark, the paper also reports a finite-horizon continuous-time CARA/LQG solution, and an identification/moment-matching vignette connects the model's parameters to price and volume moments.

1 Introduction

Overconfidence—the tendency to overestimate the precision of one's information—is a well-documented behavioral bias in financial markets and is empirically associated with excessive trading and episodes of mispricing Odean (1998); Barber and Odean (2001). A central modeling challenge is to combine heterogeneous (and potentially biased) beliefs formed from private information with endogenous price formation, while retaining an equilibrium concept that is mathematically well-posed, computable, and connectable to data. This paper develops a mean field game (MFG) framework for a market populated by a continuum of investors who filter an unobserved fundamental from noisy private signals and trade against an endogenous price impacted by mean trading rate (order flow).

The model keeps a clean stock–flow separation. Inventory $x_{i,t}$ (shares) carries over between decision times, trading rate $u_{i,t}$ (shares per unit time) satisfies $x_{i,t+\Delta t} = x_{i,t} + u_{i,t}\Delta t$, and the price equation loads on the mean flow $\bar{u}_t$ rather than on mean inventory. Overconfidence enters only through *filtering*: agents treat their private signal as more precise than it truly is, which changes posterior uncertainty and therefore trading intensity and disagreement, not through an ad hoc demand multiplier.

Early behavioral models introduced stylized agent types (noise traders, momentum traders) to demonstrate how bounded rationality can drive prices away from fundamentals De Long et al. (1990); Hong and Stein (1999); Daniel et al. (1998); Gervais and Odean (2001), but typically rely on a small number of types rather than a full distribution of beliefs. Mean field games have been applied to financial markets in several contexts: Guéant, Lasry, and Lions Guéant et al. (2010) developed MFG frameworks for execution and portfolio problems; Carmona, Fouque, and Sun Carmona et al. (2015) studied systemic risk; Lachapelle *et al.* Lachapelle et al. (2016) applied MFG ideas to high-frequency trading and price formation; and Cardaliaguet and Lehalle Cardaliaguet and Lehalle (2018) analyzed trade crowding effects.

This paper's contribution relative to existing MFG finance literature is a bounded-rational equilibrium concept that is both economically interpretable and mathematically checkable in a stock–flow microstructure setting. In the dynamic baseline, the paper studies a discrete-time *myopic mean-field equilibrium*: given a conjectured common-noise adapted mean trading rate $(\bar{u}_t)$, each agent applies a one-step CARAbest response under conditionally Gaussian price increments (using their filtered belief), and mean-field consistency closes the dynamics by requiring $\bar{u}_t$ to equal the conditional population mean of these best responses. Because the best response is linear in $(\hat{v}_{i,t} - p_t)$ and in $\bar{u}_t$, the closure reduces each time step to a scalar stock–flow fixed point. A per-step contraction condition guarantees uniqueness and well-posedness of the induced discrete-time dynamics and particle approximation (Theorem 4.6).

The simulations distinguish *level amplification* (large mispricing/volatility levels driven by weak anchoring and high noise trading) from *overconfidence effects* (incremental differences when increasing k). Across a targeted joint grid over anchoring, impact, and noise trading, the simulations show a robust mechanism separation in the baseline anchored-impact regime: microstructure parameters govern mispricing levels, while overconfidence strongly increases disagreement and trading intensity with economically small effects on price-level mispricing (Subsection 6.3.3). To make the model empirically usable, Section 6.1 provides an identification argument linking key parameters to observable price and volume moments, and a moment-match vignette illustrates the calibration bridge on a liquid ETF.

The paper's dynamic analysis has a deliberate two-model structure. (A) The object computed and simulated is the discrete-time stock–flow myopic equilibrium described above. (B) As a theoretical benchmark, Subsection 4.3 derives an exact finite-horizon continuous-time CARA/LQG best response under partial information; this analytic extension clarifies how the full intertemporal solution adds a hedging correction to the myopic rule, and the paper compares the myopic and intertemporal policies in Subsection 6.4.

The main contributions of this paper are:

- This paper formulates a mean field game with overconfident Bayesian filtering and an explicit stochastic price equation with endogenous flow impact, under a stock–flow timing that separates inventory and trading rate (Subsubsection 2.3.3).

- This paper provides a clean static benchmark with a closed-form linear price (5) and explicit comparative statics in the overconfidence parameter k.

- In the dynamic setting, the paper derives a checkable myopic CARAinventory rule under conditionally Gaussian price increments (with holding cost) and obtains a per-step stock–flow mean-field closure; an explicit contraction condition guarantees uniqueness and discrete-time well-posedness (Theorem 4.6).

- This paper reports particle-based numerical experiments (large-N simulations) across bull/bear regimes and microstructure regimes, including mechanism diagnostics (belief dispersion and perceived uncertainty), validation checks, and extensions (Section 6).

- This paper provides a minimal identification/calibration bridge: Section 6.1 links key parameters to observable price and volume moments and illustrates the mapping with a moment-match vignette.

The remainder of this paper is organized as follows. Section 2 presents the model, including the static benchmark and the dynamic price/belief dynamics. Section 3 discusses the mean-field object in the presence of common noise and the fixed-point notion of (myopic) equilibrium. Section 4 states the main analytic results, including the myopic rule and the continuous-time CARA/LQG benchmark. Section 5 collects proofs. Section 6 presents numerical experiments, the empirical bridge, and the joint-grid analysis. Section 7 concludes.

Main contributions

- This paper formulates a mean field game with overconfident Bayesian filtering and an explicit stochastic price equation with endogenous flow impact, under a stock–flow timing that separates inventory and trading rate (Subsubsection 2.3.3).
- This paper provides a clean static benchmark with a closed-form linear price (5) and explicit comparative statics in the overconfidence parameter k.
- In the dynamic setting, the paper derives a checkable myopic CARAinventory rule under conditionally Gaussian price increments (with holding cost) and obtains a per-step stock–flow mean-field closure; an explicit contraction condition guarantees uniqueness and discrete-time well-posedness (Theorem 4.6).
- This paper reports particle-based numerical experiments (large-N simulations) across bull/bear regimes and microstructure regimes, including mechanism diagnostics (belief dispersion and perceived uncertainty), validation checks, and extensions (Section 6).
- This paper provides a minimal identification/calibration bridge: Section 6.1 links key parameters to observable price and volume moments and illustrates the mapping with a moment-match vignette.

2 Problem Statement and Model

2.1 Setup and Notation

Consider a financial market with a continuum of investors indexed by $i \in [0,1]$ over a horizon $[0,T]$. Let $(\Omega, \mathcal{F}, \{\mathcal{F}_t\}_{t\geq 0}, \mathbb{P})$ support independent Brownian motions W_t (fundamental shock), Z_t (aggregate price/noise-trading shock), U_t (common signal component), and $\{B_{i,t}\}_{i\in[0,1]}$ (idiosyncratic signal noise). Write $\mathbb{E}[\cdot]$ for expectation and $\tau = 1/\sigma^2$ for precision.

Information and timing. At each decision date t (on a discrete grid with step Δt), agent i observes the public price p_t, her private signal history $(\xi_{i,s})_{s\leq t}$ (equivalently, the most recently realized normalized increment $z_{i,t} := (\xi_{i,t} - \xi_{i,t-\Delta t})/\Delta t$ in the discrete implementation), and her pre-trade inventory x_{i,t^-}. She then chooses a post-trade inventory $x_{i,t}$ (equivalently an order $\Delta x_{i,t} := x_{i,t} - x_{i,t^-}$, hence a trading rate $u_{i,t} = \Delta x_{i,t}/\Delta t$). The mean trading rate $\bar{u}_t = \int_0^1 u_{i,t}\, di$ enters the flow-impact price update over $[t, t+\Delta t]$. This stock–flow separation and the within-step ordering are made explicit in Subsubsection 2.3.3.

Model parameters: $\gamma > 0$ (absolute risk aversion), $\kappa > 0$ (fundamental anchoring strength), $\lambda > 0$ (impact strength), $k \geq 1$ (overconfidence), and volatilities $\sigma_v, \sigma_c, \sigma_\epsilon, \sigma_{\eta,\text{flow}}, \phi > 0$ (fundamental shock, common signal component, idiosyncratic signal noise, order-flow noise scale, and reduced-form price/noise-trading volatility). In the microstructure sketch below, $\sigma_{\eta,\text{flow}}$ is the volatility of exogenous noise-trader order flow and induces price noise via $\phi := \lambda\sigma_{\eta,\text{flow}}$. Overconfidence is modeled as a misperception of private-signal precision: an agent with parameter k uses perceived idiosyncratic variance σ_ϵ^2/k in belief updating (equivalently, perceived precision k/σ_ϵ^2). *Notation warning:* k denotes overconfidence (signal-precision inflation) whereas κ denotes anchoring strength in the price dynamics. *Baseline:* homogeneous overconfidence is assumed, i.e., $k_i \equiv k$ for all investors; heterogeneous k_i is considered only as a numerical extension (see Section 6).

2.2 Static Benchmark

In this static benchmark, $\nu \sim \mathcal{N}(0, \sigma_\nu^2)$ is an exogenous noise-demand shock (price level), distinct from the order-flow noise scale $\sigma_{\eta,\text{flow}}$ used in the microstructure sketch (whose induced price-noise volatility is $\phi = \lambda\sigma_{\eta,\text{flow}}$). The symbol ϕ is reserved for the dynamic price/noise-trading volatility in (8).

As a baseline, consider a static market with fundamental value $v \sim \mathcal{N}(\mu_{v,0}, \sigma_{v,0}^2)$. Each investor receives a private signal

$$s_i = v + \epsilon_i, \quad \epsilon_i \sim \mathcal{N}(0, \sigma_{\epsilon,0}^2), \tag{1}$$

and chooses demand x_i for a single risky asset with payoff v at settlement. Investors have CARAutility

$$U_i = -\mathbb{E}\left[e^{-\gamma W_i} \mid s_i\right], \quad W_i = w_0 + x_i(v - p), \tag{2}$$

and take the price impact rule (instantaneous clearing with noise demand)

$$p = \lambda \int_0^1 x_i \, di + \nu, \quad \nu \sim \mathcal{N}(0, \sigma_\nu^2). \tag{3}$$

Under Gaussian beliefs, maximizing CARAutility is equivalent to maximizing mean minus $(\gamma/2)$ times variance. Let $\tau_{v,0} := 1/\sigma_{v,0}^2$ and let $\tau'_{\epsilon,0} := k/\sigma_{\epsilon,0}^2$ denote the perceived private-signal precision. Then the (perceived) posterior variance is $\sigma_{\text{post}}^2 = 1/(\tau_{v,0} + \tau'_{\epsilon,0})$ and the posterior mean is $\hat{v}_i = (\tau_{v,0}\mu_{v,0} + \tau'_{\epsilon,0}s_i)/(\tau_{v,0} + \tau'_{\epsilon,0})$. The optimal demand is therefore

$$x_i^* = \frac{\hat{v}_i - p}{\gamma\, \sigma_{\text{post}}^2}. \tag{4}$$

To make the aggregation step explicit, consider first a finite population of size N, with signals $s_i = v + \epsilon_i$ for $i = 1, \ldots, N$, where $\{\epsilon_i\}_{i=1}^N$ are i.i.d., independent of v, with $\mathbb{E}[\epsilon_i] = 0$ and $\mathbb{E}[\epsilon_i^2] = \sigma_{\epsilon,0}^2 < \infty$, and define the sample average $\bar{s}_N := \frac{1}{N}\sum_{i=1}^N s_i$. Since $\hat{v}_i$ is affine in s_i, the cross-sectional mean belief satisfies $\frac{1}{N}\sum_{i=1}^N \hat{v}_i = \frac{\tau_{v,0}\mu_{v,0} + \tau'_{\epsilon,0}\bar{s}_N}{\tau_{v,0} + \tau'_{\epsilon,0}}$. Under the finite-$N$ clearing rule $p^N = \lambda\big(\frac{1}{N}\sum_{i=1}^N x_i\big) + \nu$, the same algebra yields

$$p^N = \frac{\lambda\tau'_{\epsilon,0}}{\gamma + \lambda(\tau_{v,0} + \tau'_{\epsilon,0})}\,\bar{s}_N + \frac{\gamma}{\gamma + \lambda(\tau_{v,0} + \tau'_{\epsilon,0})}\,\nu + \frac{\lambda\tau_{v,0}}{\gamma + \lambda(\tau_{v,0} + \tau'_{\epsilon,0})}\,\mu_{v,0}.$$

Since $\bar{s}_N = v + \frac{1}{N}\sum_{i=1}^{N} \epsilon_i$, the strong law of large numbers implies $\bar{s}_N \to v$ almost surely (conditional on v, hence also unconditionally) as $N \to \infty$, yielding the mean-field limit price[1]

$$p = \frac{\lambda \tau'_{\epsilon,0}}{\gamma + \lambda(\tau_{v,0} + \tau'_{\epsilon,0})}\, v + \frac{\gamma}{\gamma + \lambda(\tau_{v,0} + \tau'_{\epsilon,0})}\, \nu + \frac{\lambda \tau_{v,0}}{\gamma + \lambda(\tau_{v,0} + \tau'_{\epsilon,0})}\, \mu_{v,0}. \tag{5}$$

Equation (5) makes the channel explicit: higher k increases perceived precision $\tau'_{\epsilon,0}$ and therefore strengthens the price response to v while also increasing demand magnitude for a given mispricing.

Notation note. In the static benchmark (Sec. 2.2), $(\mu_{v,0}, \sigma_{v,0})$ parameterize the one-shot prior $v \sim \mathcal{N}(\mu_{v,0}, \sigma^2_{v,0})$ and $\sigma_{\epsilon,0}$ is the one-shot private-signal noise standard deviation in $s_i = v + \epsilon_i$. The ",0" subscripts are retained throughout Section 2.2 and its proofs; unsubscripted $(\mu_v, \sigma_v, \sigma_\epsilon, \ldots)$ are reserved for the dynamic model. In the dynamic model (Sec. 2.3), (μ_v, σ_v) denote the drift and instantaneous diffusion volatility of v_t in $dv_t = \mu_v\, dt + \sigma_v\, dW_t$, and σ_ϵ is the diffusion loading on idiosyncratic signal noise in $d\xi_{i,t} = v_t\, dt + \sigma_c\, dU_t + \sigma_\epsilon\, dB_{i,t}$. The benchmarks are comparable but the parameters have different time-aggregation interpretations.

2.3 Dynamic Mean Field Game Formulation

2.3.1 State Dynamics and Mean-Field Coupling

The fundamental value follows a diffusion

$$dv_t = \mu_v\, dt + \sigma_v\, dW_t, \tag{6}$$

and each investor observes a private signal process

$$d\xi_{i,t} = v_t dt + \sigma_c\, dU_t + \sigma_\epsilon\, dB_{i,t}, \tag{7}$$

where $\{B_{i,t}\}$ are independent across i and independent of (W, U, Z).

Noise sources and independence. Let (W_t, U_t, Z_t) be independent standard Brownian motions representing, respectively, fundamental shocks, the common signal component, and exogenous price/noise-trader shocks. For each investor i, let $B_{i,t}$ be a standard Brownian motion, independent across i and independent of (W, U, Z). All processes are defined on a filtered probability space satisfying the usual conditions. The common filtration is

$$\mathcal{F}^0_t := \sigma(W_s, U_s, Z_s : \ s \le t).$$

Public information (for empirics). For empirical identification and calibration, the analysis uses a coarser *public* filtration generated by observable market variables and treats it as a subfiltration of the common-noise filtration. Concretely,

$$\mathcal{F}^{\text{pub}}_t := \sigma(p_s, \widehat{\bar{u}}_s : \ s \le t) \subseteq \mathcal{F}^0_t,$$

[1] A literal continuum model with $\int_0^1 s_i\, di = v$ can be formalized under an "exact law of large numbers" framework for a continuum of independent shocks (e.g., via a Fubini extension/Loeb space). This paper avoids this measure-theoretic detour and adopts the large-N interpretation, consistent with the finite-N particle/limit perspective used later.

where $\widehat{\bar{u}}$ is a measurable order-flow proxy used for identification of λ. The common-noise filtration $\mathcal{F}^0$ is retained for the theoretical common-noise mean-field equilibrium construction. On a discrete grid with step size Δt, define the normalized increments

$$\varepsilon^v_{t+1} := \frac{W_{t+\Delta t} - W_t}{\sqrt{\Delta t}}, \quad \varepsilon^c_{t+1} := \frac{U_{t+\Delta t} - U_t}{\sqrt{\Delta t}}, \quad \varepsilon^\eta_{t+1} := \frac{Z_{t+\Delta t} - Z_t}{\sqrt{\Delta t}}, \quad \varepsilon^i_{i,t+1} := \frac{B_{i,t+\Delta t} - B_{i,t}}{\sqrt{\Delta t}}.$$

Then $\varepsilon^v_{t+1}, \varepsilon^c_{t+1}, \varepsilon^\eta_{t+1} \sim \mathcal{N}(0,1)$ are i.i.d. over t, and $\varepsilon^i_{i,t+1} \sim \mathcal{N}(0,1)$ is i.i.d. over (i,t) and independent of the common shocks. In the discrete-time implementation on a grid with step size Δt, the normalized signal increment is used (with $y_{i,t}$ below reserved for mispricing $\hat{v}_{i,t} - p_t$):

$$z_{i,t} := \frac{\xi_{i,t} - \xi_{i,t-\Delta t}}{\Delta t} = v_t + \frac{\sigma_c}{\sqrt{\Delta t}}\,\varepsilon^c_t + \frac{\sigma_\epsilon}{\sqrt{\Delta t}}\,\varepsilon^i_{i,t}, \qquad \varepsilon^c_t, \varepsilon^i_{i,t} \sim \mathcal{N}(0,1),$$

where $\varepsilon^c_t := (U_t - U_{t-\Delta t})/\sqrt{\Delta t}$ and $\varepsilon^i_{i,t} := (B_{i,t} - B_{i,t-\Delta t})/\sqrt{\Delta t}$. so $\mathrm{Var}(z_{i,t} \mid v_t) = (\sigma_c^2 + \sigma_\epsilon^2)/\Delta t$ and the perceived measurement variance is $R'(\Delta t) = (\sigma_c^2 + \sigma_\epsilon^2/k)/\Delta t$ (Appendix A). (For $\Delta t = 1$, this reduces to $z_{i,t} = v_t + \sigma_c \varepsilon^c_t + \sigma_\epsilon \varepsilon^i_{i,t}$.) The market price evolves endogenously through an anchored impact rule:

$$dp_t = \kappa(v_t - p_t)\,dt + \lambda \bar{u}_t\,dt + \phi\,dZ_t, \qquad \bar{u}_t := \int_0^1 u_{i,t}\,di. \tag{8}$$

Equation (8) is a reduced-form microstructure: prices mean-revert to fundamentals at rate κ (arbitrage/fundamental anchoring), respond to aggregate net trading flow with strength λ, and are perturbed by aggregate noise Z_t with volatility ϕ. The anchoring term $\kappa(v_t - p_t)$ should be interpreted as reduced-form arbitrage pressure toward the (latent) fundamental v_t; it is not assumed that a market maker directly observes v_t. The mean-field coupling enters through $\bar{u}_t$. In the discrete-time implementation, $u_{i,t}$ is the trading rate induced by inventory adjustments over a decision interval Δt (Subsubsection 2.3.3).

Microstructure sketch for the anchored impact rule. Equation (8) can be viewed as a reduced-form limit of competitive risk-neutral market making with inventory costs, plus an (exogenous) arbitrage/anchoring flow.

Linear impact from inventory-averse competitive market makers. Let Q_t denote aggregate net order flow hitting dealers (positive when the public buys), and let the representative dealer's inventory be q_t, with

$$dq_t = -\,dQ_t, \qquad \text{(dealers take the opposite side of net flow).}$$

Assume dealers are risk-neutral and competitive (zero expected profit), but face a quadratic inventory holding cost $\frac{\lambda}{2} q_t^2$. A standard myopic quoting / LQ argument implies the midprice is shifted linearly by inventory,

$$p_t \approx \tilde{m}_t - \lambda q_t,$$

where $\tilde{m}_t$ is the dealer's "efficient" benchmark (e.g., a fast-moving reference level). Differentiating and substituting $dq_t = -dQ_t$ gives

$$dp_t \approx d\tilde{m}_t + \lambda\,dQ_t,$$

so that (in drift form) price changes are *linear* in contemporaneous net flow. Writing $dQ_t = \bar{u}_t\,dt + \sigma_{\eta,\text{flow}}\,dZ_t$ (where $\bar{u}_t$ is the net order-flow intensity hitting dealers) yields the impact and noise terms

$$dp_t - d\tilde{m}_t \approx \lambda \bar{u}_t\,dt + (\lambda \sigma_{\eta,\text{flow}})\,dZ_t, \qquad \phi := \lambda \sigma_{\eta,\text{flow}}.$$

Here $\tilde{m}_t$ is the dealer's efficient benchmark, $\bar{u}_t$ is the net order-flow intensity hitting dealers, and Z_t is a Brownian motion; $\sigma_{\eta,\text{flow}} > 0$ is the corresponding order-flow noise volatility (shares per $\sqrt{\text{time}}$), not to be confused with the trading-cost parameter η used later. In the baseline below, inventory $x_{i,t}$ is explicitly distinguished from trading rate $u_{i,t}$ (Subsubsection 2.3.3); impact in (8) depends on the mean trading rate $\bar{u}_t$ (equivalently $\lambda\,\Delta\bar{x}_t$ over a decision interval).

Anchoring as reduced-form arbitrage pressure. To capture fast arbitrage / fundamental-anchoring, posit an additional "arbitrage" flow that leans against mispricing,

$$u_t^{\text{arb}} = a\,(v_t - p_t),$$

so total net flow is $\bar{u}_t + u_t^{\text{arb}}$ at the same impact slope λ. Then

$$dp_t \approx \lambda\big(\bar{u}_t + a(v_t - p_t)\big)\,dt + (\lambda\sigma_{\eta,\text{flow}})\,dZ_t = \kappa(v_t - p_t)\,dt + \lambda\bar{u}_t\,dt + \phi\,dZ_t, \quad \kappa := \lambda a,$$

which matches the anchored impact specification.

2.3.2 Equilibrium Price Formation

The analysis focuses on feedback strategies where demand depends on perceived mispricing. Let $\hat{v}_{i,t}$ denote investor i's Kalman–Bucy estimate of v_t under the *perceived* measurement-noise variance $R'(k)$ (Appendix A). When $k = 1$ this coincides with the true conditional mean $\mathbb{E}[v_t \mid \mathcal{F}_t^i]$; when $k \neq 1$ it should be interpreted as a *subjective* filter state computed under the investor's misperceived signal precision. Define the mean belief $m_t := \int_0^1 \hat{v}_{i,t}\,di$. A broad class of (best-response and learning-based) specifications take the affine form

$$x_{i,t} = \Theta_t(\Sigma_{i,t})\big(\hat{v}_{i,t} - p_t\big) + \tilde{\Theta}_t(\Sigma_{i,t})\,\bar{u}_t, \tag{9}$$

where $\Sigma_{i,t}$ is the agent's perceived posterior variance. *Definition (gains).* For each t, the maps $\Theta_t, \tilde{\Theta}_t : [0,\infty) \to [0,\infty)$ are (possibly time-varying) feedback gains. $\Theta_t(\Sigma)$ has units (shares/value) and measures sensitivity of inventory to mispricing; $\tilde{\Theta}_t(\Sigma)$ has units (shares per unit flow) and measures sensitivity to the mean trading rate. In the baseline myopic CARAbest response (Proposition 4.2), the gains are

$$\Theta_t(\Sigma_{i,t}) = \frac{\kappa}{\chi + \gamma\,\sigma_{p,i,t}^2}, \qquad \tilde{\Theta}_t(\Sigma_{i,t}) = \frac{\lambda}{\chi + \gamma\,\sigma_{p,i,t}^2},$$

where $\sigma_{p,i,t}^2$ is the conditional variance *rate* defined by $\text{Var}_i(\Delta p_{t+\Delta t} \mid \mathcal{F}_t^i) = \sigma_{p,i,t}^2 \Delta t$ and depends on $\Sigma_{i,t}$ through the subjective price-variance term (Eq. (30)).

2.3.3 Timing and stock–flow separation (inventory vs. trading rate)

Timing and objects (discrete decision interval Δt). At each decision date t agents enter with a *pre-trade inventory* x_{i,t^-} (shares) and choose a *post-trade inventory* $x_{i,t}$ (shares). The executed order and trading rate are

$$\Delta x_{i,t} := x_{i,t} - x_{i,t^-}, \qquad u_{i,t} := \frac{\Delta x_{i,t}}{\Delta t} \quad \text{(shares/time)}, \qquad \bar{u}_t := \int_0^1 u_{i,t}\,di.$$

Price changes over $[t, t+\Delta t]$ via *flow-based* impact,

$$\Delta p_{t+\Delta t} = \kappa(v_t - p_t)\,\Delta t + \lambda\,\bar{u}_t\,\Delta t + \phi\sqrt{\Delta t}\,\varepsilon_{t+1}^{\eta}, \qquad \varepsilon_{t+1}^{\eta} := \frac{Z_{t+\Delta t} - Z_t}{\sqrt{\Delta t}} \sim \mathcal{N}(0,1).$$

Equivalently, since $\bar{u}_t \Delta t = \Delta\bar{x}_t$ with $\bar{x}_t := \int_0^1 x_{i,t}\,di$, the impact term can be written $\lambda\,\Delta\bar{x}_t$. This timing makes explicit that x is a stock (shares) while u is a flow (shares/time), resolving the unit ambiguity when a single symbol is used for both.

2.3.4 Belief Updating via Kalman Filtering

Each investor maintains a belief state $(\hat{v}_{i,t}, \Sigma_{i,t})$ where $\hat{v}_{i,t}$ is the posterior mean of v_t and $\Sigma_{i,t}$ is the perceived posterior variance. In the linear-Gaussian setting above, $(\hat{v}_{i,t}, \Sigma_{i,t})$ satisfy Kalman–Bucy equations driven by the private signal $\xi_{i,t}$. Overconfidence enters by replacing σ_ϵ^2 with σ_ϵ^2/k in the perceived filter. Appendix A summarizes the resulting filter.

2.3.5 Objective Functional

Investor i chooses a post-trade inventory process $(x_{i,t})_t$ (shares) on the discrete decision grid. Over one step, wealth evolves as

$$W_{i,t+\Delta t} = W_{i,t} + x_{i,t}\,\Delta p_{t+\Delta t} - \frac{\chi}{2} x_{i,t}^2\,\Delta t, \qquad \chi > 0,$$

where the quadratic term penalizes inventory holding/risk over the interval. Rather than solving the full intertemporal exponential-utility control problem, the paper adopts a bounded-rational *myopic* approximation: at each decision date, the investor solves the one-step certainty-equivalent problem

$$\max_{x_{i,t}} \; x_{i,t}\,\mu_{i,t} - \frac{1}{2}\big(\gamma\,\sigma_{p,i,t}^2 + \chi\big) x_{i,t}^2\,\Delta t,$$

where $\mu_{i,t} := \mathbb{E}_i[\Delta p_{t+\Delta t} \mid \mathcal{F}_t^i] = \big(\kappa(\hat{v}_{i,t} - p_t) + \lambda \bar{u}_t\big)\Delta t$ and $\mathrm{Var}_i(\Delta p_{t+\Delta t} \mid \mathcal{F}_t^i) = \sigma_{p,i,t}^2 \Delta t$. The analysis treats $\sigma_{p,i,t}^2$ as computed from primitives; in the discrete implementation it includes belief uncertainty through the effective variance term in Section IV.

2.3.6 Mean-Field Consistency (Myopic)

Let μ_t denote the (possibly random) law of $(\hat{v}_{i,t}, \Sigma_{i,t})$ across agents. Together with (8), the paper studies a *myopic mean-field consistent* fixed point: (i) given a conjectured mean-field flow $\{\mu_t\}$ (equivalently, moments such as m_t), each agent applies the myopic CARArule in Section IV; and (ii) the resulting population law induced by the controlled belief dynamics is consistent with $\{\mu_t\}$. Section III formalizes the mean-field object and discusses the common-noise aspect induced by (W_t, U_t, Z_t).

3 Mean-Field Approximation and Limiting Equations

3.1 Mean-Field Object Under Common Noise

Common filtration. Let $W_t^0 := (W_t, U_t, Z_t)$ collect the common shocks. Define

$$\mathcal{F}_t^0 := \sigma(W_s^0 : \; s \le t) = \sigma(W_s, U_s, Z_s : \; s \le t).$$

All conditional laws $\mathcal{L}(\cdot \mid \mathcal{F}_t^0)$ in the common-noise formulation use this definition.

Because the model includes common shocks (W_t, U_t, Z_t) through the fundamental, correlated signals, and price noise, the appropriate mean-field object is the *conditional* population law given $\mathcal{F}_t^0$. Concretely, let $X_{i,t} := (\hat{v}_{i,t}, \Sigma_{i,t})$ denote investor i's internal belief state (posterior mean and perceived uncertainty), and define the mean-field flow

$$\mu_t := \mathcal{L}(X_{i,t} \mid \mathcal{F}_t^0). \tag{10}$$

The conditional mean belief $m_t := \int \hat{v}\,\mu_t(d\hat{v}\,d\Sigma)$ enters the price dynamics through the mean trading rate $\bar{u}_t$ appearing in (8); inventories and trading rates are linked by the stock–flow timing in Subsubsection 2.3.3. (Heterogeneous-k extension: if k_i varies across investors, take $X_{i,t} := (\hat{v}_{i,t}, \Sigma_{i,t}, k_i)$ and $\mu_t := \mathcal{L}(X_{i,t} \mid \mathcal{F}_t^0)$.)

3.2 Mean-Field Equilibrium (Common-Noise Formulation)

Fix a candidate flow $\{\mu_t\}_{t\in[0,T]}$ and the resulting price process $\{p_t\}$ from (8). In the bounded-rational formulation of this paper, the representative agent does not solve a full intertemporal control problem; instead, given $\{\mu_t\}$ and $\{p_t\}$ the agent applies the myopic rule from Section IV, yielding a feedback $x_{i,t} = x^{\text{myopic}}(t, X_{i,t}, p_t, \mu_t)$. The induced controlled state process generates a new conditional flow $\{\tilde{\mu}_t\}$. A myopic mean-field equilibrium is a fixed point $\mu = \tilde{\mu}$.

In common-noise settings, μ_t is random and its evolution is governed by a stochastic Kolmogorov forward equation (stochastic Fokker–Planck / SPDE) for the conditional law; see, e.g., Carmona and Delarue (2018a); Lacker (2016). Section VI computes equilibrium statistics using a particle approximation: simulate a large N-agent system driven by shared (W, U, Z) and independent $\{B_i\}$ and estimate μ_t via the empirical measure.

Scope of theoretical results. To avoid confusion, the paper explicitly states what it establishes and what it does not claim.

Per-step stock–flow fixed point and the coefficient B_t^{sf}. Suppose the one-step myopic best response has the affine form

$$x_{i,t} = \theta_{i,t}\big(\kappa(\hat{v}_{i,t} - p_t) + \lambda \bar{u}_t\big), \qquad \theta_{i,t} := \frac{\alpha_0}{\chi + \gamma\, \sigma_{p,i,t}^2} > 0,$$

where $\sigma_{p,i,t}^2 := \text{Var}_i(\Delta p_{t+\Delta t} \mid \mathcal{F}_t^i)/\Delta t$ is the conditional variance rate (so $\text{Var}_i(\Delta p_{t+\Delta t} \mid \mathcal{F}_t^i) = \sigma_{p,i,t}^2 \Delta t$). Define the common-filtration coefficients

$$A_t^{\text{sf}} := \kappa\, \mathbb{E}[\theta_{i,t}(\hat{v}_{i,t} - p_t) \mid \mathcal{F}_t^0], \qquad B_t^{\text{sf}} := \lambda\, \mathbb{E}[\theta_{i,t} \mid \mathcal{F}_t^0].$$

Then $\bar{x}_t = A_t^{\text{sf}} + B_t^{\text{sf}} \bar{u}_t$. With stock–flow timing $\bar{u}_t = (\bar{x}_t - \bar{x}_{t^-})/\Delta t$, the fixed point is

$$\bar{u}_t = \frac{A_t^{\text{sf}} - \bar{x}_{t^-}}{\Delta t - B_t^{\text{sf}}}, \qquad \bar{x}_t = A_t^{\text{sf}} + B_t^{\text{sf}}\, \bar{u}_t,$$

which is well-defined and unique whenever $\Delta t - B_t^{\text{sf}} \neq 0$; if $0 \leq B_t^{\text{sf}} < \Delta t$ then the associated per-step map is a contraction (Theorem 4.6). **Baseline object (what this paper computes and simulates):** a discrete-time, stock–flow myopic equilibrium with inventory carryover and flow-based impact. The per-step mean-field fixed point is scalar; under $0 \leq B_t^{\text{sf}} < \Delta t$ the per-step map is a contraction (Theorem 4.6), and under this condition the full discrete-time particle system is well-posed (Theorem 3.1). **Benchmarks (for comparison only):** the paper also records a continuous-time position-impact benchmark (which collapses stock and flow) where the mean-field closure becomes algebraic and admits an explicit closed form and condition (Theorem 3.2); this benchmark is not used in the baseline simulations. **What this paper does not claim:** This paper does not establish existence or uniqueness of a full optimal-control MFG equilibrium under intertemporal exponential utility maximization with endogenous filtering on prices. The myopic rule (29) is a bounded-rational approximation; Subsection 4.3 and Subsection 4.4 provide constructive continuous-time comparisons, but a complete verification of existence/uniqueness conditions for those intertemporal MFG couplings would strengthen the theoretical foundation.

3.3 Discrete-Time Myopic Mean-Field Equilibrium (What This Paper Computes)

The numerical experiments in Section VI implement a discrete-time, bounded-rational equilibrium concept consistent with the myopic rule in Section IV. Fix a time grid $t = 0, 1, \ldots, T$ (step

size $\Delta t = 1$ in the implementation) and consider the N-agent system induced by: (i) fundamental and price updates (Euler discretization of (8)), (ii) private-signal observations (normalized increments $z_{i,t} = (\xi_{i,t} - \xi_{i,t-\Delta t})/\Delta t$) and Kalman belief updates (Appendix A), and (iii) the myopic inventory rule (29) with the per-step stock–flow fixed point (Proposition 4.5).

Definition (myopic mean-field equilibrium, discrete time). Given a pre-trade mean inventory $\bar{x}_{t^-}$ and public price p_t, agent i computes a belief state $(\hat{v}_{i,t}, \Sigma_{i,t})$ and chooses a post-trade inventory $x_{i,t}$ according to the myopic rule, which depends on the mean trading rate $\bar{u}_t$. A discrete-time myopic mean-field equilibrium at time t is a pair $(\bar{x}_t, \bar{u}_t)$ such that

$$\bar{x}_t = \frac{1}{N}\sum_{i=1}^{N} x_{i,t}, \qquad \bar{u}_t = \frac{\bar{x}_t - \bar{x}_{t^-}}{\Delta t},$$

with individual choices consistent with $\bar{u}_t$. In the implementation the rule is linear in $\bar{u}_t$ and the scalar fixed point is computed in closed form (Proposition 4.5).

3.4 Discrete-Time Well-Posedness (Existence and Uniqueness of Paths)

The paper formalizes the particle implementation as a coupled discrete-time dynamical system on a fixed time grid.

Assumptions. Fix $T \in \mathbb{N}$ and $\Delta t > 0$ and assume: (A1) parameters satisfy $\kappa > 0$, $\phi > 0$, $\gamma > 0$, $\alpha_0 > 0$ and initial conditions $(v_0, p_0, \{\hat{v}_{i,0}, \Sigma_{i,0}\}_{i=1}^N)$ are finite with $\Sigma_{i,0} \geq 0$; (A2) beliefs evolve via the discrete-time Kalman recursion in Appendix A (so $(\hat{v}_{i,t}, \Sigma_{i,t})$ is uniquely defined given $(\hat{v}_{i,t-1}, \Sigma_{i,t-1})$ and the signal); (A3) for each t, the per-step stock–flow map admits a unique fixed point $\bar{x}_t$ (and hence $\bar{u}_t$), e.g., the contraction condition $0 \leq B_t^{\mathrm{sf}} < \Delta t$ in Theorem 4.6 holds; (A4) price and fundamental updates are given by the Euler discretizations of their SDEs driven by specified shock sequences.

Theorem 3.1 (Well-posedness of the discrete-time particle system)**.** *Under (A1)–(A4), for any realization of the common and idiosyncratic shock sequences, the discrete-time system defined by: (i) belief update (Appendix A), (ii) per-step myopic mean-field fixed point (Proposition 4.5), and (iii) Euler updates for (v_t, p_t), admits a unique adapted solution path*

$$(v_t, p_t, \{\hat{v}_{i,t}, \Sigma_{i,t}\}_{i=1}^N, \bar{x}_t, \bar{u}_t)_{t=0}^T.$$

3.5 Position-impact benchmark: common-noise fixed-point verification (continuous time)

This section is a diagnostic benchmark using the legacy position-impact closure; the baseline simulations use the discrete-time stock–flow equilibrium with uniqueness condition $0 \leq B_t^{\mathrm{sf}} < \Delta t$ (Proposition 4.5, Theorem 4.6).

This subsection records a self-contained fixed-point verification for a continuous-time *position-impact* benchmark (which collapses stock and flow so that $\bar{u}_t \equiv \bar{x}_t$). It is included for comparison and is not used in the baseline simulations, which use the discrete-time stock–flow closure above. The key point is that, in the information simplification used here (filtering on ξ^i only), the belief state dynamics are *conditionally i.i.d.* given the common filtration, so the mean-field object is the conditional law and the equilibrium closure reduces to an explicit algebraic fixed point.

Common and idiosyncratic noises. Recall the common filtration $(\mathcal{F}_t^0)$ generated by $W^0 = (W, U, Z)$, and idiosyncratic signal noises $\{B^i\}_{i\geq 1}$ independent across i and independent of (W, U, Z).

Finite-N (continuous-time) price-taking system. Consider the N-agent system (continuous time) with a *price-taking* interaction through the average demand $\bar{x}_t^N := \frac{1}{N}\sum_{j=1}^N x_t^{j,N}$:

$$dv_t = \mu_v\,dt + \sigma_v\,dW_t, \tag{11}$$

$$d\xi_t^i = v_t\,dt + \sigma_c\,dU_t + \sigma_\epsilon\,dB_t^i, \qquad i = 1,\dots,N, \tag{12}$$

$$dp_t^N = \kappa(v_t - p_t^N)\,dt + \lambda\bar{x}_t^N\,dt + \phi\,dZ_t. \tag{13}$$

Agents compute the subjective Kalman–Bucy filter (Appendix A) from (12):

$$\begin{aligned} d\hat{v}_t^i &= \mu_v\,dt + K_t^{(i)}\big(d\xi_t^i - \hat{v}_t^i\,dt\big),\\ K_t^{(i)} &:= \frac{\Sigma_t^{(i)}}{R'}, \quad R' := \sigma_c^2 + \sigma_\epsilon^2/k. \end{aligned} \tag{14}$$

with Riccati $\dot{\Sigma}_t^{(i)} = \sigma_v^2 - (\Sigma_t^{(i)})^2/R'$ and $\Sigma_0^{(i)} \geq 0$. (If $\Sigma_0^{(i)} \equiv \Sigma_0$, then $K_t^{(i)} \equiv K_t$ and $\Sigma_t^{(i)} \equiv \Sigma_t$ are deterministic.)

Given $(p_t^N, \bar{x}_t^N)$, the (benchmark) myopic CARA rule under Gaussian price increments (with $\chi = 0$ and $\mathrm{Var}(dp_t \mid \mathcal{F}_t^i)/dt = \phi^2$) prescribes the pointwise best response

$$x_t^{i,N} = \frac{\kappa(\hat{v}_t^i - p_t^N) + \lambda\bar{x}_t^N}{\gamma\phi^2}, \qquad i = 1,\dots,N. \tag{15}$$

Averaging (15) yields the *per-time* fixed point

$$(\gamma\phi^2 - \lambda)\,\bar{x}_t^N = \kappa(\hat{m}_t^N - p_t^N), \qquad \hat{m}_t^N := \frac{1}{N}\sum_{i=1}^N \hat{v}_t^i, \tag{16}$$

so whenever $\gamma\phi^2 > \lambda$,

$$\bar{x}_t^N = \frac{\kappa}{\gamma\phi^2 - \lambda}\,(\hat{m}_t^N - p_t^N). \tag{17}$$

Mean-field (conditional-law) system. Define the representative-agent belief state $\hat{v}_t$ solving (14) with an independent copy B (and the same common noises (W, U, Z)), and define the conditional flow

$$\begin{aligned} \mu_t &:= \mathcal{L}\big(\hat{v}_t, \Sigma_t \,\big|\, \mathcal{F}_t^0\big),\\ m_t &:= \int \hat{v}\,\mu_t(d\hat{v}\,d\Sigma) = \mathbb{E}[\hat{v}_t \mid \mathcal{F}_t^0]. \end{aligned}$$

The mean-field price satisfies

$$dp_t = \kappa(v_t - p_t)\,dt + \lambda\bar{x}_t\,dt + \phi\,dZ_t, \tag{18}$$

where $\bar{x}_t$ is required to satisfy the mean-field consistency condition

$$\bar{x}_t = \int \frac{\kappa(\hat{v} - p_t) + \lambda\bar{x}_t}{\gamma\phi^2}\;\mu_t(d\hat{v}\,d\Sigma). \tag{19}$$

Since only the mean of $\hat{v}$ enters (19), the fixed point reduces to

$$\bar{x}_t = \frac{\kappa}{\gamma\phi^2 - \lambda}\,(m_t - p_t), \qquad \text{assuming } \gamma\phi^2 > \lambda. \tag{20}$$

Theorem 3.2 (Common-noise fixed point). *Assume* $\gamma\phi^2 > \lambda$ *and* $\sup_{i\le N}\mathbb{E}[|\hat{v}_0^i|^2] < \infty$ *with* $\sup_{i\le N}\Sigma_0^{(i)} < \infty$. *For simplicity, assume initial belief states are i.i.d. across* i *conditional on* $\mathcal{F}_0^0$. *Then:*

(i) (Well-posedness.) *The* N*-agent system* (11)–(13) *with controls given by the myopic fixed point* (15) *admits a unique strong solution, and the limiting mean-field (conditional-law) system consisting of* (11)*, a representative signal equation of the form* (12) *(with an independent idiosyncratic Brownian motion), the representative filter* (14)*, and the price equation* (18) *with* $\bar{x}$ *given by* (20) *admits a unique strong solution.*

(ii) (Fixed-point verification.) *The process* $\bar{x}$ *defined by* (20) *is the unique solution to the mean-field consistency equation* (19) *(i.e., a unique myopic common-noise MFG fixed point).*

(iii) (Conditional propagation of chaos / LLN.) *Let the empirical measure of belief states be* $\mu_t^N := \frac{1}{N}\sum_{i=1}^N \delta_{(\hat{v}_t^i,\Sigma_t^{(i)})}$. *Then for each fixed* t,

$$\mu_t^N \xrightarrow[N\to\infty]{} \mu_t \quad \textit{in probability, and} \quad \hat{m}_t^N \to m_t \textit{ in } L^2.$$

Consequently, $\bar{x}_t^N \to \bar{x}_t$ *in* L^2 *and* $p_t^N \to p_t$ *in* L^2 *uniformly on* $[0,T]$.

Proof. Step 1 (Well-posedness). For each i, the filter SDE (14) is linear with adapted coefficients and admits a unique strong solution with finite second moments; the Riccati equation is a scalar ODE with global solution (Appendix A). Given $\bar{x}^N$ and p^N, the control (15) is affine in $(\hat{v}^i, p^N, \bar{x}^N)$. The averaging identity (16) yields the explicit closure (17) when $\gamma\phi^2 > \lambda$. Substituting (17) into (13) gives a linear SDE for p^N driven by (W,U,Z) and the averaged belief $\hat{m}^N$, hence a unique strong solution. Likewise, substituting (20) into (18) gives a linear SDE for p driven by (W,U,Z) and m.

Step 2 (Fixed point). Equation (19) is affine in $\bar{x}_t$:

$$\bar{x}_t = \frac{\kappa(m_t - p_t) + \lambda\bar{x}_t}{\gamma\phi^2}.$$

Rearranging gives $(\gamma\phi^2 - \lambda)\bar{x}_t = \kappa(m_t - p_t)$ and thus (20). Uniqueness follows since $\gamma\phi^2 - \lambda > 0$.

Step 3 (Conditional LLN / propagation of chaos). Conditional on $\mathcal{F}_t^0$, the idiosyncratic noises $\{B^i\}$ are independent and the filter equations (14) are driven by independent Brownian motions with the *same* common coefficients and common path (W,U,Z). Hence the collection $\{(\hat{v}_t^i, \Sigma_t^{(i)})\}_{i=1}^N$ is i.i.d. conditional on $\mathcal{F}_t^0$ (with law μ_t), and the conditional law of large numbers implies $\mu_t^N \Rightarrow \mu_t$ and

$$\mathbb{E}\big[|\hat{m}_t^N - m_t|^2 \mid \mathcal{F}_t^0\big] = \frac{1}{N}\operatorname{Var}(\hat{v}_t \mid \mathcal{F}_t^0),$$

so $\hat{m}_t^N \to m_t$ in L^2. Moreover, by Step 1 it holds that $\sup_{t\le T}\mathbb{E}[\hat{v}_t^2] < \infty$, hence $\sup_{t\le T}\mathbb{E}[\operatorname{Var}(\hat{v}_t \mid \mathcal{F}_t^0)] \le \sup_{t\le T}\mathbb{E}[\hat{v}_t^2] < \infty$ and therefore

$$\sup_{t\le T}\mathbb{E}|\hat{m}_t^N - m_t|^2 \le \frac{C_T}{N}, \qquad \int_0^T \mathbb{E}|\hat{m}_s^N - m_s|^2\,ds \le \frac{TC_T}{N} \xrightarrow[N\to\infty]{} 0.$$

Step 4 (Price convergence). Let $C := \kappa/(\gamma\phi^2 - \lambda)$ so that (17)–(20) read $\bar{x}_t^N = C(\hat{m}_t^N - p_t^N)$ and $\bar{x}_t = C(m_t - p_t)$. Substituting these into (13) and (18) gives the closed price equations

$$dp_t^N = \kappa(v_t - p_t^N)\,dt + \lambda C(\hat{m}_t^N - p_t^N)\,dt + \phi\,dZ_t, \qquad dp_t = \kappa(v_t - p_t)\,dt + \lambda C(m_t - p_t)\,dt + \phi\,dZ_t.$$

Subtracting yields a linear ODE for $\Delta p_t := p_t^N - p_t$ driven by $\Delta m_t := \hat{m}_t^N - m_t$:

$$d\Delta p_t = -(\kappa + \lambda C)\Delta p_t\,dt + \lambda C\,\Delta m_t\,dt.$$

By variation of constants, for $t \in [0,T]$,

$$\Delta p_t = e^{-(\kappa+\lambda C)t}\Delta p_0 + \lambda C \int_0^t e^{-(\kappa+\lambda C)(t-s)}\Delta m_s\, ds.$$

Assuming matching initial conditions ($\Delta p_0 = 0$), Jensen and Cauchy–Schwarz imply

$$\sup_{t\le T}\mathbb{E}|p_t^N - p_t|^2 \;\le\; (\lambda C)^2 T \int_0^T \mathbb{E}|\hat{m}_s^N - m_s|^2\, ds \;\xrightarrow[N\to\infty]{}\; 0,$$

and the L^2 uniform convergence follows.

Step 5 (Mean-field action convergence). Using again $\bar{x}_t^N = C(\hat{m}_t^N - p_t^N)$ and $\bar{x}_t = C(m_t - p_t)$,

$$\bar{x}_t^N - \bar{x}_t = C\big[(\hat{m}_t^N - m_t) - (p_t^N - p_t)\big].$$

Thus, by Step 3 and Step 4,

$$\sup_{t\le T}\mathbb{E}|\bar{x}_t^N - \bar{x}_t|^2 \le 2C^2\left(\sup_{t\le T}\mathbb{E}|\hat{m}_t^N - m_t|^2 + \sup_{t\le T}\mathbb{E}|p_t^N - p_t|^2\right) \xrightarrow[N\to\infty]{} 0.$$

□

Remark 3.3 (Stochastic Fokker–Planck equation for μ_t). For any test function $\varphi \in C_b^2(\mathbb{R}\times\mathbb{R}_+\times\mathbb{R}_+)$, the conditional law $\mu_t = \mathcal{L}(\hat{v}_t, \Sigma_t, k \mid \mathcal{F}_t^0)$ satisfies the common-noise SPDE (in weak form)

$$\begin{aligned} d\langle\mu_t,\varphi\rangle = \Big\langle \mu_t, \big(\mu_v + K_t(k)(v_t - \hat{v})\big)\,\partial_{\hat{v}}\varphi \\ + \tfrac{1}{2}K_t(k)^2\sigma_\epsilon^2\,\partial^2_{\hat{v}\hat{v}}\varphi\Big\rangle dt \\ + \Big\langle \mu_t, K_t(k)\sigma_c\,\partial_{\hat{v}}\varphi\Big\rangle dU_t. \end{aligned}$$

where $\langle\mu,\varphi\rangle := \int\varphi\, d\mu$ and $K_t(k) = \Sigma_t(k)/(\sigma_c^2 + \sigma_\epsilon^2/k)$. In the homogeneous case, μ_t is Gaussian in $\hat{v}$ conditional on $\mathcal{F}_t^0$ (with random mean m_t).

3.6 Mean-Field Limit

This section states a standard common-noise McKean–Vlasov/MFG limit as a black-box framework; the contribution is the constructive solution in the LQG specialization, given in Section 3.7.

Setting. Consider a common-noise McKean–Vlasov system on a finite horizon $[0,T]$. Let $W_t^0 := (W_t, U_t, Z_t)$ collect the common shocks and define $\mathcal{F}_t^0 := \sigma(W_s^0 :\ s \le t) = \sigma(W_s, U_s, Z_s : s \le t)$. For each $N \ge 1$ let $\{B^i\}_{i=1}^N$ be mutually independent and independent of W^0. The N-agent state processes $\{X_t^{i,N}\}_{i=1}^N$ take values in $\mathbb{R}^d$ and satisfy a coupled system whose coefficients may depend on the empirical measure $\bar{\mu}_t^N := \frac{1}{N}\sum_{j=1}^N \delta_{X_t^{j,N}}$ and on the common noise. The mean-field limit is described by a McKean–Vlasov SDE in which the conditional law $\mu_t = \mathcal{L}(X_t \mid \mathcal{F}_t^0)$ of a representative state X_t enters the drift and diffusion; see Carmona and Delarue (2018a,b); Lacker (2018).

Assumptions. The following standard conditions are imposed (see, e.g., Fournier and Guillin (2015); Lacker (2018)).

(H1) **(Lipschitz in state and measure.)** The drift $b(t,x,\mu)$ and diffusion $\sigma(t,x,\mu)$ are Lipschitz in (x,μ) uniformly in $t \in [0,T]$, with μ in the space of probability measures on $\mathbb{R}^d$ metrized by the Wasserstein distance W_2.

(H2) **(Linear growth.)** $|b(t,x,\mu)| + \|\sigma(t,x,\mu)\| \le C(1 + |x| + W_2(\mu,\delta_0))$ for some $C \ge 0$.

(H3) **(Common noise integrability.)** Common-noise coefficients are progressively measurable and square-integrable on $[0,T]$ a.s.

(H4) **(Initial condition.)** The initial states $\{X_0^{i,N}\}_{i=1}^N$ are i.i.d. with law μ_0 and satisfy $\mathbb{E}[|X_0^{i,N}|^2] < \infty$; μ_0 has finite second moment.

(H5) **(Non-degeneracy / bounded coefficients.)** The diffusion matrix $\sigma\sigma^\top$ is uniformly elliptic (or at least non-degenerate) and all coefficients are bounded when restricted to compacts in $\mathbb{R}^d \times \mathcal{P}_2(\mathbb{R}^d)$.

Under (H1)–(H5), the limiting McKean–Vlasov equation admits a unique strong solution and the N-particle system is well-posed; see Carmona and Delarue (2018a,b).

Theorem 3.4 (Convergence of empirical measures)**.** *Assume (H1)–(H5). Let $\{X^{i,N}\}_{i=1}^N$ solve the N-particle system and let X solve the limiting McKean–Vlasov equation with the same common noise W^0 and i.i.d. copies $\{B^i\}$ of the idiosyncratic driver. Then for each $t \in [0,T]$,*

$$\bar{\mu}_t^N \xrightarrow[N\to\infty]{W_2} \mu_t \quad \textit{in probability,}$$

where $\mu_t = \mathcal{L}(X_t \mid \mathcal{F}_t^0)$ is the conditional law of the limit process. In particular, propagation of chaos holds: any fixed finite marginals converge in law to the product of the limit conditional law.

Proof sketch (black-box references). Existence and uniqueness for the limit equation follow from (H1)–(H2) and fixed-point arguments in the space of flows of measures; see Carmona and Delarue (2018a). Convergence of $\bar{\mu}_t^N$ to μ_t in W_2 is a standard consequence of (H1)–(H5) and the conditional law of large numbers for the empirical measure; see Fournier and Guillin (2015) for quantitative rates and Lacker (2018) for the common-noise formulation. Propagation of chaos is then implied by the same estimates; see Carmona and Delarue (2018b). □

Proposition 3.5 (Stability of mean-field equilibrium)**.** *Under (H1)–(H5), the mean-field equilibrium flow $\{\mu_t\}_{t\in[0,T]}$ is unique in the class of admissible flows with finite second moments. Moreover, $\sup_{t\in[0,T]} \mathbb{E}[W_2(\bar{\mu}_t^N, \mu_t)^2] \le C/N$ for some constant C depending on T and the data.*

Proof sketch (black-box references). Uniqueness follows from the Lipschitz structure (H1) and Gronwall-type estimates in Wasserstein space; see Carmona and Delarue (2018a). The $O(1/N)$ bound for $\mathbb{E}[W_2(\bar{\mu}_t^N, \mu_t)^2]$ is given in Fournier and Guillin (2015) and Huang et al. (2006) for the classical and MFG settings. □

Remark 3.6 (LQG specialization). In the LQG setting (see Section IV), the coefficients are affine in state and measure, so (H1)–(H2) hold and the limit is explicit. The preceding black-box statements justify using the mean-field system as the large-N approximation for the particle implementation in Section VI.

3.7 Constructive LQG Solution via Picard Iteration

Benchmark (position impact; continuous time). This subsection is a continuous-time constructive solver for a *position-impact* formulation (it collapses stock and flow so that $\bar{u} \equiv \bar{x}$). It is included as a diagnostic/benchmark and is not used in the baseline discrete-time stock–flow simulations in Section VI.

Notation. The notation (A_t, B_t) is reserved for the continuous-time LQG/value-function coefficients in this subsection (Proposition 3.7). The per-step stock–flow fixed point uses distinct coefficients $(A_t^{\mathrm{sf}}, B_t^{\mathrm{sf}})$ (Section 3, Proposition 4.5).

Endogenous vs exogenous. Mean demand $\bar{x}$, price p, and (from the equilibrium map) mispricing $\bar{y} = m - p$ and the coefficient B_t (driven by $\bar{x}$) are *endogenous*; in equilibrium, beliefs and the filter are consistent with the chosen information. Exogenous parameters include κ, λ, ϕ, γ, and other primitives (e.g. σ_v, σ_c, σ_ϵ, k). In this formulation, belief updating conditions only on the private signal ξ and not on the price observation channel; hence the mean belief m_t is not fed back by $\bar{x}$. Price is endogenous as an outcome of $\bar{x}$ but is not used as an observation in the filter; incorporating it would require joint filtering and a richer fixed-point formulation (see Section IV).

Reduced state and dynamics. Define the (belief–price) mispricing state

$$y_t \;:=\; \hat{v}_t - p_t. \tag{21}$$

This subsection works in the homogeneous representative-agent setting with overconfidence parameter k, so $\hat{v}_t$ is the subjective Kalman estimate of v_t, Σ_t is the perceived posterior variance, and $R' := \sigma_c^2 + \sigma_\epsilon^2/k$ is the perceived measurement-noise variance. Wealth and state dynamics in innovation form are

$$dW_t = x_t \left(\kappa\, y_t + \lambda\, \bar{x}_t\right) dt + x_t\, \phi\, dI_t^p, \tag{22}$$

$$dy_t = \left(\mu_v - \kappa\, y_t - \lambda\, \bar{x}_t\right) dt + \beta_t\, dI_t^\xi - \phi\, dI_t^p, \tag{23}$$

where under the physical measure P and the agent filtration, I^p and I^ξ are independent Brownian motions (price innovation and objective signal innovation); misspecification enters only through the gain K_t (via $R'(k)$). The (subjective) unhedgeable loading is

$$\beta_t \;=\; K_t \sqrt{\sigma_c^2 + \sigma_\epsilon^2}, \qquad K_t \;=\; \frac{\Sigma_t}{R'}, \qquad R' \;=\; \sigma_c^2 + \frac{\sigma_\epsilon^2}{k}, \tag{24}$$

and the perceived posterior variance Σ_t solves the Riccati equation

$$\dot{\Sigma}_t \;=\; \sigma_v^2 - \frac{\Sigma_t^2}{R'}, \qquad \Sigma_0 \geq 0. \tag{25}$$

Fixed-point map and contraction. Theorem 3.4 provides the framework: existence, uniqueness, and convergence of the mean-field limit are from the black-box theory (assumptions (H1)–(H5)); the reduced dynamics (22)–(23), Riccati (25), and mean-field update (26) below are derived in the LQG setting used here. Given a candidate mean-field demand process $\bar{x}(\cdot)$, one can (i) solve the backward Riccati for A_t (independent of $\bar{x}$), (ii) solve the backward linear ODE for B_t driven by $\bar{x}_t$, (iii) simulate forward the coupled (v_t, m_t, p_t) and hence $\bar{y}_t = m_t - p_t$, and (iv) update $\bar{x}$ via the mean-field consistency relation. This defines a fixed-point map Φ on trajectories $\bar{x}(\cdot)$.

Fixed-point object. The fixed-point object is the map Φ on the space $\mathcal{X} := L^2_{\mathcal{F}^0}(\Omega \times [0,T])$ of candidate mean-field demand trajectories (adapted to the common filtration $\mathcal{F}^0$), equipped with the norm

$$\|\bar{x}\|_2 := \Big(\mathbb{E}\int_0^T |\bar{x}_t|^2\, dt\Big)^{1/2}.$$

Equilibrium corresponds to the unique fixed point $\bar{x}^\star = \Phi(\bar{x}^\star)$ when the contraction condition $q < 1$ below holds; see Proposition 3.7.

Proposition 3.7 (Constructive equilibrium under weak coupling / small horizon)**.** *Define the fixed-point map Φ on $\bar{x}(\cdot)$ as follows. Given $\bar{x}(\cdot)$:*

(i) Solve backward the Riccati equation for A_t with terminal condition $A_T = 0$ (as in the A-ODE of the exact CARA/LQG formulation).

(ii) Solve backward the linear ODE for B_t driven by $\bar{x}_t$, with terminal condition $B_T = 0$.

(iii) Solve forward the dynamics for (v_t, m_t, p_t) given $\bar{x}_t$, and set $\bar{y}_t = m_t - p_t$.

(iv) Update via mean-field consistency:

$$\bar{x}_t \;=\; \frac{(\kappa + \phi^2 A_t)\,\bar{y}_t + \phi^2 B_t}{\gamma\,\phi^2 - \lambda}. \tag{26}$$

Define

$$q \;:=\; \frac{\lambda T}{\gamma\phi^2 - \lambda}\,\big(2\kappa + \kappa^2 T\big). \tag{27}$$

If $\gamma\phi^2 > \lambda$ and $q < 1$, then Φ is a contraction on the space $\mathcal{X} := L^2_{\mathcal{F}^0}(\Omega \times [0,T])$ and the fixed point exists and is unique; Picard iteration converges.

Proof. The contraction argument is made fully explicit.

Functional-analytic setup. Fix a filtered probability space $(\Omega, \mathcal{F}, \mathcal{F}^0, \mathbb{P})$ supporting the common shocks (e.g. (W, U, Z) as in (32)–(34)) and the cross-sectional private noises. Let $W^0_t := (W_t, U_t, Z_t)$ collect the common shocks and define $\mathcal{F}^0_t := \sigma(W^0_s :\ s \le t) = \sigma(W_s, U_s, Z_s :\ s \le t)$. Define the Banach space

$$\mathcal{X} := L^2_{\mathcal{F}^0}(\Omega \times [0,T]), \qquad \|\bar{x}\|_2 := \Big(\mathbb{E}\int_0^T |\bar{x}_t|^2\, dt\Big)^{1/2}.$$

(If one prefers to restrict to deterministic mean-field trajectories $\bar{x} : [0,T] \to \mathbb{R}$, the same proof applies verbatim with $\|\bar{x}\|_{L^2([0,T])} := (\int_0^T |\bar{x}_t|^2 dt)^{1/2}$.)

Assume $\gamma\phi^2 > \lambda$, so the denominator in (26) is strictly positive. Also assume β is $\mathcal{F}^0$-progressively measurable and bounded on $[0,T]$ (this holds under the constant-gain closure (31), or any bounded-gain filtering specification used in Sections III–IV).

Step 1: Riccati well-posedness and a uniform bound for A. In the homogeneous case, A_t solves (44) with terminal condition $A_T = 0$:

$$-\dot{A}_t = \frac{\kappa^2}{\phi^2} - \beta_t^2 A_t^2, \qquad A_T = 0.$$

Set $\widetilde{A}_s := A_{T-s}$ for $s \in [0,T]$. Then

$$\dot{\widetilde{A}}_s = \frac{\kappa^2}{\phi^2} - \beta_{T-s}^2\, \widetilde{A}_s^2, \qquad \widetilde{A}_0 = 0.$$

Nonnegativity. The vector field $f(s,a) := \kappa^2/\phi^2 - \beta_{T-s}^2 a^2$ is continuous in s and locally Lipschitz in a, hence solutions are unique. Moreover $f(s,0) = \kappa^2/\phi^2 > 0$ for all s, so starting from $\widetilde{A}_0 = 0$ the solution becomes strictly positive immediately. If it ever became negative, let $\tau := \inf\{s > 0 : \widetilde{A}_s = 0\}$ be the first return time to 0 from above. Then $\dot{\widetilde{A}}_\tau = f(\tau, 0) > 0$, so the trajectory points into the positive half-line at τ, contradicting the definition of τ. Thus $\widetilde{A}_s \geq 0$ for all $s \in [0,T]$, hence $A_t \geq 0$ for all t. *Coarse bound.* Because the quadratic term is nonnegative,

$$\dot{\widetilde{A}}_s \leq \frac{\kappa^2}{\phi^2} \quad \Longrightarrow \quad 0 \leq \widetilde{A}_s \leq \frac{\kappa^2}{\phi^2} s,$$

hence

$$0 \leq A_t \leq \frac{\kappa^2}{\phi^2}(T-t) \leq \frac{\kappa^2}{\phi^2} T \qquad \text{for all } t \in [0,T].$$

In particular, $A \in L^\infty([0,T])$ and $\|A\|_\infty \leq \kappa^2 T/\phi^2$.

Step 2: Precise assumption on mean belief and the $\bar{y}$-Lipschitz bound. Recall $\bar{y}_t := m_t - p_t$ in Proposition III.7.

In the myopic formulation of Section IV.B, belief updating (Appendix A) is conditioned only on the private signal $\xi_{i,t}$ (and not on the endogenous price observation channel). Under this modeling choice, the mean belief process $m_t = \int_0^1 \hat{v}_{i,t}\, di$ is independent of the mean-field demand input $\bar{x}$; i.e. for two inputs $\bar{x}, \bar{x}' \in \mathcal{X}$ it follows that $m \equiv m'$.

(If one prefers not to hard-code this, it suffices to assume instead that $\bar{x} \mapsto m$ is Lipschitz in $\|\cdot\|_2$ with constant $C_m T$; the bound below then holds with λ replaced by $\lambda + C_m$.)

Now fix $\bar{x}, \bar{x}' \in \mathcal{X}$. Couple the two forward systems on the same probability space with the same common shocks and identical initial conditions (v_0, p_0). Subtracting the price equations (34) yields, pathwise,

$$d(p_t - p_t') = -\kappa(p_t - p_t')\, dt + \lambda(\bar{x}_t - \bar{x}_t')\, dt, \qquad (p_0 - p_0') = 0,$$

since the common noise term $\phi\, dZ_t$ cancels under this coupling. Solving gives

$$|p_t - p_t'| \leq \lambda \int_0^t e^{-\kappa(t-s)} |\bar{x}_s - \bar{x}_s'|\, ds \leq \lambda \int_0^t |\bar{x}_s - \bar{x}_s'|\, ds \leq \lambda\sqrt{t}\Big(\int_0^t |\bar{x}_s - \bar{x}_s'|^2\, ds\Big)^{1/2}.$$

Squaring and integrating in t, then using Fubini, yields

$$\int_0^T |p_t - p_t'|^2\, dt \leq \lambda^2 \int_0^T t \int_0^t |\bar{x}_s - \bar{x}_s'|^2\, ds\, dt \leq \lambda^2 T^2 \int_0^T |\bar{x}_s - \bar{x}_s'|^2\, ds.$$

Taking expectations gives $\|p - p'\|_2 \leq \lambda T \|\bar{x} - \bar{x}'\|_2$. Because $m \equiv m'$, it follows that $\bar{y} - \bar{y}' = -(p - p')$, hence

$$\|\bar{y} - \bar{y}'\|_2 \leq \lambda T \|\bar{x} - \bar{x}'\|_2.$$

Step 3: B-Lipschitz bound in $\bar{x}$. Given A (which does not depend on $\bar{x}$) and β (independent of $\bar{x}$ under the same information closure as above), B_t solves (45) with terminal condition $B_T = 0$:

$$-\dot{B}_t = \frac{\kappa\lambda}{\phi^2}\bar{x}_t + \mu_v A_t - \beta_t^2 A_t B_t, \qquad B_T = 0.$$

(If β is allowed to depend on $\bar{x}$, an additional Lipschitz term appears; the same contraction logic goes through with a larger constant.)

Let B, B' be the solutions corresponding to $\bar{x}, \bar{x}'$ and set $\Delta B := B - B'$. Subtracting the ODEs gives

$$-\dot{\Delta B}_t = \frac{\kappa\lambda}{\phi^2}(\bar{x}_t - \bar{x}'_t) - \beta_t^2 A_t \, \Delta B_t, \qquad \Delta B_T = 0.$$

By integrating factor,

$$\Delta B_t = \frac{\kappa\lambda}{\phi^2} \int_t^T \exp\Big(- \int_t^s \beta_u^2 A_u \, du \Big) (\bar{x}_s - \bar{x}'_s) \, ds.$$

Since $A_u \geq 0$ and $\beta_u^2 \geq 0$, the exponential factor is at most 1, yielding

$$|B_t - B'_t| \leq \frac{\kappa\lambda}{\phi^2} \int_t^T |\bar{x}_s - \bar{x}'_s| \, ds \leq \frac{\kappa\lambda}{\phi^2} \sqrt{T-t} \Big(\int_t^T |\bar{x}_s - \bar{x}'_s|^2 \, ds \Big)^{1/2}.$$

Squaring and integrating in t, then using Fubini, yields $\|B - B'\|_2 \leq (\kappa\lambda/\phi^2)\, T \, \|\bar{x} - \bar{x}'\|_2$.

Step 4: Contraction estimate for Φ and a fully checkable sufficient condition. Recall (26):

$$\Phi(\bar{x})_t = \frac{(\kappa + \phi^2 A_t)\bar{y}_t + \phi^2 B_t}{\gamma\phi^2 - \lambda}.$$

Using $\gamma\phi^2 - \lambda > 0$, boundedness of A, and the triangle inequality,

$$\|\Phi(\bar{x}) - \Phi(\bar{x}')\|_2 \leq \frac{(\kappa + \phi^2 \|A\|_\infty)\|\bar{y} - \bar{y}'\|_2 + \phi^2 \|B - B'\|_2}{\gamma\phi^2 - \lambda}.$$

Substituting the bounds from Steps 2–3 gives

$$\|\Phi(\bar{x}) - \Phi(\bar{x}')\|_2 \leq \frac{\lambda T}{\gamma\phi^2 - \lambda} \Big(2\kappa + \phi^2 \|A\|_\infty \Big) \, \|\bar{x} - \bar{x}'\|_2.$$

Finally, using $\|A\|_\infty \leq \kappa^2 T/\phi^2$ from Step 1 yields the parameter-only bound

$$\|\Phi(\bar{x}) - \Phi(\bar{x}')\|_2 \leq q \, \|\bar{x} - \bar{x}'\|_2, \qquad q := \frac{\lambda T}{\gamma\phi^2 - \lambda} \Big(2\kappa + \kappa^2 T \Big),$$

which is fully checkable from primitives.

Step 5: Banach fixed point. If $q < 1$, then Φ is a contraction on $(\mathcal{X}, \|\cdot\|_2)$, hence admits a unique fixed point $\bar{x}^\star \in \mathcal{X}$. Moreover, the Picard iteration $\bar{x}^{n+1} = \Phi(\bar{x}^n)$ converges geometrically to $\bar{x}^\star$ in $\|\cdot\|_2$.

Remark (relation to the simpler myopic scaling). In the myopic closure where hedging terms are suppressed ($A \equiv 0$, $B \equiv 0$), the Lipschitz estimate tightens to a pure $O(T)$ scaling proportional to $\kappa\lambda/(\gamma\phi^2 - \lambda)$, matching the heuristic small-horizon/weak-coupling condition discussed around (27). □

Picard iteration. A conservative Lipschitz bound is q in (27); for $q < 1$, Banach yields uniqueness. Algorithm 1 summarizes the procedure. Initialize a candidate $\bar{x}^0(\cdot)$ (e.g., identically zero or the myopic closure $\bar{x}_t^0 = \kappa\bar{y}_t^0/(\gamma\phi^2 - \lambda)$ from a forward run with $\bar{x} \equiv 0$), then iterate: compute Σ, K, β from (25)–(24), solve A backward, solve B backward using the current $\bar{x}^n$, forward-simulate (v, m, p) and $\bar{y}^n$, update $\bar{x}^{n+1}$ via (26), and stop when the residual (e.g., $\|\bar{x}^{n+1} - \bar{x}^n\|$ in L^2 or sup-norm over the time grid) is below a tolerance.

Algorithm 1 Picard iteration for LQG mean-field equilibrium

Input: Horizon T, parameters $(\kappa, \lambda, \gamma, \phi, \mu_v, \sigma_v, \sigma_c, \sigma_\epsilon, k)$, initial conditions $(v_0, p_0, \hat{v}_0, \Sigma_0)$, tolerance ϵ, max iterations $N_{\max}$.
Initialize: Set $\bar{x}_t^0 \leftarrow 0$ (or myopic seed) for $t \in [0,T]$. Set $n \leftarrow 0$.
repeat
  Compute Σ_t, K_t, β_t on $[0,T]$ from (25) and (24).
  Solve backward for A_t (Riccati, $A_T = 0$).
  Solve backward for B_t given $\bar{x}_t^n$ (linear ODE, $B_T = 0$).
  Forward-simulate (v_t, m_t, p_t) and $\bar{y}_t^n = m_t - p_t$ using $\bar{x}_t^n$ in the dynamics.
  Update $\bar{x}_t^{n+1} \leftarrow \frac{(\kappa+\phi^2 A_t)\bar{y}_t^n + \phi^2 B_t}{\gamma\phi^2 - \lambda}$ for $t \in [0,T]$.
  Compute residual $r_n \leftarrow \|\bar{x}^{n+1} - \bar{x}^n\|$ (e.g., L^2 or sup over grid).
  $n \leftarrow n+1$.
until $r_{n-1} < \epsilon$ or $n \geq N_{\max}$
Output: Equilibrium mean-field demand $\bar{x}^* \approx \bar{x}^n$ and associated $(A, B, \bar{y})$.

Implementation and reproducibility. The Picard iteration in Algorithm 1 is implemented in a MATLAB script; the path and run instructions will be specified in the replication package. All reported equilibrium paths and statistics use this routine with a fixed tolerance and time discretization.

3.8 Reproducibility and numerical verification

The equilibrium is computed via Algorithm 1 implemented in `code/matlab/mfg_lqg_common_noise_demo.m`. Diagnostics include the fixed-point residual along Picard iterates, a time-step refinement test under decreasing dt, and an N-convergence test comparing particle moments to the mean-field limit.[2]

Remark (discrete-time certification). At the discrete-time level, uniqueness of the numerical fixed point can be certified via a Banach fixed-point argument on trajectories endowed with a sup-norm metric. A machine-checkable backbone for this contraction argument is provided in `lean/MFGContraction.lean`; it does not attempt to formalize the full stochastic propagation-of-chaos theorem.

4 Main Results

4.1 Static Benchmark: Price Sensitivity and Overconfidence

The closed-form static price (5) yields explicit comparative statics with respect to overconfidence.

Proposition 4.1 (Static price response increases with overconfidence)**.** *Let* $\tau_{v,0} := 1/\sigma_{v,0}^2$ *and* $\tau'_{\epsilon,0} := k/\sigma_{\epsilon,0}^2$. *In the static benchmark, the coefficient on* v *in* (5) *is*

$$a(k) = \frac{\lambda \tau'_{\epsilon,0}}{\gamma + \lambda(\tau_{v,0} + \tau'_{\epsilon,0})}, \tag{28}$$

which is increasing in k *and satisfies* $0 < a(k) < 1$.

[2] Outputs and plots can be regenerated by running the script.

4.2 Myopic Trading Rule and Mean-Field Consistency

Next, a checkable *myopic* inventory rule is derived for the discrete-time timing in Subsubsection 2.3.3. Fix a decision interval Δt and treat the mean trading rate $\bar{u}_t$ and the public price p_t as given. For tractability, belief updating (Appendix A) conditions only on the private signal ξ_i; incorporating endogenous prices as an additional observation channel would require joint filtering and a richer fixed-point formulation. Conditional on the investor's information $\mathcal{F}_t^i$, the one-step price increment $\Delta p_{t+\Delta t}$ is Gaussian with conditional mean $(\kappa(\hat{v}_{i,t} - p_t) + \lambda \bar{u}_t)\Delta t$ and conditional variance $\sigma_{p,i,t}^2 \Delta t$.

Proposition 4.2 (Myopic CARAinventory choice with holding cost and flow impact)**.** *Fix a decision interval Δt. Suppose conditional on $\mathcal{F}_t^i$ the price increment is Gaussian with $\mathbb{E}_i[\Delta p_{t+\Delta t}] = (\kappa(\hat{v}_{i,t} - p_t) + \lambda \bar{u}_t)\Delta t$ and $Var_i(\Delta p_{t+\Delta t}) = \sigma_{p,i,t}^2 \Delta t$. With one-step wealth $\Delta W_{i,t} = x_{i,t}\Delta p_{t+\Delta t} - (\chi/2)x_{i,t}^2 \Delta t$ and CARAutility, the unique maximizer is*

$$x_{i,t}^\star = \frac{\kappa(\hat{v}_{i,t} - p_t) + \lambda \bar{u}_t}{\chi + \gamma\, \sigma_{p,i,t}^2}. \tag{29}$$

Define the corresponding *mispricing gain* (shares per unit price) as the coefficient on $(\hat{v}_{i,t} - p_t)$ in (29). Under the Euler increment (8) over Δt and conditioning on $\mathcal{F}_t^i$, $\sigma_{p,i,t}^2 = \phi^2 + \kappa^2 \Sigma_{i,t} \Delta t$, so

$$\Theta_t(\Sigma_{i,t}) := \frac{\kappa}{\chi + \gamma\, \sigma_{p,i,t}^2} = \frac{\kappa}{\chi + \gamma\big(\phi^2 + \kappa^2 \Sigma_{i,t} \Delta t\big)}. \tag{30}$$

Moreover,

$$\partial_\Sigma \Theta_t(\Sigma) = -\frac{\gamma \kappa^3 \Delta t}{\big(\chi + \gamma(\phi^2 + \kappa^2 \Sigma \Delta t)\big)^2} \leq 0,$$

so Θ_t is weakly decreasing in Σ.

Position-impact benchmark (reduced form; not used in baseline simulations). If one collapses stock and flow (so $\bar{u}_t \equiv \bar{x}_t$) and sets $\chi = 0$ and $\sigma_{p,i,t}^2 \equiv \phi^2$, then averaging (29) yields the familiar homogeneous closure (assuming $\gamma\phi^2 > \lambda$):

$$\bar{x}_t = \frac{\kappa}{\gamma\phi^2 - \lambda}\,(m_t - p_t), \tag{31}$$

where $m_t := \int_0^1 \hat{v}_{i,t}\, di$ is the mean belief. This reduced form is retained only as a transparent diagnostic benchmark; the baseline simulations solve the discrete-time stock–flow fixed point with inventory carryover and uniqueness condition $0 \leq B_t^{\text{sf}} < \Delta t$ (Proposition 4.5 and Theorem 4.6).

4.3 Exact continuous-time CARA/LQG control with filtering and mean-field coupling

This subsection replaces the infinitesimal-horizon (myopic) CARA rule with the finite-horizon continuous-time exponential-utility optimum under partial information. This subsection keeps the same fundamental/signal/price dynamics (32)–(34) and the same Kalman–Bucy filtering structure for subjective beliefs.

Dynamics and information. Let the fundamental and price evolve as

$$dv_t = \mu_v\,dt + \sigma_v\,dW_t, \tag{32}$$
$$d\xi_{i,t} = v_t\,dt + \sigma_c\,dU_t + \sigma_\epsilon\,dB_{i,t}, \tag{33}$$
$$dp_t = \kappa\,(v_t - p_t)\,dt + \lambda\,\bar{u}_t\,dt + \phi\,dZ_t, \tag{34}$$

where $\bar{u}_t := \int_0^1 u_{j,t}\,dj$ is the mean-field trading rate (taken as exogenous by an infinitesimal agent). Agent i observes $(p_s, \xi_{i,s})_{s\le t}$ and forms a subjective filtered estimate $\hat{v}_{i,t}$.

Subjective Kalman filter (with overconfidence). As in Appendix A, agent i runs a (possibly misspecified) Kalman–Bucy filter

$$\begin{aligned} d\hat{v}_{i,t} &= \mu_v\,dt + K_t^{(i)}\big(d\xi_{i,t} - \hat{v}_{i,t}\,dt\big), \\ K_t^{(i)} &:= \frac{\Sigma_t^{(i)}}{R'}, \qquad R' := \sigma_c^2 + \frac{\sigma_\epsilon^2}{k}, \end{aligned} \tag{35}$$

with Riccati equation

$$\dot{\Sigma}_t^{(i)} \;=\; \sigma_v^2 - \frac{(\Sigma_t^{(i)})^2}{R'}, \qquad \Sigma_0^{(i)} \ge 0. \tag{36}$$

(When convenient, one may use the constant-gain approximation $K_t^{(i)} \approx K^\star = \sigma_v/\sqrt{R'}$.)

Innovation form and reduced state. Define the (belief-based) mispricing state

$$y_{i,t} := \hat{v}_{i,t} - p_t. \tag{37}$$

Under the agent's filtration, write the observed price in innovations form

$$dp_t \;=\; \big[\kappa\,y_{i,t} + \lambda\,\bar{u}_t\big]dt \;+\; \phi\,dI_{i,t}^p, \tag{38}$$

where I_i^p is a Brownian motion (price innovation).

Objective innovation and misspecified residual. Let $(\Omega, \mathcal{F}, \{\mathcal{F}_t\}, P)$ denote the physical probability space. Define the objective conditional mean

$$m_{i,t} := \mathbb{E}^P[v_t \mid \mathcal{F}_t^i].$$

The corresponding (normalized) objective innovation is

$$d\tilde{I}_{i,t}^\xi := \frac{d\xi_{i,t} - m_{i,t}\,dt}{\sqrt{\sigma_c^2 + \sigma_\epsilon^2}}.$$

Under P and the agent filtration $\{\mathcal{F}_t^i\}$, $\tilde{I}_i^\xi$ is a standard Brownian motion. When $k \neq 1$, the agent's filter state $\hat{v}_{i,t}$ is misspecified and generally differs from $m_{i,t}$. Define the deviation

$$\delta_{i,t} := \hat{v}_{i,t} - m_{i,t}.$$

Then the standardized residual based on $\hat{v}_{i,t}$ decomposes as

$$\frac{d\xi_{i,t} - \hat{v}_{i,t}\,dt}{\sqrt{\sigma_c^2 + \sigma_\epsilon^2}} = d\tilde{I}_{i,t}^\xi - \frac{\delta_{i,t}}{\sqrt{\sigma_c^2 + \sigma_\epsilon^2}}\,dt,$$

so it coincides with a Brownian innovation only in the correctly specified case $k = 1$ (when $\delta_{i,t} \equiv 0$). For notational simplicity, set $I^{\xi}_{i,t} := \tilde{I}^{\xi}_{i,t}$ in what follows.

Consequently, the controlled wealth and the state satisfy

$$dW_{i,t} = x_{i,t}\, dp_t \;=\; x_{i,t}\big[\kappa\, y_{i,t} + \lambda\, \bar{u}_t\big]dt + x_{i,t}\phi\, dI^{p}_{i,t}, \tag{39}$$

$$dy_{i,t} = \big[\mu_v - \kappa\, y_{i,t} - \lambda\, \bar{u}_t\big]dt + \beta^{(i)}_t\, dI^{\xi}_{i,t} \;-\; \phi\, dI^{p}_{i,t}, \tag{40}$$

where I^{ξ}_i is the objective signal-innovation Brownian motion (defined above), independent of the price innovation I^{p}_i, and the (subjective) unhedgeable belief-noise loading is

$$\beta^{(i)}_t \;:=\; K^{(i)}_t \sqrt{\sigma_c^2 + \sigma_\epsilon^2}. \tag{41}$$

Note that $K^{(i)}_t$ depends on the perceived measurement-noise variance $R'(k)$, whereas the innovation volatility factor $\sqrt{\sigma_c^2 + \sigma_\epsilon^2}$ reflects the true signal-noise variance in $d\xi_{i,t}$.

Using the decomposition above, the diffusion term in (35) is $\beta^{(i)}_t\, dI^{\xi}_{i,t}$ with I^{ξ} the objective innovation; overconfidence affects only $K^{(i)}_t$ (through $R'(k)$).

(Under constant gain, $\beta^{(i)}_t \approx \beta^{\star} = K^{\star}\sqrt{\sigma_c^2 + \sigma_\epsilon^2}$ is constant.)

Diffusions entering the HJB. In the innovation representation (39)–(40), the controlled state is $(W_{i,t}, y_{i,t})$ and is driven by two independent Brownian motions: the *price innovation* I^{p}_i with volatility ϕ and the *filter innovation* I^{ξ}_i with volatility $\beta^{(i)}_t$. The HJB is written under the physical measure P using the objective innovation Brownian motions $(I^{p}_i, \tilde{I}^{\xi}_i)$; misspecification enters only through the gain $K^{(i)}_t$ (computed from the perceived variance $R'(k)$), while the factor $\sqrt{\sigma_c^2 + \sigma_\epsilon^2}$ is the true signal-noise volatility. Consequently, the HJB/Itô generator contains the variance terms $\frac{1}{2}x^2_{i,t}\phi^2 V_{ww}$ and $\frac{1}{2}\big((\beta^{(i)}_t)^2 + \phi^2\big)V_{yy}$. Moreover, because the same $dI^{p}_{i,t}$ appears in both $dW_{i,t}$ and $dy_{i,t}$, the cross-variation is $d\langle W_i, y_i\rangle_t = -x_{i,t}\phi^2\, dt$, which produces the mixed derivative term $-x_{i,t}\phi^2 V_{wy}$ in the HJB and is exactly the source of the intertemporal hedging correction in (48).

Control objective. Agent i maximizes exponential utility of terminal wealth:

$$\sup_{x_i \in \mathcal{A}} \mathbb{E}\Big[-\exp\big(-\gamma_i W_{i,T}\big)\,\Big|\,\mathcal{F}^{i}_t\Big], \tag{42}$$

over admissible progressively measurable controls $\mathcal{A}$ with $\mathbb{E}\int_0^T x^2_{i,t}\, dt < \infty$.

Exact CARA/LQG solution (finite horizon).

Proposition 4.3 (Exponential-quadratic value and optimal feedback)**.** *Fix a mean-field trading-rate process $(\bar{u}_t)_{t\in[0,T]}$. The value function admits the exponential-quadratic form*

$$V_i(t, w, y) \;=\; -\exp\!\left(-\gamma_i w - \frac{1}{2}A^{(i)}_t y^2 - B^{(i)}_t y - C^{(i)}_t\right), \tag{43}$$

where $(A^{(i)}_t, B^{(i)}_t, C^{(i)}_t)$ solve the backward ODE system with terminal conditions $A^{(i)}_T = B^{(i)}_T =$

$C_T^{(i)} = 0$:

$$-\dot{A}_t^{(i)} = \frac{\kappa^2}{\phi^2} - \big(\beta_t^{(i)}\big)^2\big(A_t^{(i)}\big)^2, \tag{44}$$

$$-\dot{B}_t^{(i)} = \frac{\kappa\lambda}{\phi^2}\,\bar{u}_t \;+\; \mu_v\, A_t^{(i)} \;-\; \big(\beta_t^{(i)}\big)^2 A_t^{(i)} B_t^{(i)}, \tag{45}$$

$$-\dot{C}_t^{(i)} = \frac{1}{2}\Big(\big((\beta_t^{(i)})^2 + \phi^2\big)A_t^{(i)} - (\beta_t^{(i)})^2\big(B_t^{(i)}\big)^2\Big) \tag{46}$$

$$+\,\mu_v B_t^{(i)} + \frac{\lambda^2}{2\phi^2}\bar{u}_t^2. \tag{47}$$

The optimal control is the affine feedback

$$x_{i,t}^{\star} \;=\; \frac{\kappa\, y_{i,t} + \lambda\,\bar{u}_t}{\gamma_i \phi^2} \;+\; \frac{A_t^{(i)} y_{i,t} + B_t^{(i)}}{\gamma_i}. \tag{48}$$

The first term is the myopic (instantaneous) demand. The second term is an intertemporal hedging correction induced by the correlation between the state $y_{i,t}$ and traded return noise in (40).

Constant-gain closed form (tight approximation). Under the constant-gain approximation $K_t^{(i)} \approx K^\star$ so that $\beta_t^{(i)} \approx \beta^\star$ is constant, (44) has the explicit solution

$$\begin{aligned} A_t^{(i)} &\approx \frac{\kappa}{\phi\,\beta^\star}\,\tanh\!\left(\frac{\kappa\,\beta^\star}{\phi}(T-t)\right), \\ \beta^\star &:= K^\star\sqrt{\sigma_c^2 + \sigma_\epsilon^2}, \\ K^\star &:= \frac{\sigma_v}{\sqrt{\sigma_c^2 + \sigma_\epsilon^2/k}}. \end{aligned} \tag{49}$$

The remaining $(B_t^{(i)}, C_t^{(i)})$ follow from linear ODEs once $\bar{u}_t$ is specified.

Mean-field consistency. With flow-based impact, the endogenous mean-field object is the trading rate $\bar{u}_t$ rather than the inventory $\bar{x}_t$. Closing the loop therefore requires an explicit link between inventory adjustments and trading rates; Subsection 2.3.3 fixes the discrete-time timing used in the baseline particle implementation, and Subsection 4.4 sketches a continuous-time flow-control extension.

4.4 Continuous-time CARA/LQG with inventory dynamics and quadratic trading costs (flow-control extension)

This subsection provides a continuous-time benchmark consistent with the stock–flow separation (inventory x versus trading rate u). It is included only as an extension and is not used in the baseline discrete-time simulations.

Let $u_{i,t}$ denote the agent's trading rate and let inventory evolve as

$$dx_{i,t} = u_{i,t}\,dt. \tag{50}$$

Under the innovation representation (Proposition 4.3), price evolves with flow-based impact,

$$dp_t = (\kappa y_{i,t} + \lambda\bar{u}_t)\,dt + \phi\,dI_{i,t}^p, \tag{51}$$

and wealth is augmented with quadratic trading and holding costs,

$$dW_{i,t} = x_{i,t}\,dp_t - \eta\,u_{i,t}^2\,dt - \frac{\chi}{2}x_{i,t}^2\,dt, \qquad \eta > 0,\ \chi > 0. \tag{52}$$

Consider the exponential-utility value function with state (w, x, y),

$$V(t, w, x, y) := \sup_{(u_s)_{s\in[t,T]}} \mathbb{E}\big[-\exp(-\gamma W_{i,T}) \mid (W_{i,t}, x_{i,t}, y_{i,t}) = (w, x, y)\big],$$

taking the mean-field path $\bar{u}_t$ as given. With the CARA ansatz

$$V(t, w, x, y) = -\exp\big(-\gamma(w + f(t, x, y))\big),$$

the HJB takes the standard risk-sensitive LQG form, and the control enters only through

$$\sup_u \big\{u\,\partial_x f(t, x, y) - \eta\,u^2\big\},$$

so the optimal trading rate is

$$u_{i,t}^\star = \frac{\partial_x f(t, x_{i,t}, y_{i,t})}{2\eta}. \tag{53}$$

Under a quadratic specification for $f(t, x, y)$, $\partial_x f$ is affine in (x, y) and hence $u_{i,t}^\star$ is linear in (x, y). Substituting the quadratic ansatz into the HJB yields a coupled system of Riccati ODEs for the quadratic coefficients and linear ODEs for the affine terms, with forcing that depends on the (given) mean-field flow $\bar{u}_t$; this is the usual LQG structure.

4.5 Level Amplification vs. Overconfidence Effects

In the baseline simulations, the calibration intentionally uses strong anchoring ($\kappa = 0.005$) and moderate impact ($\lambda = 0.20$), and the resulting k-treatment effect on mean absolute mispricing is modest ($|\Delta\mathbb{E}[|p - v|]| \approx 0.004$; Section 6.3). This subsection distinguishes two notions: (i) *level amplification*—large mispricing/volatility levels driven by weak anchoring and/or high noise trading; and (ii) *overconfidence (treatment) effects*—incremental differences when increasing k from 1 to 3. In the simulations of Section 6.3, stress regimes exhibit substantial level amplification, while k-effects on mispricing remain modest across the explored parameterizations. The following proposition gives an analytical mechanism for why k predominantly affects disagreement rather than mispricing.

Proposition 4.4 (Mechanism: mean-belief closure and why k shifts dispersion more than price)**.** *Within the myopic mean-field equilibrium (per-step stock–flow closure in Proposition 4.5):*

(i) ***Closure depends only on the mean belief.*** *The per-step fixed point for $(\bar{x}_t, \bar{u}_t)$ depends on the belief distribution only through cross-sectional averages of $\hat{v}_{i,t} - p_t$ (equivalently, the mean belief $m_t := \int_0^1 \hat{v}_{i,t}\,di$) and the predetermined pre-trade mean inventory $\bar{x}_{t^-}$. In particular, cross-sectional variance (disagreement) does not enter the mean-field fixed point except through the risk denominators $D_{i,t}$ (and in the homogeneous benchmark $D_{i,t}$ is common across agents). (In the particle implementation, the one-step myopic rule uses the effective variance $\mathrm{Var}_{i,t}^{\mathrm{eff}} = \phi^2 + \kappa^2\Sigma_{i,t}\Delta t$ (Proposition 4.5); in the homogeneous benchmark $\Sigma_{i,t}$ is common across agents, so this term only rescales $\bar{x}_t$ and does not introduce dependence on disagreement.)*

(ii) ***Decomposition of mispricing.*** *For additional closed-form intuition, under the reduced-form position-impact benchmark closure* (31) *(which collapses stock and flow), let* $y_t := p_t - v_t$ *(mispricing) and* $e_t := m_t - v_t$ *(mean-belief tracking error). Under the constant-gain approximation, the pair* (y_t, e_t) *satisfies the linear system* (65)*: mispricing dynamics are driven by (a)* microstructure regime (κ, λ, ϕ) *through the coefficient* $c := \lambda\kappa/(\gamma\phi^2 - \lambda)$ *and the mean-reversion rate* $\kappa + c$*; and (b) the* mean-belief term e_t*, which is the only channel through which the belief distribution affects price. Thus* $\mathbb{E}[|p - v|]$ *and stationary mispricing variance are determined by* (κ, λ, ϕ) *and the stationary law of* e_t*.*

(iii) ***Why*** k ***predominantly affects disagreement.*** *Under the information structure of Appendix A, each agent's belief has a common component (loading* $K^*(k)\sigma_c$ *on* dU_t*) and an idiosyncratic component (loading* $K^*(k)\sigma_\epsilon$ *on* $dB_{i,t}$*). The cross-sectional mean* m_t *aggregates beliefs, so the idiosyncratic components average out and* m_t *is driven only by the common noise and the fundamental. By Proposition 4.8, disagreement variance* $V_\infty^\delta(k) = Var(\hat{v}_{i,t} - m_t \mid \mathcal{F}^0)$ *is* strictly increasing *in* k*. By Proposition 4.9, the mean-belief error* $e_t = m_t - v_t$ *has stationary variance* $Var(e_\infty)$ *that depends on* k *only through* $K^*(k)$ *and is* strictly decreasing *in* k*. Hence incremental increases in* k *raise cross-sectional variance (disagreement) and trading intensity by construction, while the mean belief—and therefore equilibrium demand and mispricing—respond only weakly because they depend on* e_t*, whose variance is bounded and not uniformly amplified in* k*.*

Level amplification from market microstructure. In the simulations, weak anchoring ($\kappa < 0.002$) and/or high noise trading ($\phi > 0.75$) can generate large mispricing and volatility *levels* (e.g., $\mathbb{E}[|p - v|]$ exceeding 3–9 vs. ≈ 1.9 in baseline). This level amplification is primarily driven by (κ, ϕ) rather than the overconfidence parameter k: within stress cases, outcomes are nearly unchanged between $k = 1$ and $k = 3$ (Table 16).

Overconfidence effects: primarily on disagreement and trading intensity. In the simulations (baseline and stress calibrations), increasing k from 1 to 3 primarily increases cross-sectional disagreement ($\Delta\mathbb{E}[\sigma_i(\hat{v}_i)] \approx +0.059$) and trading intensity, while effects on mispricing levels remain modest ($|\Delta\mathbb{E}[|p - v|]| \approx 0.004$ in baseline, similarly small in stress cases). This contrast with the static benchmark is expected: in the static market-clearing price, perceived precision enters directly through the price coefficient $a(k)$ (Proposition 4.1), whereas in the anchored-impact dynamics the belief distribution affects price only through the cross-sectional mean belief m_t (Proposition 4.4). Under the reduced-form closure, mispricing $y_t := p_t - v_t$ and the mean-belief tracking error $e_t := m_t - v_t$ satisfy the 2D system (65), so k enters mispricing only through $K^*(k)$ and only via the coupling $c = \lambda\kappa/(\gamma\phi^2 - \lambda)$ (Proposition 4.10 and Corollary 4.11); if $c = 0$, y_t reduces to a univariate OU with $\mathrm{Var}(y_\infty) = (\phi^2 + \sigma_v^2)/(2\kappa)$, independent of k. Moreover, in the calibrations the belief-uncertainty contribution $\kappa^2\Sigma_{i,t}\Delta t$ is tiny relative to ϕ^2, so $D_{i,t} = \chi + \gamma(\phi^2 + \kappa^2\Sigma_{i,t}\Delta t)$ and hence the demand gains change only weakly with k (see Remark in Proposition 4.5).

Structural extensions (potential mechanisms). The model can be extended with structural mechanisms that could amplify mispricing persistence or volatility: (i) *State-dependent anchoring*: $\kappa(t) = \kappa_{\text{base}} \exp(-\alpha_\kappa |p_t - v_t|)$ weakens arbitrage pressure under extreme mispricing (limits to arbitrage); (ii) *Endogenous fundamental feedback*: $dv_t = \mu_v\, dt + \sigma_v\, dW_t + \beta_{\text{feedback}}(p_t - v_t)\, dt$ creates reflexive price–fundamental loops; (iii) *Overconfidence-dependent impact*: $\lambda_{\text{eff}} = \lambda_{\text{base}}(1 + \beta_\lambda(\bar{k}_t - 1))$ makes impact increase with aggregate overconfidence. These extensions are implemented in the codebase (Section 6.3) but are not the focus of the current numerical results, which demonstrate level amplification from (κ, ϕ) rather than k-driven amplification.

Scope and interpretation. Proposition 4.3 relies on the price-taking mean-field specification and on the simplification that belief updating conditions only on the private signal (Appendix A). The particle simulations implement a discrete-time mean-field consistent dynamics: at each step $(\bar{x}_t, \bar{u}_t)$ is computed from the scalar stock–flow fixed point in Proposition 4.5. In the baseline calibration the per-step contraction condition $0 \le B_t^{\mathrm{sf}} < \Delta t$ is verified along the simulated path (Theorem 4.6). Equation (31) is retained only as a transparent position-impact benchmark (not used in baseline simulations).

Remark (Contraction vs. existence). Since the per-step map is affine, a unique fixed point exists whenever $\Delta t - B_t^{\mathrm{sf}} \neq 0$ (Proposition 4.5). The contraction condition $0 \le B_t^{\mathrm{sf}} < \Delta t$ ensures stability of the per-step map (Theorem 4.6) and is the sufficient criterion used in the baseline calibration. When $B_t^{\mathrm{sf}} > \Delta t$, the fixed point remains well-defined but Φ_t is expanding and the fixed point is repelling under Picard iteration; results in that regime are interpreted as comparative statics rather than outcomes of a convergent per-step iteration.

Proposition 4.5 (Per-step fixed point in the particle implementation)**.** *In the discrete-time particle implementation, an effective variance is used*

$$\mathrm{Var}_{i,t}^{\mathrm{eff}} := \phi^2 + \kappa^2 \Sigma_{i,t}\, \Delta t, \tag{54}$$

i.e. the variance rate in Proposition 4.2 is instantiated as $\sigma_{p,i,t}^2 = \mathrm{Var}_{i,t}^{\mathrm{eff}}$, and define the effective risk/holding-cost term

$$D_{i,t} := \chi + \gamma\, \mathrm{Var}_{i,t}^{\mathrm{eff}}. \tag{55}$$

Remark (Scale). *Using the steady-state approximation $\Sigma_{i,t} \approx \Sigma^*(k) = \sigma_v \sqrt{R'(k)}$ (Lemma A.1) and $\Delta t = 1$, baseline parameters (Table 2) imply $\kappa^2 \Sigma^*(k) \Delta t / \phi^2 \approx 8.1 \times 10^{-6}$ for $k = 1$ and 4.7×10^{-6} for $k = 3$. In the "Weak+high" stress case of Table 16 ($\kappa = 0.001$, $\phi = 1.00$), the corresponding ratios are 8.1×10^{-8} and 4.7×10^{-8}. Thus $D_{i,t}$ is dominated by $\chi + \gamma\phi^2$ in the calibrations, so k-induced changes in $\Sigma_{i,t}$ barely move the demand gains through $D_{i,t}$. The myopic rule takes the linear form*

$$x_{i,t} = \frac{\alpha_0}{D_{i,t}} \Big(\kappa(\hat{v}_{i,t} - p_t) + \lambda \bar{u}_t \Big). \tag{56}$$

Remark (Normalization). *Since $\frac{\alpha_0}{\chi + \gamma V} = \frac{1}{(\chi/\alpha_0) + (\gamma/\alpha_0) V}$ (with $V = \mathrm{Var}_{i,t}^{\mathrm{eff}}$), one may normalize $\alpha_0 = 1$ without loss of generality provided (χ, γ) are treated as free parameters; if χ is treated as fixed, α_0 acts as an additional scale parameter. This form follows by applying Proposition 4.2 to the flow-based Euler increment $\Delta p_{t+1} := p_{t+1} - p_t = \kappa(v_t - p_t)\Delta t + \lambda \bar{u}_t \Delta t + \phi \sqrt{\Delta t}\, \varepsilon_{t+1}^{\eta}$: conditional on $\mathcal{F}_t^i$, the drift depends on $\hat{v}_{i,t}$ and the variance satisfies $Var_{i,t}(\Delta p_{t+1}) = \phi^2 \Delta t + \kappa^2 \Sigma_{i,t} (\Delta t)^2 = \mathrm{Var}_{i,t}^{\mathrm{eff}}\, \Delta t$. Hence the optimal one-step inventory depends on the effective variance rate $\mathrm{Var}_{i,t}^{\mathrm{eff}} = \phi^2 + \kappa^2 \Sigma_{i,t} \Delta t$. The scalar $\alpha_0 > 0$ is an optional position-size (risk-budget) scale (set to $\alpha_0 = 1$ in the baseline); when $\chi = 0$ it can be absorbed into a rescaling of γ (e.g., $\gamma \leftarrow \gamma/\alpha_0$), whereas for $\chi > 0$ absorbing α_0 requires a joint rescaling of (χ, γ) (see Remark (Normalization)). Define*

$$A_t^{\mathrm{sf}} := \frac{1}{N} \sum_{i=1}^{N} \frac{\alpha_0 \kappa (\hat{v}_{i,t} - p_t)}{D_{i,t}}, \qquad B_t^{\mathrm{sf}} := \frac{1}{N} \sum_{i=1}^{N} \frac{\alpha_0 \lambda}{D_{i,t}}.$$

Let $\bar{x}_{t^-} := \frac{1}{N} \sum_{i=1}^{N} x_{i,t^-}$ denote the pre-trade mean inventory and note that the mean trading rate satisfies $\bar{u}_t = (\bar{x}_t - \bar{x}_{t^-})/\Delta t$. If $\Delta t - B_t^{\mathrm{sf}} \neq 0$, the scalar fixed point exists and is unique and is given by

$$\bar{x}_t = \frac{A_t^{\mathrm{sf}} - (B_t^{\mathrm{sf}}/\Delta t) \bar{x}_{t^-}}{1 - B_t^{\mathrm{sf}}/\Delta t}, \qquad \bar{u}_t = \frac{\bar{x}_t - \bar{x}_{t^-}}{\Delta t}. \tag{57}$$

Theorem 4.6 (Contraction and uniqueness of the per-step mean-field closure)**.** *Fix time t and treat the belief states $(\hat{v}_{i,t}, \Sigma_{i,t})$, the public price p_t, and the pre-trade mean inventory $\bar{x}_{t^-}$ as given. Define the affine mean-field map*

$$\Phi_t(\bar{x}) := A_t^{\mathrm{sf}} + \frac{B_t^{\mathrm{sf}}}{\Delta t}\bar{x} - \frac{B_t^{\mathrm{sf}}}{\Delta t}\bar{x}_{t^-}, \tag{58}$$

where $A_t^{\mathrm{sf}}, B_t^{\mathrm{sf}}$ are as in Proposition 4.5. Since Φ_t is affine with slope $B_t^{\mathrm{sf}}/\Delta t$, it has a unique fixed point whenever $B_t^{\mathrm{sf}} \neq \Delta t$. If additionally $0 \le B_t^{\mathrm{sf}} < \Delta t$, then Φ_t is a contraction on $\mathbb{R}$ with constant $B_t^{\mathrm{sf}}/\Delta t$. Moreover, since $\mathrm{Var}_{i,t}^{\mathrm{eff}} \ge \phi^2$ and $D_{i,t} \ge \chi + \gamma\phi^2$, a simple sufficient condition ensuring $B_t^{\mathrm{sf}} < \Delta t$ uniformly is

$$\frac{\alpha_0 \lambda}{\Delta t\,(\chi + \gamma\phi^2)} < 1. \tag{59}$$

Remark (Time-step refinement). *If α_0 is interpreted as a per-unit-time risk budget, then under grid refinement set $\alpha_0(\Delta t) = \alpha_0\,\Delta t$. In that convention, the sufficient proxy in (59) becomes $\alpha_0\lambda/(\chi + \gamma\phi^2) < 1$, i.e. it is invariant to Δt. In the homogeneous case $D_{i,t} \equiv D_t$, one has $B_t^{\mathrm{sf}} = \alpha_0\lambda/D_t$, so $0 \le B_t^{\mathrm{sf}} < \Delta t$ is equivalent to $D_t > \alpha_0\lambda/\Delta t$, i.e. $\chi + \gamma\,\mathrm{Var}_t^{\mathrm{eff}} > \alpha_0\lambda/\Delta t$.*

Proposition 4.7 (Closed-loop stability in a homogeneous benchmark)**.** *Assume the homogeneous closure (31) holds and, for this benchmark calculation, that the mean belief tracks the fundamental ($m_t = v_t$). Then the mispricing $y_t := p_t - v_t$ satisfies the linear SDE*

$$\begin{aligned} dy_t &= -\kappa_{\mathrm{eff}}\, y_t\, dt - \mu_v\, dt + \phi\, dZ_t - \sigma_v\, dW_t, \\ \kappa_{\mathrm{eff}} &:= \kappa\,\frac{\gamma\phi^2}{\gamma\phi^2 - \lambda}. \end{aligned} \tag{60}$$

In particular, if $\gamma\phi^2 > \lambda$ then $\kappa_{\mathrm{eff}} > 0$ and y_t is mean-reverting (Ornstein–Uhlenbeck). If additionally $\mu_v = 0$, the stationary variance is $Var(y_\infty) = (\phi^2 + \sigma_v^2)/(2\kappa_{\mathrm{eff}})$.

4.6 Uniqueness and Stability Conditions (Multiplicity and Blow-Ups)

The following conditions rule out multiple equilibria and blow-ups. **Continuous-time LQG map Φ** (position-impact benchmark; Section 3.7): if $\gamma\phi^2 > \lambda$ (positive denominator) and $q < 1$, then Φ is a contraction on $(\mathcal{X}, \|\cdot\|_2)$, so the fixed point is unique and Picard iteration does not blow up (see Proposition 3.7). **Discrete-time per-step (baseline stock–flow):** if $0 \le B_t^{\mathrm{sf}} < \Delta t$, the scalar stock–flow fixed point for $(\bar{x}_t, \bar{u}_t)$ is unique (Proposition 4.5); a sufficient uniform condition is (59) (see Theorem 4.6). **Closed-loop paths (mispricing OU benchmark):** under the position-impact benchmark closure (31), if $\gamma\phi^2 > \lambda$ then $\kappa_{\mathrm{eff}} > 0$ and mispricing is mean-reverting (Proposition 4.7). **Black-box MFG limit (benchmark):** under (H1)–(H5), the equilibrium flow is unique and $\bar{\mu}_t^N$ converges to μ_t at rate $O(1/N)$ (see Proposition 3.5 in the mean-field limit subsection).

4.7 Option B: Stationary Moments With Explicit k-Dependence

This subsection is a diagnostic benchmark built on the reduced-form position-impact closure (31); the baseline simulations use the discrete-time stock–flow equilibrium with uniqueness condition $0 \le B_t^{\mathrm{sf}} < \Delta t$ (Proposition 4.5, Theorem 4.6).

Proposition 4.7 provides a transparent OU benchmark for mispricing, but it removes the overconfidence channel by imposing $m_t = v_t$. The paper now records complementary stationary-moment calculations in which k enters explicitly through the steady-state filtering gain (Appendix A). Lemma A.1 shows that the perceived Riccati equation converges exponentially to

the steady state, motivating the constant-gain approximation used below (interpretable as an asymptotic stationary regime after burn-in).

Proposition 4.8 (Stationary disagreement and monotonicity in k (constant-gain approximation)). *Assume a homogeneous overconfidence type k and approximate the Kalman–Bucy gain by its steady-state value $K^*(k) = \sigma_v/\sqrt{R'(k)}$, where $R'(k) = \sigma_c^2 + \sigma_\epsilon^2/k$ (Appendix A). Let $m_t := \int_0^1 \hat{v}_{i,t}\, di$ and define the cross-sectional deviation $\tilde{\delta}_{i,t} := \hat{v}_{i,t} - m_t$. Conditioning on the common filtration $\mathcal{F}_t^0$, the deviations satisfy the OU dynamics*

$$d\tilde{\delta}_{i,t} = -K^*(k)\,\tilde{\delta}_{i,t}\,dt + K^*(k)\sigma_\epsilon\,dB_{i,t}. \tag{61}$$

Consequently, the conditional disagreement variance $V_t^\delta := Var(\hat{v}_{i,t} \mid \mathcal{F}_t^0) = Var(\tilde{\delta}_{i,t} \mid \mathcal{F}_t^0)$ admits the stationary value

$$V_\infty^\delta(k) = \frac{K^*(k)\sigma_\epsilon^2}{2} = \frac{\sigma_v\sigma_\epsilon^2}{2\sqrt{\sigma_c^2 + \sigma_\epsilon^2/k}}, \tag{62}$$

which is strictly increasing in k.

Proposition 4.9 (Stationary mean-belief tracking error (constant-gain approximation)). *Under the same constant-gain approximation, define the mean-belief tracking error $e_t := m_t - v_t$. Then*

$$de_t = -K^*(k)\,e_t\,dt + K^*(k)\sigma_c\,dU_t - \sigma_v\,dW_t, \tag{63}$$

and the stationary variance is

$$Var(e_\infty) = \frac{(K^*(k))^2\sigma_c^2 + \sigma_v^2}{2K^*(k)} = \frac{K^*(k)\sigma_c^2}{2} + \frac{\sigma_v^2}{2K^*(k)}. \tag{64}$$

In particular, k enters the stationary tracking quality through $K^*(k)$ and $Var(e_\infty)$ is strictly decreasing in k (and converges to $\sigma_v\sigma_c$ as $k \to \infty$ when $\sigma_c > 0$).

Proposition 4.10 (Stationary mispricing with belief feedback (2D OU / Lyapunov form)). *Assume $\mu_v = 0$ and use the homogeneous closure (31). Under the constant-gain approximation above, the pair (y_t, e_t) with $y_t := p_t - v_t$ satisfies the linear system*

$$\begin{aligned} dy_t &= -(\kappa + c)\,y_t\,dt + c\,e_t\,dt + \phi\,dZ_t - \sigma_v\,dW_t, \\ de_t &= -K^*(k)\,e_t\,dt + K^*(k)\sigma_c\,dU_t - \sigma_v\,dW_t, \end{aligned} \tag{65}$$

where $c := \lambda\kappa/(\gamma\phi^2 - \lambda)$. If $\gamma\phi^2 > \lambda$ and $K^*(k) > 0$, then the drift matrix

$$A(k) := \begin{bmatrix} -(\kappa + c) & c \\ 0 & -K^*(k) \end{bmatrix}$$

is Hurwitz and the stationary covariance $P(k) = \mathbb{E}[X_\infty X_\infty^\top]$ for $X_t = (y_t, e_t)$ is the unique solution of the Lyapunov equation

$$A(k)P(k) + P(k)A(k)^\top + Q(k) = 0, \tag{66}$$

where $Q(k)$ is the diffusion covariance implied by (65). Thus $Var(y_\infty)$ depends on k explicitly through $K^*(k)$.

Corollary 4.11 (Closed-form stationary variances for Proposition 4.10). *In the setting of Proposition 4.10, write $K := K^*(k)$ and define the noise covariances $q_{11} := \phi^2 + \sigma_v^2$, $q_{12} := \sigma_v^2$, and*

$q_{22} := K^2\sigma_c^2 + \sigma_v^2$. *Then the Lyapunov equation* (66) *has the explicit solution* $P = \begin{pmatrix} p_{11} & p_{12} \\ p_{12} & p_{22} \end{pmatrix}$ *with*

$$\begin{aligned} p_{22} &= \frac{q_{22}}{2K} = \frac{K\sigma_c^2}{2} + \frac{\sigma_v^2}{2K}, \\ p_{12} &= \frac{c\,p_{22} + q_{12}}{\kappa + c + K}, \\ p_{11} &= \frac{c\,p_{12} + q_{11}/2}{\kappa + c}. \end{aligned} \tag{67}$$

In particular, $Var(y_\infty) = p_{11}$ *depends on* k *through* $K^*(k)$.

4.8 Connection to Numerical Results

Section VI simulates a large-N particle system implementing (8), Kalman belief updates (Appendix A), and the feedback policy (29) (implemented in discrete time with an effective variance that includes belief uncertainty). Overconfidence enters only through belief updating (misperceived signal precision), and the paper reports price/mispricing/volatility statistics across bull/bear drifts μ_v and overconfidence levels k.

5 PROOFS

Proof of Proposition 4.1

Proof. From the static price equation (5), the coefficient on v is

$$a(k) = \frac{\lambda\tau'_{\epsilon,0}}{\gamma + \lambda(\tau_{v,0} + \tau'_{\epsilon,0})}, \qquad \tau'_{\epsilon,0} = \frac{k}{\sigma^2_{\epsilon,0}}, \quad \tau_{v,0} = \frac{1}{\sigma^2_{v,0}}.$$

Set $u := \tau'_{\epsilon,0} > 0$ and define $f(u) := \frac{\lambda u}{\gamma + \lambda(\tau_{v,0}+u)}$. Then $a(k) = f(\tau'_{\epsilon,0})$ and

$$f'(u) = \frac{\lambda(\gamma + \lambda\tau_{v,0})}{\big(\gamma + \lambda(\tau_{v,0} + u)\big)^2} > 0,$$

so f is strictly increasing in u, hence $a(k)$ is strictly increasing in k. Moreover, $a(k) > 0$ is immediate since all parameters are positive, and

$$a(k) < 1 \iff \lambda u < \gamma + \lambda(\tau_{v,0} + u) \iff 0 < \gamma + \lambda\tau_{v,0},$$

which holds. Thus $0 < a(k) < 1$ and $a(k)$ increases with k. □

Proof of Proposition 4.2

Proof. Fix a decision interval Δt and condition on $\mathcal{F}_t^i$. By the proposition's assumptions, $\Delta p_{t+\Delta t}$ is Gaussian with

$$\mu_{i,t} := \mathbb{E}_i[\Delta p_{t+\Delta t}] = \big(\kappa(\hat{v}_{i,t} - p_t) + \lambda\bar{u}_t\big)\Delta t, \qquad \mathrm{Var}_i(\Delta p_{t+\Delta t}) = \sigma^2_{p,i,t}\Delta t.$$

The one-step wealth increment is

$$\Delta W_{i,t} = x_{i,t}\Delta p_{t+\Delta t} - \frac{\chi}{2}x^2_{i,t}\Delta t,$$

hence $\Delta W_{i,t}$ is Gaussian conditional on $\mathcal{F}_t^i$ with

$$\mathbb{E}_i[\Delta W_{i,t}] = x_{i,t}\mu_{i,t} - \frac{\chi}{2}x_{i,t}^2\Delta t, \qquad \mathrm{Var}_i(\Delta W_{i,t}) = x_{i,t}^2\sigma_{p,i,t}^2\Delta t.$$

For CARA utility $U(w) = -e^{-\gamma w}$ and Gaussian $X \sim N(m, s^2)$, the standard identity gives $\mathbb{E}[-e^{-\gamma X}] = -\exp(-\gamma m + (\gamma^2/2)s^2)$. Applying this with $X = W_{i,t} + \Delta W_{i,t}$ (where $W_{i,t}$ is $\mathcal{F}_t^i$-measurable), maximizing conditional expected utility over $x_{i,t}$ is equivalent to maximizing the certainty-equivalent quadratic

$$x_{i,t}\mu_{i,t} - \frac{\gamma}{2}x_{i,t}^2\sigma_{p,i,t}^2\Delta t - \frac{\chi}{2}x_{i,t}^2\Delta t.$$

The first-order condition yields $\mu_{i,t} - (\gamma\sigma_{p,i,t}^2 + \chi)x_{i,t}\Delta t = 0$, so

$$x_{i,t}^\star = \frac{\mu_{i,t}/\Delta t}{\chi + \gamma\sigma_{p,i,t}^2} = \frac{\kappa(\hat{v}_{i,t} - p_t) + \lambda\bar{u}_t}{\chi + \gamma\sigma_{p,i,t}^2},$$

which is (29). □

Proof of Proposition 4.5

Proof. Work on the discrete grid with step Δt and the Euler increment

$$\begin{aligned}\Delta p_{t+1} := p_{t+1} - p_t &= \kappa(v_t - p_t)\Delta t + \lambda\bar{u}_t\Delta t \\ &\quad + \phi\sqrt{\Delta t}\,\varepsilon_{t+1}^\eta, \\ \varepsilon_{t+1}^\eta &:= \frac{Z_{t+\Delta t} - Z_t}{\sqrt{\Delta t}} \sim N(0,1).\end{aligned}$$

Conditional on investor i's information $\mathcal{F}_t^i$, one has $\mathbb{E}[v_t \mid \mathcal{F}_t^i] = \hat{v}_{i,t}$ and $\mathrm{Var}(v_t \mid \mathcal{F}_t^i) = \Sigma_{i,t}$. Hence

$$\mathbb{E}[\Delta p_{t+1} \mid \mathcal{F}_t^i] = \big(\kappa(\hat{v}_{i,t} - p_t) + \lambda\bar{u}_t\big)\Delta t,$$

and, using independence of ε_{t+1}^η from $\mathcal{F}_t^i$ and from v_t,

$$\begin{aligned}\mathrm{Var}(\Delta p_{t+1} \mid \mathcal{F}_t^i) &= \kappa^2\,\mathrm{Var}(v_t \mid \mathcal{F}_t^i)(\Delta t)^2 + \phi^2\Delta t \\ &= \kappa^2\Sigma_{i,t}(\Delta t)^2 + \phi^2\Delta t.\end{aligned}$$

Under the one-step myopic CARA approximation (Proposition 4.2), the investor chooses $x_{i,t}$ to maximize the certainty-equivalent quadratic

$$x_{i,t}\,\mathbb{E}[\Delta p_{t+1} \mid \mathcal{F}_t^i] - \frac{\gamma}{2}x_{i,t}^2\,\mathrm{Var}(\Delta p_{t+1} \mid \mathcal{F}_t^i) - \frac{\chi}{2}x_{i,t}^2\,\Delta t.$$

Substituting the conditional moments above and dividing by the common factor $\Delta t > 0$ gives the equivalent problem

$$\max_{x_{i,t}}\; x_{i,t}\big(\kappa(\hat{v}_{i,t} - p_t) + \lambda\bar{u}_t\big) - \frac{1}{2}\Big(\gamma\big(\phi^2 + \kappa^2\Sigma_{i,t}\Delta t\big) + \chi\Big)x_{i,t}^2.$$

The unique maximizer is

$$x_{i,t}^* = \frac{\kappa(\hat{v}_{i,t} - p_t) + \lambda\bar{u}_t}{\chi + \gamma(\phi^2 + \kappa^2\Sigma_{i,t}\Delta t)}.$$

Including the optional scale $\alpha_0 > 0$ (risk-budget/position-size parameter) yields (56) with

$$\mathrm{Var}_{i,t}^{\mathrm{eff}} := \phi^2 + \kappa^2\Sigma_{i,t}\Delta t,$$

Write (56) as $x_{i,t} = a_{i,t} + b_{i,t}\bar{u}_t$ with

$$a_{i,t} := \frac{\alpha_0\kappa(\hat{v}_{i,t} - p_t)}{\chi + \gamma \mathrm{Var}_{i,t}^{\mathrm{eff}}}, \qquad b_{i,t} := \frac{\alpha_0\lambda}{\chi + \gamma \mathrm{Var}_{i,t}^{\mathrm{eff}}}.$$

Averaging over $i = 1, \ldots, N$ gives $\bar{x}_t = A_t^{\mathrm{sf}} + B_t^{\mathrm{sf}}\bar{u}_t$ where $A_t^{\mathrm{sf}}, B_t^{\mathrm{sf}}$ are as defined in the paper. Using $\bar{u}_t = (\bar{x}_t - \bar{x}_{t^-})/\Delta t$ gives

$$\bar{x}_t = A_t^{\mathrm{sf}} + \frac{B_t^{\mathrm{sf}}}{\Delta t}\bar{x}_t - \frac{B_t^{\mathrm{sf}}}{\Delta t}\bar{x}_{t^-}.$$

Rearranging yields $\big(1 - B_t^{\mathrm{sf}}/\Delta t\big)\bar{x}_t = A_t^{\mathrm{sf}} - (B_t^{\mathrm{sf}}/\Delta t)\bar{x}_{t^-}$. If $\Delta t - B_t^{\mathrm{sf}} \neq 0$, the unique solution is

$$\bar{x}_t = \frac{A_t^{\mathrm{sf}} - (B_t^{\mathrm{sf}}/\Delta t)\bar{x}_{t^-}}{1 - B_t^{\mathrm{sf}}/\Delta t}, \qquad \bar{u}_t = \frac{\bar{x}_t - \bar{x}_{t^-}}{\Delta t},$$

as claimed. □

Proof of Theorem 4.6

Proof. By Proposition 4.5, for fixed $(\hat{v}_{i,t}, \Sigma_{i,t})_{i=1}^N$, p_t, and $\bar{x}_{t^-}$, the per-step map is affine:

$$\Phi_t(\bar{x}) = A_t^{\mathrm{sf}} + \frac{B_t^{\mathrm{sf}}}{\Delta t}\bar{x} - \frac{B_t^{\mathrm{sf}}}{\Delta t}\bar{x}_{t^-}.$$

For any $\bar{x}, \bar{x}'$,

$$|\Phi_t(\bar{x}) - \Phi_t(\bar{x}')| = \frac{|B_t^{\mathrm{sf}}|}{\Delta t}\,|\bar{x} - \bar{x}'|.$$

Thus if $0 \le B_t^{\mathrm{sf}} < \Delta t$, Φ_t is a contraction on $\mathbb{R}$ with contraction constant $B_t^{\mathrm{sf}}/\Delta t$ and has a unique fixed point, given in closed form in Proposition 4.5.

For the sufficient uniform condition: since $\Sigma_{i,t} \ge 0$ and $\Delta t > 0$, one has $\mathrm{Var}_{i,t}^{\mathrm{eff}} = \phi^2 + \kappa^2\Sigma_{i,t}\Delta t \ge \phi^2$, hence $D_{i,t} = \chi + \gamma\mathrm{Var}_{i,t}^{\mathrm{eff}} \ge \chi + \gamma\phi^2$ and therefore

$$B_t^{\mathrm{sf}} = \frac{1}{N}\sum_{i=1}^N \frac{\alpha_0\lambda}{D_{i,t}} \le \frac{1}{N}\sum_{i=1}^N \frac{\alpha_0\lambda}{\chi + \gamma\phi^2} = \frac{\alpha_0\lambda}{\chi + \gamma\phi^2}.$$

Therefore $\alpha_0\lambda/(\Delta t(\chi + \gamma\phi^2)) < 1$ implies $B_t^{\mathrm{sf}} < \Delta t$ for all t. □

Proof of Theorem 3.1 (Well-posedness of the discrete-time particle system)

Proof. Fix $T \in \mathbb{N}$, $\Delta t > 0$, and fix a realization of all common and idiosyncratic shock sequences used by the algorithm. It is shown by induction on $t = 0, 1, \ldots, T$ that the state

$$S_t = (v_t, p_t, \{(\hat{v}_{i,t}, \Sigma_{i,t})\}_{i=1}^N, \bar{x}_t)$$

is uniquely determined and adapted.

At $t = 0$, $(v_0, p_0, \{\hat{v}_{i,0}, \Sigma_{i,0}\}_{i=1}^N)$ are given by assumption (A1). Suppose the system is uniquely defined up to time t. Then:

1. By (A2), the discrete-time Kalman recursion in Appendix A defines each $(\hat{v}_{i,t}, \Sigma_{i,t})$ uniquely from $(\hat{v}_{i,t-1}, \Sigma_{i,t-1})$ and the realized private signal increment $z_{i,t}$ at time t (which is a measurable function of the fixed shock sequences and v_t).

2. Given $(\hat{v}_{i,t}, \Sigma_{i,t})_{i=1}^N$ and p_t, the per-step demand map Φ_t is well-defined by Proposition 4.5. By (A3) (e.g. $\Delta t - B_t^{\mathrm{sf}} \neq 0$), Φ_t has a unique fixed point $\bar{x}_t$ (and hence $\bar{u}_t$), and then each $x_{i,t}$ is uniquely determined.

3. Finally, by (A4), the Euler updates for v_{t+1} and p_{t+1} are explicit measurable functions of (v_t, p_t), $\bar{u}_t$, and the realized shocks at time $t+1$, hence define unique (v_{t+1}, p_{t+1}).

Thus S_{t+1} is uniquely determined from S_t and the fixed shocks, and is adapted to the natural filtration generated by the shocks. Induction completes the proof, yielding a unique adapted solution path on $\{0, 1, \ldots, T\}$. □

Proof of Proposition 4.8 (Constant-gain approximation)

Proof. Assume a homogeneous type k and adopt the constant-gain approximation $K_t \equiv K^*(k) =: K > 0$. From Appendix A, the (subjective) Kalman–Bucy filter is

$$d\hat{v}_{i,t} = \mu_v \, dt + K\big(d\xi_{i,t} - \hat{v}_{i,t} \, dt\big).$$

Using the observation equation (33),

$$d\xi_{i,t} = v_t \, dt + \sigma_c \, dU_t + \sigma_\epsilon \, dB_{i,t},$$

so substituting gives

$$\begin{aligned} d\hat{v}_{i,t} &= \mu_v \, dt + K\big((v_t - \hat{v}_{i,t}) \, dt + \sigma_c \, dU_t + \sigma_\epsilon \, dB_{i,t}\big) \\ &= \big(\mu_v + K(v_t - \hat{v}_{i,t})\big) \, dt + K\sigma_c \, dU_t + K\sigma_\epsilon \, dB_{i,t}. \end{aligned}$$

Let $m_t := \int_0^1 \hat{v}_{i,t} \, di$ be the cross-sectional mean belief. Under a continuum (or large-N) approximation, the idiosyncratic noises average out, i.e. $\int_0^1 dB_{i,t} \, di = 0$ in the sense of laws/LLN, while the common term U_t persists. Averaging the SDE over i yields

$$dm_t = \big(\mu_v + K(v_t - m_t)\big) \, dt + K\sigma_c \, dU_t.$$

Define the deviation $\tilde{\delta}_{i,t} := \hat{v}_{i,t} - m_t$. Subtracting the m_t equation from the $\hat{v}_{i,t}$ equation cancels the common-noise terms and gives

$$\begin{aligned} d\tilde{\delta}_{i,t} &= -K(\hat{v}_{i,t} - m_t) \, dt + K\sigma_\epsilon \, dB_{i,t} \\ &= -K\tilde{\delta}_{i,t} \, dt + K\sigma_\epsilon \, dB_{i,t}, \end{aligned}$$

which is (61).

Now condition on the common filtration $\mathcal{F}_t^0 := \sigma(W_s, U_s, Z_s : s \leq t)$. Conditional on $\mathcal{F}_t^0$, $\tilde{\delta}_{i,t}$ solves an OU SDE driven only by the idiosyncratic Brownian motion $B_{i,t}$, so its conditional variance $V_t^\delta := \mathrm{Var}(\tilde{\delta}_{i,t} \mid \mathcal{F}_t^0) = \mathbb{E}[\tilde{\delta}_{i,t}^2 \mid \mathcal{F}_t^0]$ satisfies (Itô + tower property)

$$\begin{aligned} d(\tilde{\delta}_{i,t}^2) &= 2\tilde{\delta}_{i,t} \, d\tilde{\delta}_{i,t} + (d\tilde{\delta}_{i,t})^2 \\ &= \big(-2K\tilde{\delta}_{i,t}^2 + K^2\sigma_\epsilon^2\big) \, dt + 2K\sigma_\epsilon\tilde{\delta}_{i,t} \, dB_{i,t}. \end{aligned}$$

Taking $\mathcal{F}_t^0$-conditional expectation kills the martingale term and yields the linear ODE

$$\frac{d}{dt} V_t^\delta = -2KV_t^\delta + K^2\sigma_\epsilon^2.$$

Hence $V_t^\delta \to V_\infty^\delta := \frac{K^2\sigma_\epsilon^2}{2K} = \frac{K\sigma_\epsilon^2}{2}$, giving (62).

Finally, with $R'(k) = \sigma_c^2 + \sigma_\epsilon^2/k$ one has $K^*(k) = \sigma_v/\sqrt{R'(k)}$, which is strictly increasing in k because $R'(k)$ is strictly decreasing in k; therefore $V_\infty^\delta(k) = (K^*(k)\sigma_\epsilon^2)/2$ is strictly increasing in k. □

Proof of Proposition 4.9 (Constant-gain approximation)

Proof. Under the constant-gain approximation (same setting as Proposition 4.8), the derivation gives

$$dm_t = \big(\mu_v + K(v_t - m_t)\big)\,dt + K\sigma_c\,dU_t.$$

The fundamental satisfies $dv_t = \mu_v\,dt + \sigma_v\,dW_t$. Define $e_t := m_t - v_t$. Then

$$\begin{aligned} de_t &= dm_t - dv_t \\ &= \big(\mu_v + K(v_t - m_t)\big)\,dt + K\sigma_c\,dU_t - \mu_v\,dt - \sigma_v\,dW_t \\ &= -Ke_t\,dt + K\sigma_c\,dU_t - \sigma_v\,dW_t, \end{aligned}$$

which is (63).

Since U and W are independent Brownian motions, e_t is an OU process with mean-reversion rate K and diffusion variance rate $K^2\sigma_c^2 + \sigma_v^2$. The stationary variance is the standard OU value

$$\mathrm{Var}(e_\infty) = \frac{K^2\sigma_c^2 + \sigma_v^2}{2K} = \frac{K\sigma_c^2}{2} + \frac{\sigma_v^2}{2K},$$

which is (64).

To see monotonicity in k, view $\mathrm{Var}(e_\infty)$ as a function of $K > 0$:

$$g(K) := \frac{K\sigma_c^2}{2} + \frac{\sigma_v^2}{2K}, \qquad g'(K) = \frac{\sigma_c^2}{2} - \frac{\sigma_v^2}{2K^2}.$$

If $\sigma_c = 0$, then $g(K) = \sigma_v^2/(2K)$ is strictly decreasing in K, and since $K^*(k)$ is strictly increasing in k, $\mathrm{Var}(e_\infty)$ is strictly decreasing in k. If $\sigma_c > 0$, then $g'(K) < 0$ on $K \in (0, \sigma_v/\sigma_c)$ and $K^*(k) = \sigma_v/\sqrt{R'(k)} \le \sigma_v/\sigma_c$ since $R'(k) = \sigma_c^2 + \sigma_\epsilon^2/k \ge \sigma_c^2$. Thus g is decreasing along the range of $K^*(k)$, so $\mathrm{Var}(e_\infty)$ is strictly decreasing in k. □

Proof of Proposition 4.10 (2D OU / Lyapunov form)

Proof. Assume $\mu_v = 0$ and the homogeneous closure (31):

$$\bar{x}_t = \frac{\kappa}{\gamma\phi^2 - \lambda}(m_t - p_t).$$

Write $y_t := p_t - v_t$ and $e_t := m_t - v_t$. Using $m_t - p_t = (m_t - v_t) - (p_t - v_t) = e_t - y_t$, the price SDE (8) becomes

$$\begin{aligned} dp_t &= \kappa(v_t - p_t)\,dt + \lambda\bar{x}_t\,dt + \phi\,dZ_t \\ &= -\kappa y_t\,dt + \frac{\lambda\kappa}{\gamma\phi^2 - \lambda}(e_t - y_t)\,dt + \phi\,dZ_t. \end{aligned}$$

Let $c := \lambda\kappa/(\gamma\phi^2 - \lambda)$. Then

$$dp_t = -(\kappa + c)y_t\,dt + ce_t\,dt + \phi\,dZ_t.$$

Since $\mu_v = 0$, $dv_t = \sigma_v\,dW_t$, hence

$$dy_t = dp_t - dv_t = -(\kappa + c)y_t\,dt + ce_t\,dt + \phi\,dZ_t - \sigma_v\,dW_t.$$

From Proposition 4.9, the mean-belief tracking error satisfies

$$de_t = -Ke_t\,dt + K\sigma_c\,dU_t - \sigma_v\,dW_t, \qquad K := K^*(k) > 0.$$

Stacking $X_t = (y_t, e_t)^\top$ yields the linear system (65) with drift matrix

$$A(k) = \begin{pmatrix} -(\kappa + c) & c \\ 0 & -K \end{pmatrix}$$

and diffusion matrix $G(k)$ as stated.

If $\gamma\phi^2 > \lambda$ then $c > 0$ and $\kappa + c > 0$; also $K > 0$ by definition. The eigenvalues of $A(k)$ are $-(\kappa+c)$ and $-K$, hence strictly negative: $A(k)$ is Hurwitz. For a Hurwitz A, the continuous-time Lyapunov equation

$$AP + PA^\top + GG^\top = 0$$

has a unique symmetric positive semidefinite solution P, which equals the stationary covariance $P = \mathbb{E}[X_\infty X_\infty^\top]$. This gives (66) and shows $\mathrm{Var}(y_\infty)$ depends on k through $K^*(k)$. □

Proof of Corollary 4.11 (Closed-form stationary variances)

Proof. Let $A = \begin{pmatrix} -(\kappa + c) & c \\ 0 & -K \end{pmatrix}$ and $Q := GG^\top$. Because dZ_t, dU_t, dW_t are independent, from (65) one has

$$Q = \begin{pmatrix} \phi^2 + \sigma_v^2 & \sigma_v^2 \\ \sigma_v^2 & K^2\sigma_c^2 + \sigma_v^2 \end{pmatrix} =: \begin{pmatrix} q_{11} & q_{12} \\ q_{12} & q_{22} \end{pmatrix}.$$

Write $P = \begin{pmatrix} p_{11} & p_{12} \\ p_{12} & p_{22} \end{pmatrix}$. Compute

$$AP = \begin{pmatrix} -(\kappa + c)p_{11} + cp_{12} & -(\kappa + c)p_{12} + cp_{22} \\ -Kp_{12} & -Kp_{22} \end{pmatrix},$$

$$PA^\top = \begin{pmatrix} -(\kappa + c)p_{11} + cp_{12} & -Kp_{12} \\ -(\kappa + c)p_{12} + cp_{22} & -Kp_{22} \end{pmatrix}.$$

Thus the Lyapunov equation $AP + PA^\top + Q = 0$ yields the entrywise system:

$$\begin{aligned} (2,2):&\ -2Kp_{22} + q_{22} = 0, \\ (1,2):&\ -(\kappa + c + K)p_{12} + cp_{22} + q_{12} = 0, \\ (1,1):&\ -2(\kappa + c)p_{11} + 2cp_{12} + q_{11} = 0. \end{aligned}$$

Solving sequentially gives

$$p_{22} = \frac{q_{22}}{2K} = \frac{K^2\sigma_c^2 + \sigma_v^2}{2K} = \frac{K\sigma_c^2}{2} + \frac{\sigma_v^2}{2K},$$

$$p_{12} = \frac{cp_{22} + q_{12}}{\kappa + c + K}, \qquad p_{11} = \frac{cp_{12} + q_{11}/2}{\kappa + c},$$

which matches the closed-form expressions in Corollary 4.11. □

Proof of Proposition 4.7 (Homogeneous closed-loop stability benchmark)

Proof. Assume the homogeneous closure (31) holds and, for this benchmark, $m_t = v_t$. Then

$$\bar{x}_t = \frac{\kappa}{\gamma\phi^2 - \lambda}(v_t - p_t),$$

and substituting into (8) gives

$$\begin{aligned} dp_t &= \kappa(v_t - p_t)\,dt + \lambda\frac{\kappa}{\gamma\phi^2 - \lambda}(v_t - p_t)\,dt + \phi\,dZ_t \\ &= -\kappa_{\text{eff}}(p_t - v_t)\,dt + \phi\,dZ_t, \end{aligned}$$

where

$$\kappa_{\text{eff}} := \kappa\Big(1 + \frac{\lambda}{\gamma\phi^2 - \lambda}\Big) = \kappa\frac{\gamma\phi^2}{\gamma\phi^2 - \lambda}.$$

Define $y_t := p_t - v_t$. Using $dv_t = \mu_v\,dt + \sigma_v\,dW_t$,

$$dy_t = dp_t - dv_t = -\kappa_{\text{eff}} y_t\,dt - \mu_v\,dt + \phi\,dZ_t - \sigma_v\,dW_t,$$

as claimed. If $\gamma\phi^2 > \lambda$ then $\kappa_{\text{eff}} > 0$ and y_t is an OU process. When $\mu_v = 0$, y_t has diffusion variance rate $\phi^2 + \sigma_v^2$ and mean-reversion rate κ_{eff}, so its stationary variance is

$$\text{Var}(y_\infty) = \frac{\phi^2 + \sigma_v^2}{2\kappa_{\text{eff}}}.$$

□

6 Numerical Examples

Design. Summary statistics are computed for the *myopic mean-field consistent dynamics* in Sections II–IV using a particle approximation: simulate N agents with shared common shocks (W, U, Z) and independent idiosyncratic signal noises $\{B_i\}$, with trading governed by the myopic rule (29) and belief updates given by the Kalman filter in Appendix A (implemented in discrete time via Euler/Kalman recursions). Four baseline scenarios are reported: (i) bull regime ($\mu_v > 0$) with $k = 1$, (ii) bull regime with $k = 3$, (iii) bear regime ($\mu_v < 0$) with $k = 1$, (iv) bear regime with $k = 3$. Each scenario is averaged over M independent random seeds.

Metrics. Reported metrics include mean absolute mispricing $\mathbb{E}[|p_t - v_t|]$ (computed using the simulated fundamental v_t) and a disagreement proxy $\sigma_i(\hat{v}_{i,t})$, defined as the cross-sectional standard deviation across agents of the filtered fundamental estimates $\hat{v}_{i,t}$ at time t; figures/tables report time averages and treatment differences (e.g., Δ_k denotes $k = 3$ minus $k = 1$).

Implementation. Simulations and plotting are reproducible from the repository using `code/scripts/build_paper_artifacts.py`, which writes run-level CSVs and aggregated figures into `paper_artifacts/` . Table 2 lists the baseline parameters. The baseline parameters satisfy the per-step contraction/uniqueness condition $0 \le B_t^{\text{sf}} < \Delta t$ (Theorem 4.6), uniformly along the simulated path. Unless otherwise stated, the baseline uses time step $\Delta t = 1$; Table 8 reports a coarse time-step sensitivity check. Because $z_{i,t} = (\xi_{i,t} - \xi_{i,t-\Delta t})/\Delta t$ implies $R(\Delta t) \propto 1/\Delta t$, the Kalman measurement variance is updated accordingly when Δt changes. To keep economic aggressiveness comparable across Δt, the optional position-scale α_0 is treated as a per-unit-time risk budget and set to $\alpha_0(\Delta t) = \alpha_0\,\Delta t$ in time-step refinement runs. The *calendar-time* horizon is also held fixed: with baseline $T_{\text{days}} = 400$ trading days, $T_{\text{steps}} = T_{\text{days}}/\Delta t$ steps are simulated when Δt changes. Under this convention, the sufficient contraction proxy $\alpha_0(\Delta t)\lambda/(\Delta t(\chi+\gamma\phi^2))$ is Δt-invariant. **Timing.** Within each discrete step $t \to t+1$ (decision interval Δt), agents: (i) observe their most recently realized private signal increment (equivalently, the normalized increment $z_{i,t} = (\xi_{i,t} - \xi_{i,t-\Delta t})/\Delta t$) and update $(\hat{v}_{i,t}, \Sigma_{i,t})$; (ii) compute the post-trade mean inventory $\bar{x}_t$ from the closed-form stock–flow fixed point using the pre-trade mean $\bar{x}_{t^-} = \bar{x}_{t-1}$ (Proposition 4.5); (iii) set $\bar{u}_t = (\bar{x}_t - \bar{x}_{t-1})/\Delta t$; (iv) compute each agent's post-trade inventory

Channel / mechanism	Analytic model (math)	Particle implementation (code)	Alignment / notes
Time convention	Continuous time (dt); myopic rule uses infinitesimal scaling.	Discrete grid with step Δt (baseline $\Delta t = 1$).	State Δt explicitly when translating between dp_t and Δp_{t+1}.
Price formation	Anchored impact SDE $dp_t = \kappa(v_t - p_t)\,dt + \lambda \bar{u}_t\,dt + \phi\,dZ_t$.	Euler update $p_{t+1} = p_t + \kappa(v_t - p_t)\Delta t + \lambda \bar{u}_t \Delta t + \phi\sqrt{\Delta t}\,\varepsilon^{\eta}_{t+1}$.	Note (stock–flow/units): x is inventory (shares) and u is trading rate (shares/time); the baseline uses flow impact $\lambda \bar{u}_t\,dt$ (equivalently $\lambda\,d\bar{x}_t$ under Euler, since $\bar{u}_t \Delta t = \Delta \bar{x}_t$). For the legacy position-impact benchmark (not used in baseline simulations), one may collapse stock and flow and write $\bar{u}_t \equiv \bar{x}_t$ (Section 3.5).
Signal / observation	Flow signal $d\xi_{i,t} = v_t\,dt + \sigma_c\,dU_t + \sigma_\epsilon\,dB_{i,t}$.	Normalized increment $z_{i,t} = (\xi_{i,t} - \xi_{i,t-\Delta t})/\Delta t$; for $\Delta t = 1$, $z_{i,t} = v_t +$ noise.	Aligned; normalization makes the observation noise scale with $1/\sqrt{\Delta t}$.
Belief state $(\hat{v}_{i,t}, \Sigma_{i,t})$	Kalman–Bucy filter; Σ solves Riccati.	Discrete-time Kalman recursion for $(\hat{v}_{i,t}, \Sigma_{i,t})$ (Appendix A).	Aligned at the state level.
Trading rule (risk term)	Continuous-time myopic CARA uses variance rate ϕ^2 (drift uncertainty is $O(dt^2)$).	One-step mean–variance uses $\mathrm{Var}_{i,t}(\Delta p_{t+1}) = \phi^2 \Delta t + \kappa^2 \Sigma_{i,t} (\Delta t)^2$, hence $\mathrm{Var}^{\mathrm{eff}}_{i,t} = \phi^2 + \kappa^2 \Sigma_{i,t} \Delta t$ in the denominator.	This is the extra Σ-channel present in the particle rule; it is a discretization-consistent correction.
Mean-field fixed point	Homogeneous mean-only closure: $\bar{x}_t$ depends on beliefs only through $m_t - p_t$.	Per-step fixed point uses $A^{\mathrm{sf}}_t, B^{\mathrm{sf}}_t$ built from $\gamma\,\mathrm{Var}^{\mathrm{eff}}_{i,t}$; if $\Sigma_{i,t}$ is common across agents it cancels.	Homogeneous case stays mean-only; with heterogeneous k (hence heterogeneous Σ) $\bar{x}_t$ becomes a weighted mean.
Information set	Baseline: filtering on private signal only (no price in the filter).	Baseline matches; robustness variant adds an implicit noisy price observation.	Aligned; document the robustness toggle explicitly.
Intertemporal hedging	Present in the LQG benchmark (hedging terms via A_t, B_t).	Main experiments use myopic per-step rule; optional intertemporal correction exists as a separate toggle.	Keep benchmark vs experiment distinction explicit.

Table 1: Alignment table: mechanism "channels" present in the analytic model versus the particle implementation used in Section VI.

$x^\star_{i,t}$ from the myopic rule given $\bar{u}_t$ and set $u_{i,t} = (x^\star_{i,t} - x_{i,t^-})/\Delta t$ with $x_{i,t^-} = x_{i,t-1}$; (v) update price via flow impact, $\Delta p_{t+1} = \kappa(v_t - p_t)\Delta t + \lambda \bar{u}_t \Delta t + \phi\sqrt{\Delta t}\,\varepsilon^{\eta}_{t+1}$; (vi) update wealth $W_{i,t+1} = W_{i,t} + x^\star_{i,t}\Delta p_{t+1} - (\chi/2)(x^\star_{i,t})^2 \Delta t$; and (vii) set next pre-trade inventory $x_{i,t+1^-} = x^\star_{i,t}$. In the price-augmented robustness variant, agents then incorporate p_{t+1} via the implicit observation in Appendix A (updating beliefs for time $t+1$). Thus, no future price information is used at decision time. In Table 1, the price-impact term is written in flow form $\lambda \bar{u}_t$ (equivalently $\lambda\,\Delta \bar{x}_t$ under Euler, since $\bar{u}_t \Delta t = \Delta \bar{x}_t$). Earlier drafts displayed $\bar{x}_t$ in that row; the baseline model and simulations use flow impact as in (8) and the timing step (v) above.

Variance-rate diagnostic. In the particle implementation, the effective risk term is $D_{i,t} = \chi + \gamma(\phi^2 + \kappa^2 \Sigma_{i,t} \Delta t)$ (Proposition 4.5), so the denominator includes the discrete-time correction $\kappa^2 \Sigma_{i,t} \Delta t$ coming from belief uncertainty. As a scale diagnostic, the statistic $\rho_{i,t} := (\kappa^2 \Sigma_{i,t} \Delta t)/\phi^2$ is tracked (cross-sectional mean over i); when $\rho_{i,t} \ll 1$ the discrete-time rule is a small perturbation of the continuous-time mean-only denominator.

LQG fixed-point verification (continuous-time demo). As a numerical diagnostic for the constructive LQG solver in Section 3.7, `code/matlab/mfg_lqg_common_noise_demo.m` is runwith $\Delta t = 10^{-3}$ and $N = 2000$. The Picard fixed point converges in 16 iterations with final relative residual 9.59×10^{-7}. Over the time grid, the reported RMS differences between the particle approximation and the limiting paths are: 8.52×10^{-3} for the mean belief m,

2.09×10^{-3} for the price p, 8.42×10^{-3} for the mean demand $\bar{x}$ (position-impact benchmark), and 7.13×10^{-3} for the disagreement variance benchmark. **Scheme (map form).** Let $S_t = (v_t, p_t, \{(\hat{v}_{i,t}, \Sigma_{i,t}, x_{i,t^-})\}_{i=1}^N)$. For fixed shocks (common and idiosyncratic) the algorithm defines a measurable one-step map

$$S_{t+1} = \Psi_{\Delta t, N}(S_t; \text{shocks}), \tag{68}$$

obtained by composing: (a) the Kalman update (Appendix A), (b) the per-step mean-field fixed point (Theorem 4.6), and (c) the Euler updates for (v, p). Under the contraction condition (59), the fixed-point step is stable and the full map is well-defined (Theorem 3.1).

Discrete-time shock laws and Euler scaling. Fix $\Delta t > 0$. Let $(\Delta W_t, \Delta U_t, \Delta Z_t)$ be the common-noise increments with

$$\Delta W_t = \sqrt{\Delta t}\, \varepsilon^v_{t+1}, \quad \Delta U_t = \sqrt{\Delta t}\, \varepsilon^c_{t+1}, \quad \Delta Z_t = \sqrt{\Delta t}\, \varepsilon^\eta_{t+1},$$

where $\varepsilon^v_{t+1}, \varepsilon^c_{t+1}, \varepsilon^\eta_{t+1} \sim \mathcal{N}(0,1)$ are i.i.d. over t. For idiosyncratic signal noise, let $\varepsilon^i_{i,t+1} \sim \mathcal{N}(0,1)$ i.i.d. over (i,t), independent of the common shocks, and define $\Delta B_{i,t} := \sqrt{\Delta t}\, \varepsilon^i_{i,t+1}$. The Euler updates are

$$v_{t+\Delta t} = v_t + \mu_v \Delta t + \sigma_v \Delta W_t,$$
$$p_{t+\Delta t} = p_t + \kappa(v_t - p_t)\Delta t + \lambda \bar{u}_t \Delta t + \phi \Delta Z_t.$$

Observation normalization and variance scaling. Define the normalized observation

$$z_{i,t} := \frac{\xi_{i,t} - \xi_{i,t-\Delta t}}{\Delta t} = v_t + \frac{\sigma_c}{\sqrt{\Delta t}}\, \varepsilon^c_t + \frac{\sigma_\epsilon}{\sqrt{\Delta t}}\, \varepsilon^i_{i,t}.$$

where $\varepsilon^c_t := (U_t - U_{t-\Delta t})/\sqrt{\Delta t}$ and $\varepsilon^i_{i,t} := (B_{i,t} - B_{i,t-\Delta t})/\sqrt{\Delta t}$. Therefore the objective measurement variance is

$$R(\Delta t) = \mathrm{Var}(z_{i,t} - v_t) = \frac{\sigma_c^2 + \sigma_\epsilon^2}{\Delta t},$$

and agents' perceived variance under overconfidence $k \geq 1$ is

$$R'(\Delta t) = \frac{\sigma_c^2 + \sigma_\epsilon^2/k}{\Delta t}.$$

Any Δt-refinement diagnostics must update $R(\Delta t)$ and $R'(\Delta t)$ with the same $1/\Delta t$ scaling.

Discrete-time Kalman recursion used in simulations. Let $(\hat{v}_{i,t}, \Sigma_{i,t})$ denote agent i's subjective posterior mean and variance for v_t at time t. Prediction:

$$\hat{v}^-_{i,t} = \hat{v}_{i,t-\Delta t} + \mu_v\, \Delta t, \qquad \Sigma^-_{i,t} = \Sigma_{i,t-\Delta t} + \sigma_v^2\, \Delta t.$$

With measurement variance $R'(\Delta t)$, the Kalman gain is

$$K_{i,t} = \frac{\Sigma^-_{i,t}}{\Sigma^-_{i,t} + R'(\Delta t)}.$$

Update:

$$\hat{v}_{i,t} = \hat{v}^-_{i,t} + K_{i,t}\big(z_{i,t} - \hat{v}^-_{i,t}\big), \qquad \Sigma_{i,t} = (1 - K_{i,t})\Sigma^-_{i,t}.$$

Algorithm 2 Particle approximation (one scenario)

Fix parameters, scenario (μ_v, k), horizon T, population size N, and seeds $m = 1, \dots, M$.
for $m = 1$ to M **do**
  Simulate one realization of common shocks $(\Delta W_t, \Delta U_t, \Delta Z_t)_{t=0}^{T-1}$.
  Initialize (v_0, p_0) and agent beliefs $(\hat{v}_{i,0}, \Sigma_{i,0})$ for $i = 1, \dots, N$.
  Initialize inventories $x_{i,0^-}$ and wealth $W_{i,0}$ for $i = 1, \dots, N$.
  for $t = 0$ to $T - 1$ **do**
    For each agent i, draw idiosyncratic signal noise $\Delta B_{i,t}$ and update $(\hat{v}_{i,t}, \Sigma_{i,t})$ via the (perceived) Kalman recursion.
    Compute $(\bar{x}_t, \bar{u}_t)$ from the per-step stock–flow fixed point using pre-trade inventories (Proposition 4.5).
    For each agent i, set $x_{i,t} = x^\star_{i,t}$ from the myopic rule given $\bar{u}_t$ and compute trading rate $u_{i,t} = (x_{i,t} - x_{i,t^-})/\Delta t$.
    Update (v_{t+1}, p_{t+1}) using the Euler discretization of (8) (flow-based impact).
    Update wealth $W_{i,t+1} = W_{i,t} + x_{i,t}\Delta p_{t+1} - (\chi/2)x_{i,t}^2 \Delta t$ and set $x_{i,t+1^-} = x_{i,t}$.
  end for
  Record seed-level time series (price, fundamental, returns, mispricing, demand moments).
end for
Report scenario figures/tables by averaging statistics across seeds (Monte Carlo over the common and idiosyncratic shocks).

Per-step stock–flow fixed point. Given the myopic CARA best response (as stated in the main results),

$$x_{i,t} = \theta_{i,t}\Big(\kappa(\hat{v}_{i,t} - p_t) + \lambda\, \bar{u}_t\Big), \qquad \theta_{i,t} := \frac{\alpha_0}{\chi + \gamma\, \sigma^2_{p,i,t}} > 0,$$

define the common-filtration coefficients

$$A^{\mathrm{sf}}_t := \kappa\, \mathbb{E}[\theta_{i,t}(\hat{v}_{i,t} - p_t) \mid \mathcal{F}^0_t], \qquad B^{\mathrm{sf}}_t := \lambda\, \mathbb{E}[\theta_{i,t} \mid \mathcal{F}^0_t].$$

Then $\bar{x}_t = A^{\mathrm{sf}}_t + B^{\mathrm{sf}}_t \bar{u}_t$. With stock–flow timing $\bar{u}_t = (\bar{x}_t - \bar{x}_{t^-})/\Delta t$, the fixed point is

$$\bar{u}_t = \frac{A^{\mathrm{sf}}_t - \bar{x}_{t^-}}{\Delta t - B^{\mathrm{sf}}_t}, \qquad \bar{x}_t = A^{\mathrm{sf}}_t + B^{\mathrm{sf}}_t\, \bar{u}_t,$$

which is well-defined and unique whenever $\Delta t - B^{\mathrm{sf}}_t \neq 0$; if $0 \leq B^{\mathrm{sf}}_t < \Delta t$ then the associated per-step map is a contraction (Theorem 4.6). In all experiments, $(\bar{x}_t, \bar{u}_t)$ is computed in closed form from the above expressions (not via Picard iteration of the per-step map).

6.1 Parameter identification and calibration strategy

While full empirical estimation is beyond the scope of this paper, the paper provides an identification argument showing which observable moments pin down the key structural parameters $(\kappa, \lambda, \phi, \sigma_\epsilon, \sigma_v)$ in principle. This clarifies what data would be needed for calibration and establishes the model's testability.

Identification via observable moments. Under the myopic mean-field equilibrium, the following moments are observable (or proxied) from price and volume data:

1. **Return volatility** $\mathrm{std}(r_t)$**:** In the model, "return" is the price increment $r_t := \Delta p_t$ (value units). Empirically one often works with log returns $\Delta \log P_t$; for small moves, $\Delta \log P_t \approx$

$\Delta P_t/P_t$, so a simple scaling can map model increments to empirical log-return units when needed. From the Euler discretization of (8),

$$\Delta p_{t+\Delta t} = \mu_t\,\Delta t + \phi\,\Delta Z_{t+\Delta t}, \qquad \mu_t := \kappa(v_t - p_t) + \lambda \bar{u}_t,$$

where $\Delta Z_{t+\Delta t} \sim \mathcal{N}(0, \Delta t)$ is independent of $\mathcal{F}_t^{\text{pub}}$ (and of $\mathcal{F}_t^0$) by the independence assumptions in Section II. Hence, conditioning on the public filtration,

$$\mathrm{Var}(\Delta p_{t+\Delta t} \mid \mathcal{F}_t^{\text{pub}}) = \mathrm{Var}(\mu_t \mid \mathcal{F}_t^{\text{pub}})\,(\Delta t)^2 + \phi^2 \Delta t,$$

with

$$\mathrm{Var}(\mu_t \mid \mathcal{F}_t^{\text{pub}}) = \kappa^2 \mathrm{Var}(v_t - p_t \mid \mathcal{F}_t^{\text{pub}}) + \lambda^2 \mathrm{Var}(\bar{u}_t \mid \mathcal{F}_t^{\text{pub}}) + 2\kappa\lambda\,\mathrm{Cov}(v_t - p_t, \bar{u}_t \mid \mathcal{F}_t^{\text{pub}}).$$

Equivalently, the variance rate satisfies

$$\frac{1}{\Delta t}\mathrm{Var}(\Delta p_{t+\Delta t} \mid \mathcal{F}_t^{\text{pub}}) = \phi^2 + \mathrm{Var}(\mu_t \mid \mathcal{F}_t^{\text{pub}})\,\Delta t.$$

The cross term $\mathrm{Cov}(\mu_t \Delta t, \phi \Delta Z_{t+\Delta t} \mid \mathcal{F}_t^{\text{pub}})$ vanishes because $\Delta Z_{t+\Delta t}$ is independent of $\mathcal{F}_t^{\text{pub}}$ and has mean zero. Because impact is flow-based, the relevant object is the mean trading rate $\bar{u}_t$ (not the inventory stock $\bar{x}_t$). Using $\bar{u}_t = (\bar{x}_t - \bar{x}_{t^-})/\Delta t$, any stock-based variance proxy must be rescaled by $1/\Delta t^2$ to match $\mathrm{Var}(\bar{u}_t \mid \mathcal{F}_t^{\text{pub}})$. In steady state, $\mathrm{std}(r_t) = \mathrm{std}(\Delta p_t)$ depends on ϕ, λ, and κ through both the diffusion scale ϕ^2 and the drift variability $\mathrm{Var}(\mu_t \mid \mathcal{F}_t^{\text{pub}})$, whose contributions depend on the sampling interval Δt and on the price–flow covariation moments above.

2. **Effective mean-reversion speed (κ_{eff}):** The autocorrelation of price deviations from a moving average of fundamentals (or a proxy like a slow-moving average of prices) identifies an *effective* (closed-loop) mean-reversion rate κ_{eff}. Specifically, under (8), the half-life of price deviations is approximately $(\ln 2)/\kappa_{\text{eff}}$. When order flow is exogenous (or when feedback is negligible), $\kappa_{\text{eff}} = \kappa$; with endogenous trading feedback, κ_{eff} is reduced-form and need not equal the primitive anchoring parameter κ.

$$h = \frac{\ln 2}{\kappa_{\text{eff}}}, \qquad \kappa_{\text{eff}} = \frac{\ln 2}{h}. \tag{69}$$

   In particular, closed-loop feedback can make κ_{eff} differ materially from κ: for example, in the homogeneous benchmark with position-impact closure, $\kappa_{\text{eff}} = \kappa\,\gamma\phi^2/(\gamma\phi^2 - \lambda)$ (Proposition 4.7).

3. **Impact coefficient λ:** The predictive relation between price increments and (predetermined) order flow identifies λ up to mean-field scaling. In discrete time, the model implies Δp_{t+1} loads on $\bar{u}_t$; empirically this requires either a predetermined flow proxy (e.g., lagged daily flow or opening-imbalance-style measures) or an IV/GMM approach if flow is contemporaneous with the return interval.

4. **Fundamental volatility σ_v:** The long-run variance of fundamentals (estimated from a slow-moving filter of prices or from fundamental proxies like earnings/dividends) identifies σ_v. Alternatively, σ_v can be identified from the steady-state variance of the Kalman filter innovation process.

5. **Signal noise σ_ϵ:** The cross-sectional dispersion in beliefs (proxied by analyst forecast dispersion or survey-based disagreement) relative to the fundamental variance identifies the signal-to-noise ratio σ_v/σ_ϵ. Given σ_v, this pins down σ_ϵ.

Identification chain (estimated vs. inferred vs. normalized). Two empirical workflows are distinguished. *Track 1 (price-only):* from price-only data one can estimate κ_{eff} from a half-life diagnostic (item 2) and calibrate or estimate an effective price/noise-trading volatility ϕ from return volatility (item 1, after the unit mapping to log-return units if desired). *Track 2 (price + predetermined flow proxy; Option C):* to separately identify the primitive anchoring κ and impact λ under endogenous trading, the approach estimates the joint dynamics of $(\Delta p_{t+1}, \widehat{\widehat{u}}_t)$, jointly recovering (κ, λ) and feedback parameters (e.g., θ, ρ_u), and then reporting the implied κ_{eff} (Section 6.2). In the baseline simulation parameterization, λ is treated as a normalization choice (Table 2); in the SPY vignette the paper instead estimates $(\kappa, \lambda, \theta, \phi, \dots)$ by Kalman-filter maximum likelihood on a bivariate price–flow system. *Practical note:* the variance-rate identity in item 1 implies $\Delta t^{-1}\text{Var}(\Delta p_{t+\Delta t} \mid \mathcal{F}_t^{\text{pub}})$ is approximately affine in Δt for small Δt, with intercept $\approx \phi^2$ and slope $\approx \text{Var}(\mu_t \mid \mathcal{F}_t^{\text{pub}})$; this can be used as a diagnostic across sampling intervals, but half-life alone identifies only κ_{eff} when trading is endogenous.

Option C (joint estimation from price and flow). To separate the primitive anchoring parameter κ from the reduced-form κ_{eff} under endogenous trading, the joint dynamics of $(\Delta p_{t+1}, \widehat{\widehat{u}}_t)$ are estimated in a bivariate/state-space system with latent (v_t, u_t) and an explicit feedback term $u_{t+1} = \rho_u u_t + \theta(v_t - p_t) + \cdots$. Operationally, the key timing requirement is that the flow proxy used in the Δp_{t+1} equation is predetermined at time t (e.g., lagged daily flow, or opening-imbalance-style measures for intraday data).

Baseline parameterization. The baseline values in Table 2 are chosen to satisfy the per-step uniqueness condition $0 \le B_t^{\text{sf}} < \Delta t$ (Theorem 4.6) and to generate return volatilities and mean-reversion speeds in a reasonable range for daily/weekly financial data. A simple sufficient condition ensuring $B_t^{\text{sf}} < \Delta t$ uniformly is (59). Specifically:

- $\kappa = 0.005$ corresponds to an *intrinsic* anchoring half-life of $\ln(2)/\kappa \approx 139$ steps in the no-feedback limit (e.g., $\lambda = 0$); with endogenous trading feedback, the closed-loop half-life is governed by κ_{eff} (Option C).
- $\lambda = 0.20$, $\phi = 0.50$, and $\chi = 0.05$ (with $\alpha_0 = 1$ and $\Delta t = 1$) yield $\lambda/\kappa = 40$ and satisfy the sufficient contraction condition $\alpha_0\lambda/(\Delta t(\chi + \gamma\phi^2)) < 1$, generating price-increment volatilities $\text{std}(\Delta p)$ in the 0.5–1.0 range per step (value units).
- $\sigma_v = 0.10$ and $\sigma_\epsilon = 0.80$ yield a signal-to-noise ratio $\sigma_v/\sigma_\epsilon = 0.125$, consistent with moderate information quality in private signals.

A full calibration would target these moments jointly via method of moments or maximum likelihood on price/volume panel data. The identification argument above shows that the model is in principle testable given appropriate data.

6.2 One-asset moment match vignette

This vignette illustrates how the identification mapping in §6.1 can be operationalized using a single liquid ETF (SPY). Before turning to SPY-specific mapping and estimates, brief implementation checks are reported under the baseline parameterization (particle convergence in N and λ-sensitivity; Tables 5–6).

Units and mapping. In the baseline calibration, $\Delta t = 1$ is set (one step = one trading day). With endogenous trading feedback, the empirical half-life of price deviations identifies an

effective (closed-loop) mean-reversion rate κ_{eff}, not the primitive anchoring parameter κ; half-life is therefore treated as a diagnostic and (κ, λ) are estimated jointly from a bivariate system (Section 6.1). Under time-step refinement diagnostics, Δt is interpreted as a fraction of a trading day and calendar time is kept fixed, using the usual Euler scaling (e.g., $\kappa\Delta t$ in the drift and $\phi\sqrt{\Delta t}$ in the diffusion). The model (8) uses the *price increment* dp_t (i.e., Δp in value units), not log returns $\Delta \log p$ or simple returns $\Delta p/p$. Empirically, log returns $\Delta \log P_t$ are used; for small moves, $\Delta \log P_t \approx \Delta P_t / P_t$. The linearization $\Delta \log P_t \approx s\, \Delta p_t$ with $s := 1/\bar{P}$, where $\bar{P}$ is the sample mean price level (reported in Table 9). Given this mapping, ϕ is reported in value units (dollars) and compared to the naive mapping $\phi \approx \sigma_r / s$. Table 10 reports the implied variance shares in the SPY regime under the joint estimate. This calibration is variance-consistent with the decomposition implied by $\Delta p_t = \kappa(v_t - p_t)\Delta t + \lambda \bar{u}_t \Delta t + \phi\sqrt{\Delta t}\, \varepsilon_t$: in stationary simulation $\mathrm{Var}(\Delta p)$ can be attributed to the fundamental pull term, the endogenous flow-impact term, the exogenous innovation ϕ, and the cross term $2\mathrm{Cov}(\kappa(v-p)\Delta t, \lambda\bar{u}\Delta t)$. Identifying λ itself requires an order-flow proxy; in this vignette daily volume is used as a coarse proxy (details below) and λ is estimated jointly with κ.

From daily close and volume data (Stooq; 1,927 trading days, 2018 –2026), a joint price–flow system is estimated and the primitive (κ, λ), the flow-feedback gain θ, and the implied κ_{eff} are reported; the half-life implied by κ_{eff} is then compared to the empirical half-life as a diagnostic.

Audit-able estimation procedure. The script `scripts/estimate_moment_match_option_c.py` implements the following, fully reproducible from the data. (i) **Predetermined flow proxy:** An order-flow proxy $\widehat{u}_t$ is built from daily volume, oriented and normalized so that "positive" flow corresponds to buying pressure. To respect the filtration timing, Δp_{t+1} is modeled using $\widehat{u}_t$ (lagged flow relative to the next-day price increment). (ii) **Joint estimation (state-space / Kalman MLE):** A linear-Gaussian state-space is estimated with latent fundamentals v_t and latent flow u_t, where

$$\Delta p_{t+1} = \kappa(v_t - p_t)\Delta t + \lambda u_t \Delta t + \phi\sqrt{\Delta t}\, \varepsilon^{\eta}_{t+1}, \qquad u_{t+1} = \rho_u u_t + \theta(v_t - p_t) + \sigma_u \varepsilon^{u}_{t+1},$$

and the observables are p_t and a noisy proxy $\widehat{u}_t = u_t + \sigma_{u,\text{meas}} \varepsilon^{u,\text{meas}}_t$. Parameters are estimated by maximum likelihood using the Kalman filter. (iii) **Half-life as a diagnostic:** A proxy mispricing series is formed $y_t := (P_t - \mathrm{MA}_t)/\mathrm{MA}_t$, where MA_t is a slow moving average (200-day, or $\min(200, n/4)$ for shorter series), and compute the empirical AR(1) half-life h_{emp}. The model-implied half-life h_{model} is then reported from the estimated closed-loop linear system for (y_t, u_t), where $y_t := v_t - p_t$. Concretely, setting innovations to zero and $\Delta t = 1$, the deterministic transition is

$$\begin{pmatrix} y_{t+1} \\ u_{t+1} \end{pmatrix} = \underbrace{\begin{pmatrix} 1-\kappa & -\lambda \\ \theta & \rho_u \end{pmatrix}}_{M} \begin{pmatrix} y_t \\ u_t \end{pmatrix} + (\text{constant drift}).$$

so the decay rate is governed by the spectral radius $\rho_\star$ of M. Define $\kappa_{\text{eff}} := -\ln(\rho_\star)$ and set $h_{\text{model}} = \ln(2)/\kappa_{\text{eff}}$. **Calibration check (variance shares).** Under the joint estimate, Table 10 reports the variance shares of the price increment Δp across the three channels in (8) and the cross term. This diagnostic makes explicit whether the $\kappa(v-p)$ and $\lambda\bar{u}$ channels are negligible relative to ϕ, and reports the reconstruction error of the variance identity.

Results. Table 9 reports the moment match and regime classification. The estimates are produced by running `python code/scripts/estimate_moment_match.py -ticker SPY -csv PATH_TO_CSV`; outputs are written to `paper_artifacts/moment_match/` . Figure 1 plots the

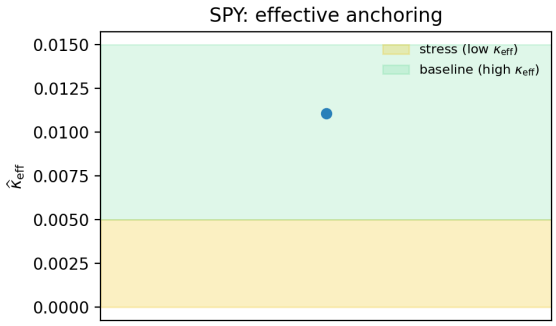

Figure 1: One-asset moment match: estimated κ_{eff} for SPY vs. baseline and stress regions (regime by effective anchoring strength).

estimated κ_{eff} against the baseline and stress regions (regime is determined by effective anchoring strength). SPY has an empirical half-life $h_{\text{emp}} \approx 62.7$ trading days; Table 9 reports the implied h_{model} as a diagnostic match.

Why mispricing does not move with k: architecture bridge. The model architecture explains why mispricing remains largely unchanged when increasing k across the joint grid (Subsection 6.3.3) and one-at-a-time sweeps (Subsection 6.3.4). Overconfidence k enters only through the Kalman filter (Appendix A): it scales the perceived idiosyncratic signal variance σ_ϵ^2/k (equivalently, the perceived measurement-noise variance $R' = \sigma_c^2 + \sigma_\epsilon^2/k$), so higher k yields tighter beliefs and more aggressive demand. But the price dynamics (8) have two channels: (a) $\kappa(v_t - p_t)$ pulls the price toward fundamentals (arbitrage/anchoring), and (b) $\lambda \bar{u}_t$ reflects flow-based impact from trading rates. Under strong anchoring (high κ), the $\kappa(v_t - p_t)$ term dominates: prices track fundamentals regardless of belief dispersion. Thus k loads mainly onto disagreement and trading intensity (belief dispersion, perceived precision, demand aggressiveness) rather than onto the price level itself. This structural separation—k shifts dispersion and intensity, whereas (κ, λ, ϕ) govern mispricing magnitudes—matches what the paper reports in Tables 3–11.

Caveats. The fundamental v_t is unobservable; the moving average is a rough proxy.

6.3 Parameter regimes and stress diagnostics

Preview of findings. Two distinct notions matter in this model: (i) *level amplification*—large mispricing/volatility levels under weak anchoring and/or high noise trading; and (ii) *overconfidence (treatment) effects*—differences in outcomes when increasing perceived signal precision from $k = 1$ to $k = 3$. The simulations show substantial *level amplification* under stress regimes (Table 16), while the incremental k-effects on average mispricing are modest in both baseline and stress calibrations (Tables 3–4).

6.3.1 Stress regimes: when mispricing *levels* become economically large

Table 16 reports "stress diagnostics" in which anchoring is weakened (κ reduced) and/or noise trading increases (ϕ increased). In this reported stress suite, anchoring stresses vary κ holding (λ, ϕ) fixed, and noise-trading stresses vary ϕ holding (λ, κ) fixed; moreover, all reported stress cases satisfy the OU mean-reversion condition $\gamma\phi^2 > \lambda$ (Proposition 4.7) and the sufficient per-step contraction proxy (59) (Theorem 4.6). Weak anchoring and high ϕ generate large mispricing and volatility *levels* (e.g., $\mathbb{E}[|p - v|]$ exceeding 3–9 in stress cases vs. ≈ 1.9 in baseline).

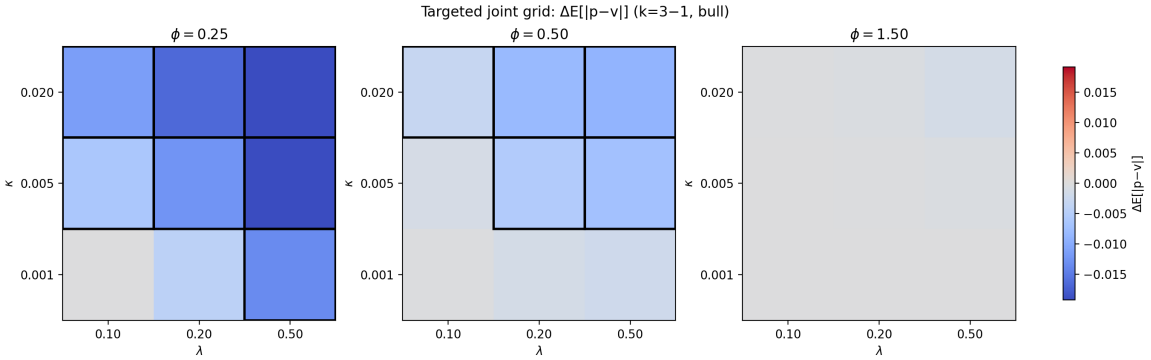

Figure 2: Joint-grid treatment effects $\Delta_k \mathbb{E}[|p-v|]$ across (κ, λ) for three ϕ slices, where mispricing is mean absolute $|p_t - v_t|$ (simulated v_t) and Δ_k denotes $k = 3$ minus $k = 1$.

Importantly, these level shifts are primarily driven by (κ, ϕ): within each stress case, outcomes are nearly unchanged between $k = 1$ and $k = 3$. This demonstrates that level amplification comes from market microstructure parameters (anchoring strength, noise trading) rather than the overconfidence treatment.

6.3.2 Baseline benchmark: k primarily increases disagreement and trading intensity

Next, the baseline bull/bear scenarios are reported under the benchmark calibration (Table 2). In this parameterization, increasing overconfidence primarily increases cross-sectional disagreement and trading intensity (e.g., $\Delta\mathbb{E}[\sigma_i(\hat{v}_i)] \approx +0.059$ and $\Delta\mathbb{E}[\sigma_i(x_i)] \approx +0.001$), while changes in mean absolute mispricing remain modest ($|\Delta\mathbb{E}[|p-v|]| \approx 0.004$). Mispricing tail and persistence diagnostics (Table 4) are essentially unchanged across k. This baseline serves as a robustness check: it demonstrates that the model does not always amplify mispricing, and that overconfidence's primary channel is through belief dispersion and trading intensity rather than price levels.

6.3.3 Targeted joint-move grid: k-effects on mispricing are robustly small

A natural concern is that one-at-a-time sweeps may miss interaction effects: overconfidence-induced amplification might require *simultaneous* changes in anchoring strength, price impact, and noise trading. To test this directly, a targeted $3 \times 3 \times 3$ grid over (κ, λ, ϕ) in the bull regime using paired random seeds and compare $k = 3$ against $k = 1$ within each cell.

Table 11 reports cell-by-cell differences in key diagnostics, and Figures 2–3 visualize the resulting treatment effects. A cell is classified as *non-negligible* if (i) the 95% confidence interval for $\Delta_k \mathbb{E}[|p-v|]$ excludes zero and (ii) $|\Delta_k \mathbb{E}[|p-v|]|$ exceeds 5% of the baseline $\mathbb{E}[|p-v|]$ in the same cell.

Negative result (robust across the joint grid). In the joint-grid simulations, $k = 3 - 1$ differences in $\mathbb{E}[|p-v|]$ are economically small: in Table 11, $\Delta_k \mathbb{E}[|p-v|]$ ranges from 0 to about -0.02 and only 2 out of 27 cells meet the "non-negligible" flag threshold. In several cells the 95% confidence interval excludes zero, but the magnitude remains small relative to the baseline mispricing level (order 1–10 depending on the regime), including in cells where weak anchoring and high noise trading generate large *levels* of mispricing. By contrast, disagreement and trading-intensity proxies move systematically with k. In these simulations, overconfidence primarily loads onto belief dispersion and trading intensity rather than price-level mispricing.

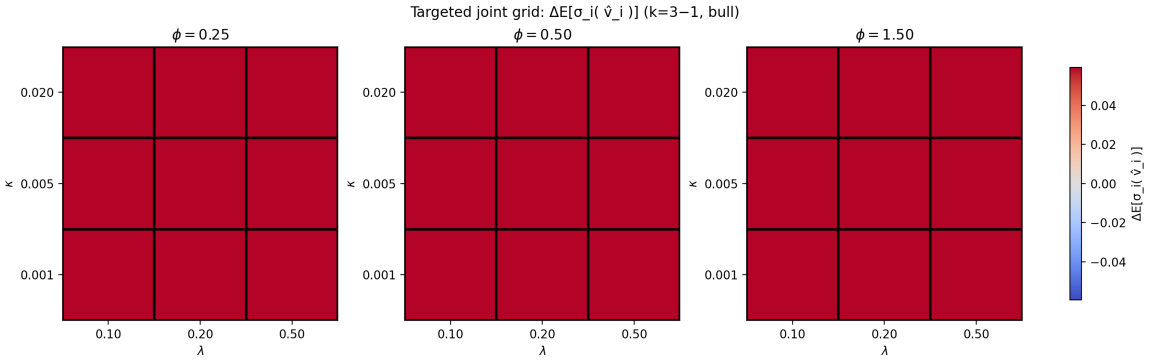

Figure 3: Joint-grid treatment effects on disagreement $\Delta_k \mathbb{E}[\sigma_i(\hat{v}_i)]$ across (κ, λ) for three ϕ slices, where $\sigma_i(\hat{v}_{i,t})$ is the cross-sectional standard deviation of $\hat{v}_{i,t}$ across agents and Δ_k denotes $k = 3$ minus $k = 1$.

6.3.4 One-at-a-time sweeps: why they rarely generate large k-effects

The joint-grid above (Subsection 6.3.3) establishes that the obvious concern was checked: simultaneous changes in (κ, λ, ϕ) do not reveal hidden k-driven mispricing amplification. One-at-a-time sweeps are now reported over the key levers highlighted by the model: the impact-to-anchoring ratio (λ/κ), signal-to-noise in private information, anchoring strength κ, and regime drift magnitude $|\mu_v|$.

Economic significance (Flag). The "Flag" column in Tables 12–15 and in the joint grid (Table 11) marks cells where the $k = 3{-}1$ effect is *economically meaningful* by the following criteria. *Mispricing:* flag if $|\Delta\mathbb{E}[|p - v|]| \geq \max(\theta_{\text{abs}},\ \theta_{\text{rel}} \times \text{baseline } \mathbb{E}[|p - v|])$. For the one-at-a-time sweeps, use $\theta_{\text{rel}} = 10\%$ and $\theta_{\text{abs}} = 0.10$; for the joint grid, use $\theta_{\text{rel}} = 5\%$ and $\theta_{\text{abs}} = 0$ so that any cell with a nontrivial relative change in mispricing is flagged; the impaired-arbitrage extension (Table 19) uses $\theta_{\text{rel}} = 5\%$ and $\theta_{\text{abs}} = 0.05$. *Return volatility:* flag if $|\Delta\,\text{std}(r)| \geq 20\%$ of the baseline $\text{std}(r)$ in that cell. These thresholds are chosen so that "meaningful" corresponds to a material relative change in mispricing (5–10% of baseline) or a substantive change in return volatility (20%); in the baseline, $\mathbb{E}[|p - v|] \approx 1.9$ (Table 3), so $\theta_{\text{abs}} = 0.10$ is about 5% of baseline. A sensitivity check using $\theta_{\text{rel}} \in \{5\%, 15\%\}$ for mispricing and 15% or 25% for return volatility leaves the set of flagged cells nearly unchanged in the sweeps; the conclusion that k-effects on mispricing are small is robust to these alternatives.

In these one-at-a-time sweep simulations (Tables 12–15), k-effects on mispricing diagnostics remain small, consistent with the baseline's strong anchoring channel ($\kappa = 0.005$) suppressing mispricing regardless of other parameters. Even when sweeping impact strength λ up to 0.50 (Table 12), the k-effect on mispricing remains small (often negative) because anchoring remains strong. The sweeps therefore map where outcomes become fragile in *levels* and clarify which parameters would need to be jointly re-estimated in a full calibration exercise targeting economically meaningful mispricing episodes.

6.4 Extensions and Validation Checks

6.4.1 Myopic vs. intertemporal policy

In the simulations, the core qualitative decomposition is robust across equilibrium concepts: the main k-loading remains on disagreement and trading intensity, while price-level mispricing is comparatively less sensitive to k under both myopic and intertemporal LQG policies. Comparisons use the same random seeds (paired shocks) and regime parameters; only the policy toggle and k differ. Table 18 and Figures 8–10 report the results. The policy decomposition (Figure 10)

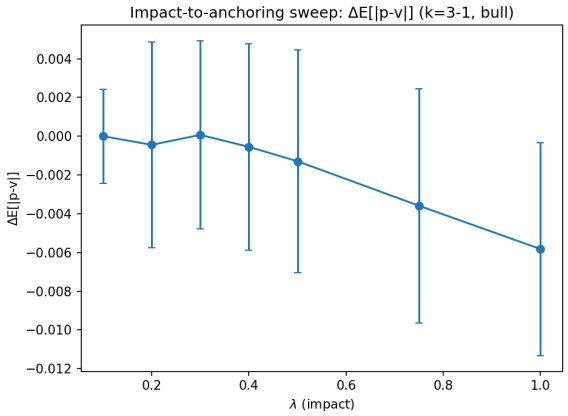

Figure 4: Effect of λ (impact) on $\Delta\mathbb{E}[|p-v|]$ (Bull regime; Δ denotes $k=3$ minus $k=1$).

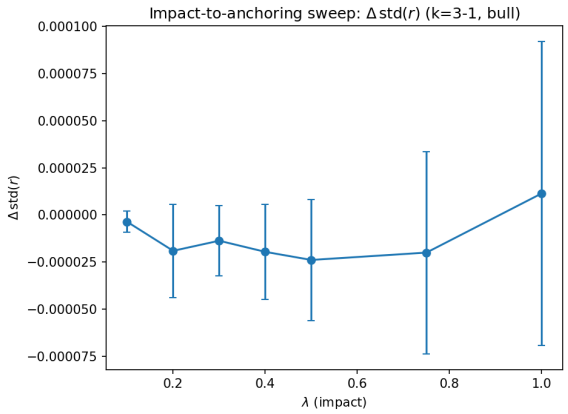

Figure 5: Effect of λ (impact) on $\Delta\,\mathrm{std}(r)$ (Bull regime; Δ denotes $k=3$ minus $k=1$).

confirms the intertemporal hedging term is numerically active. Mispricing is slightly lower under the intertemporal policy than under the myopic rule, and the k-treatment effect remains tiny under both; the modest negative $\Delta\mathbb{E}[|p-v|]$ when increasing k is consistent with stronger perceived precision inducing faster corrective trading against mispricing under strong anchoring, so price levels do not blow out—what changes with k is dispersion and trading intensity rather than the level of mispricing.

6.4.2 Extension: when k can move mispricing

In the baseline anchored-impact microstructure (relevant for SPY-like regimes), k does not materially move mispricing in the simulations. When arbitrage pressure is impaired—e.g., via state-dependent anchoring $\kappa(t) = \kappa_0 \exp(-\alpha|p-v|)$ so that κ weakens under large mispricing—k can in principle transmit into price-level mispricing. Table 19 and Figure 11 report the sensitivity to α. In the parameter range shown ($\alpha \in [0, 0.2]$), $\Delta\mathbb{E}[|p-v|]$ ($k=3-1$) remains small (around -0.004 to -0.005); even under modest state-dependence, k-effects on mispricing stay small. Larger arbitrage impairment (e.g., higher α, lower baseline κ_0, or higher ϕ) would be required for k to materially amplify mispricing. The negative result is not built into linearity; it is regime-specific: in the baseline (strong anchoring), k loads onto disagreement/intensity; in sufficiently impaired-arbitrage regimes, k can amplify mispricing.

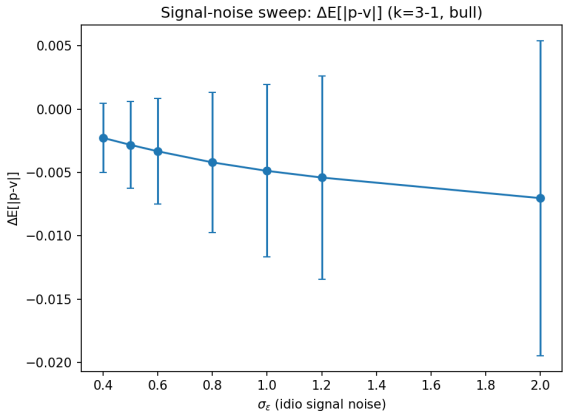

Figure 6: Effect of σ_ϵ on $\Delta\mathbb{E}[|p - v|]$ (Bull regime; Δ denotes $k = 3$ minus $k = 1$).

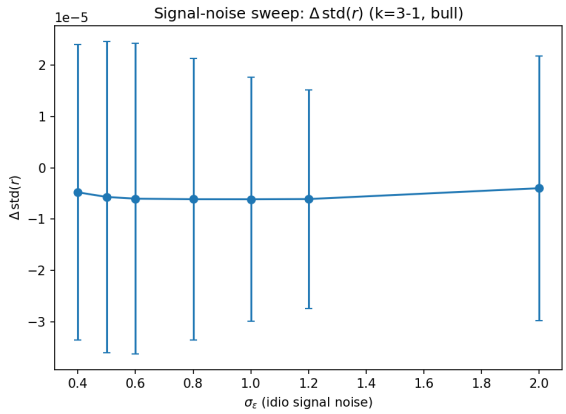

Figure 7: Effect of σ_ϵ on $\Delta\,\mathrm{std}(r)$ (Bull regime; Δ denotes $k = 3$ minus $k = 1$).

6.4.3 Empirical stylized fact: volume–volatility relation is time-varying in the SPY sample

A commonly documented empirical regularity is that trading volume and return volatility are positively related in many markets and samples (treated here as an external face-validity check for the model's intensity channel rather than as an identification of "disagreement"). In the SPY sample, however, the unconditional correlation between log volume and realized return volatility is economically small and statistically indistinguishable from zero: Table 20 reports point estimates that are slightly negative (e.g., Full sample -0.018 with Newey–West $t = -0.766$). At the same time, Figure 12 shows that the rolling correlation fluctuates around zero and exhibits episodic positive co-movement around some high-volatility periods, consistent with a time-varying relation rather than a stable unconditional sign.

Belief dispersion cannot be directly measured without survey/analyst microdata; uncertainty proxies are therefore used as reduced-form correlates. Analyst forecast dispersion, options-implied disagreement, or survey-based disagreement are natural next steps for tighter empirical tests. Stress episodes are defined mechanically as the top decile of realized return volatility (no cherry-picking).

Figure 12 plots the rolling correlation; Table 20 reports correlations in stress vs. non-stress with Newey–West t-statistics. In particular, the full-sample correlation is -0.018 (Newey–West

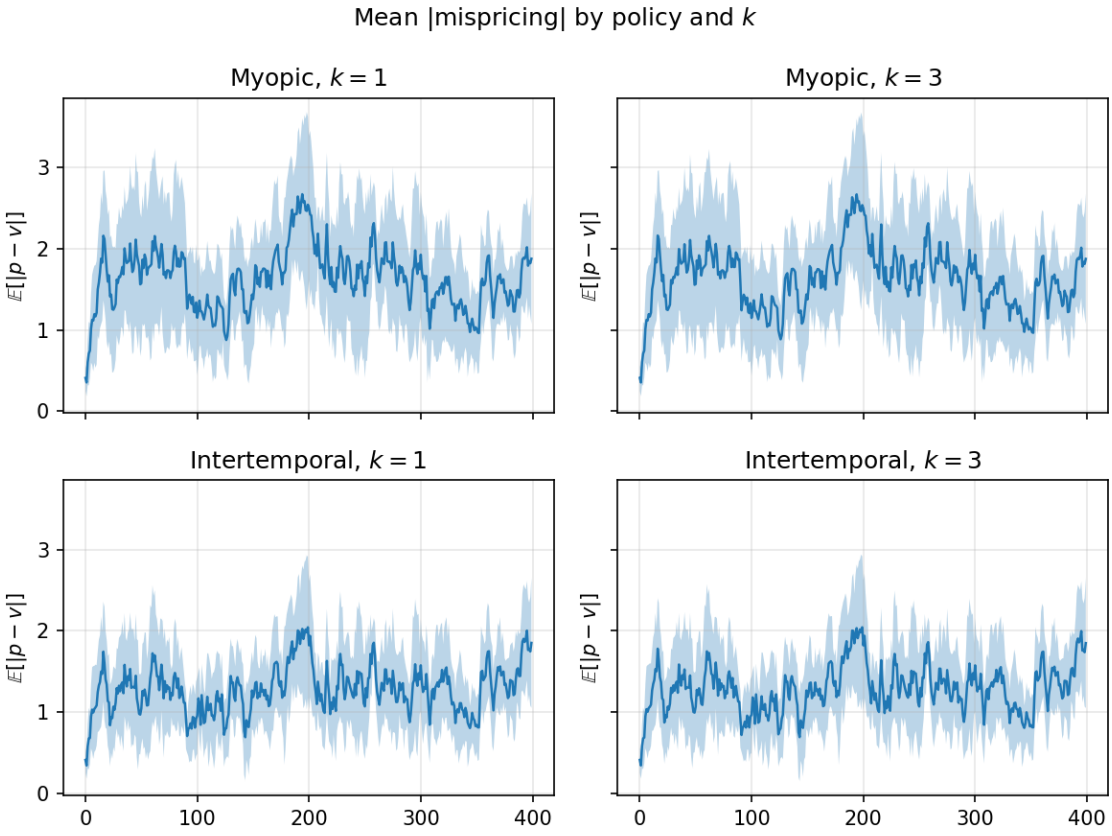

Figure 8: Mean $|p - v|$ by policy (myopic/intertemporal) and k (2×2 grid; 95% CI bands).

$t = -0.766$), and the stress/non-stress estimates are likewise small and statistically indistinguishable from zero. The model provides a mechanism for episodic co-movement: overconfidence increases disagreement and trading intensity; when intensity is elevated, volatility rises and trading activity increases, which can strengthen the (conditional) volume–volatility relation even if the unconditional correlation is close to zero.

Baseline results (benchmark). Figure 13 reports the mean price path across baseline scenarios. Figure 14 reports mean absolute mispricing $\mathbb{E}[|p_t - v_t|]$ (computed from the simulated fundamental), and Figure 15 reports a rolling volatility proxy based on realized returns. Table 3 complements the plots with seed-averaged moments and treatment effects ($k = 3$ vs. $k = 1$). **In these baseline simulations, the k-effect on mispricing is weak ($|\Delta\mathbb{E}[|p-v|]| \approx 0.004$), and mispricing tail/persistence diagnostics (Table 4) are essentially unchanged across k.** Proposition 4.4 explains this analytically: the mean-field closure depends only on the mean belief $m_t - p_t$, so mispricing is driven by microstructure (κ, λ, ϕ) and the mean-belief error $e_t = m_t - v_t$; under the filter structure, k raises disagreement (strictly in k) and trading intensity while affecting the mean belief only weakly, hence small price effects. Increasing overconfidence primarily increases cross-sectional disagreement and trading intensity (e.g., $\Delta\mathbb{E}[\sigma_i(\hat{v}_i)] \approx +0.059$ and lower perceived $\mathbb{E}[\bar{\Sigma}]$), consistent with that mechanism. The qualitative asymmetry remains visible in paths: bull regimes exhibit more persistent overvaluation episodes, while bear regimes exhibit noisier oscillations around fundamentals.

Discussion. The particle simulations are intended as computational evidence for the feedback mechanism highlighted by the model: misperceived signal precision affects belief dispersion and demand, which in turn impacts prices through (8). A full numerical fixed-point verification

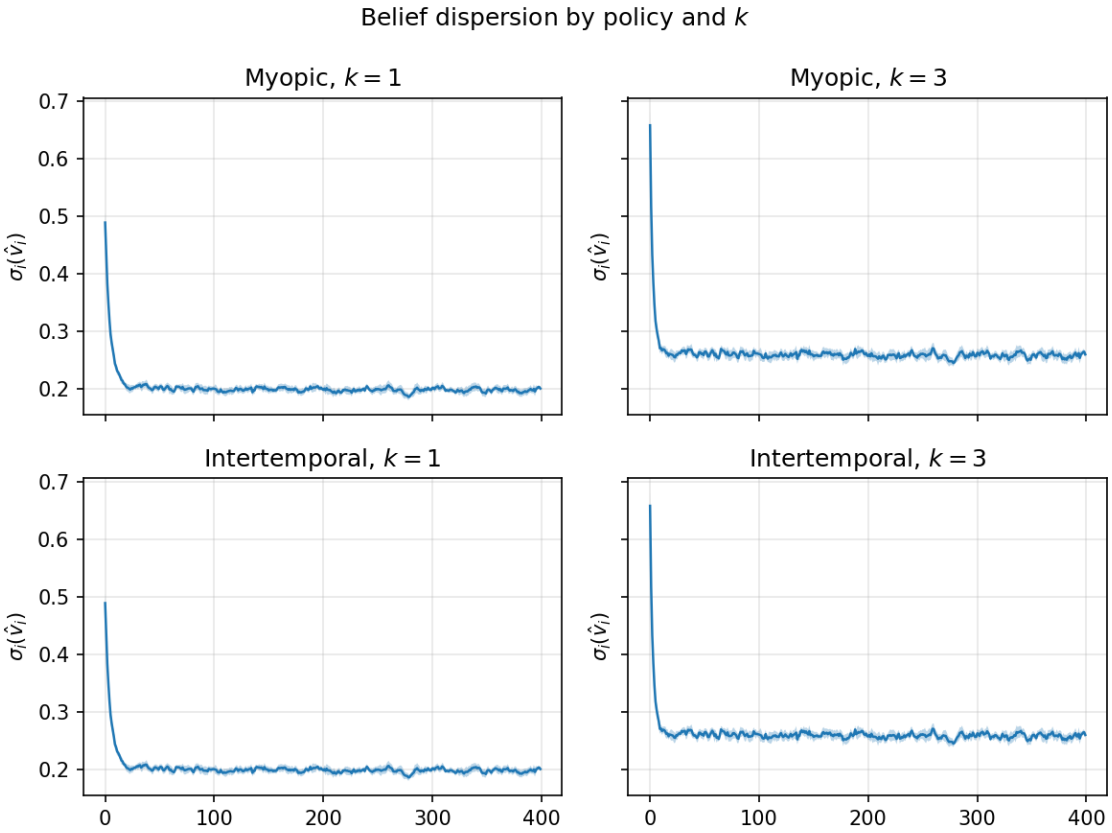

Figure 9: Belief dispersion $\sigma_i(\hat{v}_{i,t})$ (cross-sectional standard deviation across agents of $\hat{v}_{i,t}$) by policy and k.

for the common-noise mean-field limit (e.g., via conditional-law SPDE solvers) is left for future work. As a robustness check for the informational simplification (filtering on ξ_i only), the artifact script also produces a "price-augmented" filtering variant aligned with the Euler price update: it uses the realized increment $p_{t+1} - p_t$ to form an implicit noisy observation of v_t (Appendix A). The qualitative k-effects on perceived uncertainty and disagreement remain similar in that check (Table 7).

7 Conclusion

This paper formulates a mean-field game framework for modeling financial markets with heterogeneous overconfident investors. The model couples Bayesian belief updating (with misperceived signal precision) to endogenous price formation through a stochastic anchored-impact price equation. The main pipeline is a myopic mean-field consistent equilibrium: a checkable CARAbest response is derived under Gaussian price increments and a per-step stock–flow closure is obtained linking mean inventory/trading rates to mean belief. Separately, continuous-time CARA/LQG benchmarks are recorded as constructive comparisons.

The simulations demonstrate a clean *mechanism separation*: (i) *mispricing levels* are governed primarily by the microstructure regime (κ, λ, ϕ)—weak anchoring and high noise trading generate large mispricing and volatility levels; and (ii) *overconfidence (k)* robustly loads onto disagreement and trading intensity, but does not materially move price-level mispricing across a broad joint grid (Subsection 6.3.3), even when mispricing levels become large. This structural separation—

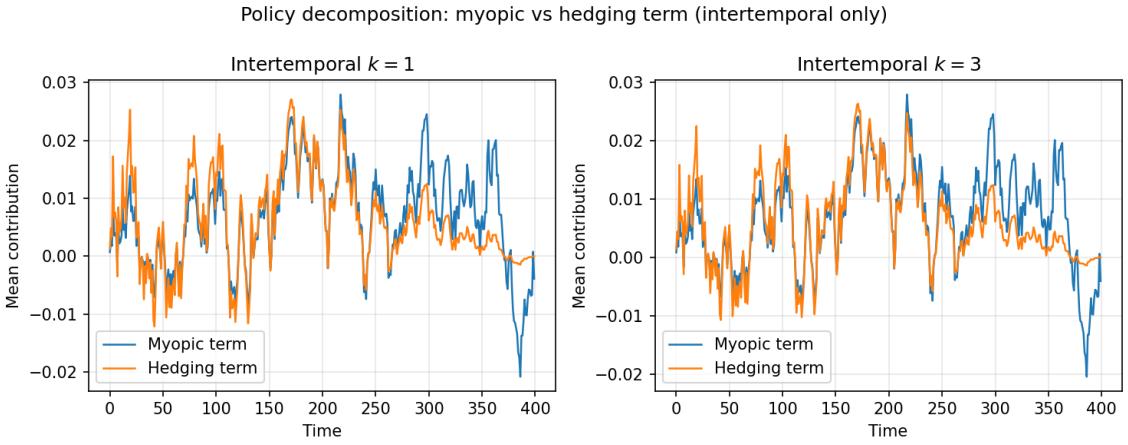

Figure 10: Policy decomposition: myopic vs. hedging term contribution (intertemporal runs).

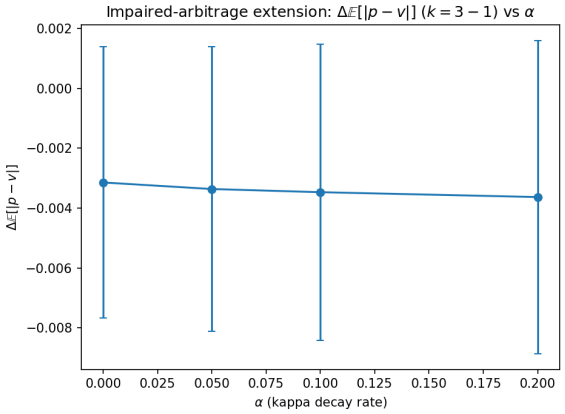

Figure 11: Impaired-arbitrage extension: $\Delta\mathbb{E}[|p - v|]$ $(k = 3 - 1)$ vs. α.

k shifts belief dispersion and intensity, whereas (κ, λ, ϕ) govern mispricing magnitudes—is the main empirical takeaway. The identification argument (Section 6.1) makes the model empirically testable, clarifying which observable moments pin down the structural parameters.

Several limitations and open questions remain. First, the baseline equilibrium concept and main simulation grid use the myopic CARAbest response under conditionally Gaussian price increments. As a validation check, Subsection 6.4.1 implements an unconstrained finite-horizon CARA/LQG intertemporal policy and finds similar qualitative k-effects. A fully constrained intertemporal formulation and a complete optimal-control MFG verification with endogenous filtering on prices remain future work. Second, while Subsection 6.1 provides an identification argument showing which moments pin down $(\kappa, \lambda, \sigma_v, \sigma_\epsilon, \phi)$ in principle, a full empirical calibration targeting these moments from price and volume data would strengthen the quantitative predictions. Third, the single-population framework abstracts from strategic and institutional heterogeneity; multi-population extensions (e.g., retail vs. institutional) could produce richer belief distributions and feedback. Finally, Section III establishes well-posedness of the discrete-time particle system under the per-step contraction/uniqueness condition $0 \leq B_t^{\mathrm{sf}} < \Delta t$ (Theorems 4.6 and 3.1). A complete verification of existence/uniqueness conditions for the full intertemporal optimal-control MFG equilibrium (with endogenous filtering on prices) would strengthen the theoretical foundation.

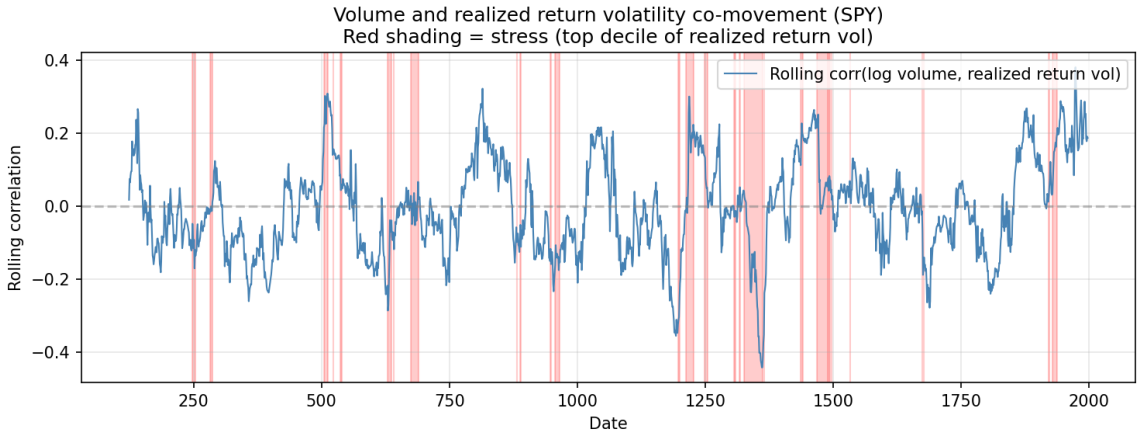

Figure 12: Rolling correlation of log volume and realized return volatility (SPY). The rolling correlation fluctuates around zero and becomes positive in some high-volatility windows. Red shading indicates stress episodes (top decile of realized return volatility).

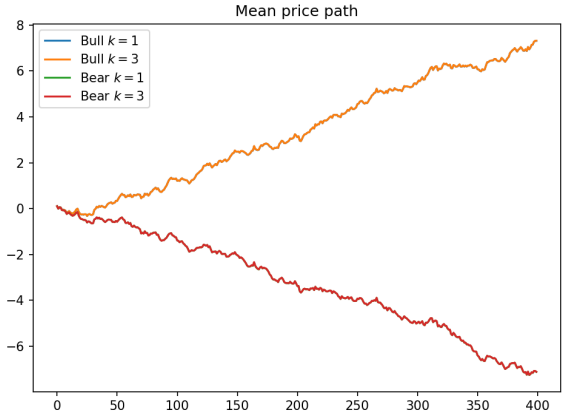

Figure 13: Mean price path across baseline scenarios (bull/bear regimes; $k \in \{1, 3\}$).

Statements and Declarations

Competing interests

The author declares that there are no competing financial or non-financial interests.

Funding

This work was not supported by external funding.

Data and code availability

Code and data used in this study are available from the corresponding author upon reasonable request. Replication package will be provided upon acceptance.

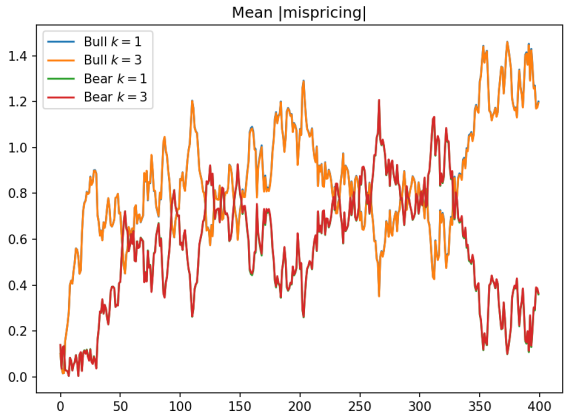

Figure 14: Mean absolute mispricing $\mathbb{E}[|p_t - v_t|]$ across baseline scenarios, computed using the simulated fundamental v_t.

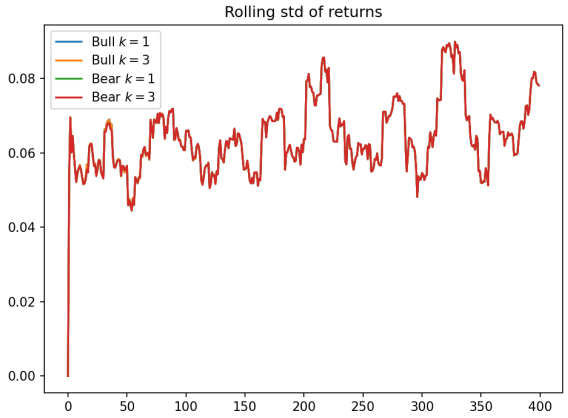

Figure 15: Rolling volatility proxy (standard deviation of returns) across baseline scenarios.

Author contributions

The author contributed to the study conception, model development, numerical work, drafting, and writing.

Ethics approval

Ethics approval is not applicable (N/A) to this study.

A Kalman–Bucy Filter With Misperceived Signal Precision

This appendix summarizes the Kalman–Bucy filter used for belief updating in Section II.

A.1 State and Observation Equations

The (unobserved) fundamental evolves as a linear diffusion

$$dv_t = \mu_v \, dt + \sigma_v \, dW_t, \tag{70}$$

and investor i observes a private signal

$$d\xi_{i,t} = v_t\,dt + \sigma_c\,dU_t + \sigma_\epsilon\,dB_{i,t}, \tag{71}$$

where W, U, and B_i are independent Brownian motions and U is common across investors.

A.2 Filter and Riccati Equation

Let $\hat{v}_{i,t}$ and $\Sigma_{i,t}$ denote investor i's Kalman–Bucy belief mean and posterior variance computed under the *perceived* measurement-noise variance $R'(k)$ below. When $k = 1$, $\hat{v}_{i,t}$ coincides with the true conditional mean $\mathbb{E}[v_t \mid \mathcal{F}_t^i]$ and $\Sigma_{i,t}$ with the true conditional variance. When $k \neq 1$ they are best interpreted as *subjective* filter states under the investor's misspecified noise model. Let $m_{i,t} := \mathbb{E}^P[v_t \mid \mathcal{F}_t^i]$ denote the objective conditional mean and define the deviation $\delta_{i,t} := \hat{v}_{i,t} - m_{i,t}$. Under P, the objective innovation $dI_{i,t}^{\xi} := (d\xi_{i,t} - m_{i,t}\,dt)/\sqrt{\sigma_c^2 + \sigma_\epsilon^2}$ is an $\{\mathcal{F}_t^i\}$-Brownian motion, and $\frac{d\xi_{i,t} - \hat{v}_{i,t}\,dt}{\sqrt{\sigma_c^2+\sigma_\epsilon^2}} = dI_{i,t}^{\xi} - \frac{\delta_{i,t}}{\sqrt{\sigma_c^2+\sigma_\epsilon^2}}\,dt$ (see Section 4.3).

A.2.1 Belief-mean SDE and diffusion decomposition

The belief state is $(\hat{v}_{i,t}, \Sigma_{i,t})$. Only $\hat{v}_{i,t}$ is stochastic; $\Sigma_{i,t}$ follows a scalar Riccati ODE. Starting from the Kalman–Bucy form

$$\begin{aligned} d\hat{v}_{i,t} &= \mu_v\,dt + K_{i,t}\big(d\xi_{i,t} - \hat{v}_{i,t}\,dt\big), \\ K_{i,t} &= \frac{\Sigma_{i,t}}{R'}, \quad R' = \sigma_c^2 + \frac{\sigma_\epsilon^2}{k}. \end{aligned} \tag{72}$$

and using the signal SDE $d\xi_{i,t} = v_t\,dt + \sigma_c\,dU_t + \sigma_\epsilon\,dB_{i,t}$, this yields the explicit diffusion decomposition

$$d\hat{v}_{i,t} = \big(\mu_v + K_{i,t}(v_t - \hat{v}_{i,t})\big)\,dt + K_{i,t}\sigma_c\,dU_t + K_{i,t}\sigma_\epsilon\,dB_{i,t}. \tag{73}$$

Thus the belief-mean diffusion has (i) a *common* component $K_{i,t}\sigma_c\,dU_t$ and (ii) an *idiosyncratic* component $K_{i,t}\sigma_\epsilon\,dB_{i,t}$. The perceived posterior variance satisfies the Riccati ODE

$$\dot{\Sigma}_{i,t} = \sigma_v^2 - \frac{\Sigma_{i,t}^2}{R'}, \tag{74}$$

and carries no diffusion term.

Here R' is the *perceived* measurement-noise variance. Overconfidence corresponds to $k > 1$, i.e., investors treat their signal as more precise than it truly is. The common component $\sigma_c\,dU_t$ prevents the law-of-large-numbers collapse of aggregate signal noise in the continuum limit and is the source of common-noise randomness in Section III. (Heterogeneous-k extension: replace k by k_i and write $R_i' = \sigma_c^2 + \sigma_\epsilon^2/k_i$.)

The scalar Riccati equation admits an explicit solution and converges exponentially to its steady state:

Lemma A.1 (Riccati convergence to steady state)**.** *Fix $R' > 0$ and $\sigma_v > 0$ and let Σ_t solve (74) with $\Sigma_0 \geq 0$. Then $\Sigma_t \to \Sigma^* := \sigma_v\sqrt{R'}$ as $t \to \infty$ and there exist constants $C, c > 0$ (depending on Σ_0, σ_v, R') such that*

$$|\Sigma_t - \Sigma^*| \leq Ce^{-ct}, \qquad c = \frac{2\sigma_v}{\sqrt{R'}}. \tag{75}$$

Consequently, the gain $K_t = \Sigma_t/R'$ converges exponentially to $K^* = \sigma_v/\sqrt{R'}$.

Proof. Fix $R' > 0$ and $\sigma_v > 0$ and consider the scalar Riccati ODE (74):

$$\frac{d\Sigma_t}{dt} = \sigma_v^2 - \frac{\Sigma_t^2}{R'}.$$

Let $\Sigma^* := \sigma_v\sqrt{R'}$ (the positive equilibrium) and write $a := \sigma_v/\sqrt{R'}$. Set $u_t := \Sigma_t/\Sigma^*$. Then u_t solves

$$\dot{u}_t = a(1 - u_t^2), \qquad u_0 = \Sigma_0/\Sigma^*.$$

Define the ratio $\rho_t := \frac{1-u_t}{1+u_t}$ (well-defined since $u_t \geq 0$). Differentiating gives

$$\dot{\rho}_t = -2a\,\rho_t,$$

hence $\rho_t = \rho\, e^{-2at}$ with $\rho := \rho_0 = \frac{1-u_0}{1+u_0} = \frac{\Sigma^*-\Sigma_0}{\Sigma^*+\Sigma_0}$. Solving for u_t yields the explicit solution

$$\Sigma_t = \Sigma^* \frac{1 - \rho\, e^{-2at}}{1 + \rho\, e^{-2at}}.$$

In all cases with $\Sigma_0 \geq 0$, the denominator satisfies $1 + \rho e^{-2at} > 0$ and $\Sigma_t \geq 0$ for all t, and $\Sigma_t \to \Sigma^*$ as $t \to \infty$ since $e^{-2at} \to 0$.

Moreover,

$$\Sigma_t - \Sigma^* = \Sigma^*\Big(\frac{1 - \rho e^{-2at}}{1 + \rho e^{-2at}} - 1\Big) = -\frac{2\Sigma^*\,\rho\, e^{-2at}}{1 + \rho e^{-2at}},$$

so the convergence is exponential with rate constant $c = 2a = 2\sigma_v/\sqrt{R'}$. For the prefactor, note: if $\rho \geq 0$ (equivalently $\Sigma_0 \leq \Sigma^*$), then $1 + \rho e^{-2at} \geq 1$ and

$$|\Sigma_t - \Sigma^*| \leq 2\Sigma^*|\rho|\, e^{-2at}.$$

If $\rho < 0$ (equivalently $\Sigma_0 > \Sigma^*$), then $1 + \rho e^{-2at} \geq 1 + \rho = 1 - |\rho|$ and

$$|\Sigma_t - \Sigma^*| \leq \frac{2\Sigma^*|\rho|}{1 - |\rho|}\, e^{-2at}.$$

Thus the claimed bound holds with, e.g., $C := 2\Sigma^*|\rho|$ when $\Sigma_0 \leq \Sigma^*$ and $C := \frac{2\Sigma^*|\rho|}{1-|\rho|}$ when $\Sigma_0 > \Sigma^*$ (both depending only on Σ_0, σ_v, R'). Since $K_t = \Sigma_t/R'$, it follows that $K_t \to K^* = \Sigma^*/R' = \sigma_v/\sqrt{R'}$ at the same exponential rate. □

A.3 Steady State

In steady state, (74) gives

$$\Sigma^* = \sigma_v\sqrt{R'} = \sigma_v\sqrt{\sigma_c^2 + \frac{\sigma_\epsilon^2}{k}}, \tag{76}$$

and the corresponding steady-state gain is $K^* = \Sigma^*/R' = \sigma_v/\sqrt{R'}$. Thus larger k increases the Kalman gain and reduces perceived posterior variance, generating more aggressive belief updating and, through the trading rule, larger demand responses to perceived mispricing.

A.4 Discrete-Time Recursion Used in Simulations

Section VI implements a discrete-time Kalman recursion consistent with the continuous-time signal model (72)–(73). On a grid with step size $\Delta t > 0$, the simulated fundamental evolves as

$v_{t+1} = v_t + \mu_v\Delta t + \sigma_v\sqrt{\Delta t}\,\varepsilon_{t+1}^v, \qquad \varepsilon_{t+1}^v \sim \mathcal{N}(0,1)$, (where $\varepsilon_{t+1}^v = (W_{t+\Delta t} - W_t)/\sqrt{\Delta t}$, as in the Section II nois

and investor i observes a discrete-time signal obtained from the *flow* observation $d\xi_{i,t}$ by taking increments and normalizing by Δt:

$$z_{i,t} := \frac{\xi_{i,t} - \xi_{i,t-\Delta t}}{\Delta t} = v_t + \frac{\sigma_c}{\sqrt{\Delta t}}\,\varepsilon_t^c + \frac{\sigma_\epsilon}{\sqrt{\Delta t}}\,\varepsilon_{i,t}^i, \qquad \varepsilon_t^c, \varepsilon_{i,t}^i \sim \mathcal{N}(0,1),$$

where $\varepsilon_t^c := (U_t - U_{t-\Delta t})/\sqrt{\Delta t}$ is common across investors and $\varepsilon_{i,t}^i := (B_{i,t} - B_{i,t-\Delta t})/\sqrt{\Delta t}$ is idiosyncratic. (With $\Delta t = 1$, this reduces to $z_{i,t} = v_t + \sigma_c\varepsilon_t^c + \sigma_\epsilon\varepsilon_{i,t}^i$.) Thus $\mathrm{Var}(z_{i,t} \mid v_t) = (\sigma_c^2 + \sigma_\epsilon^2)/\Delta t$; write $R(\Delta t) := (\sigma_c^2 + \sigma_\epsilon^2)/\Delta t$ for the objective measurement variance. Overconfidence scales only the idiosyncratic component, so the perceived measurement variance for $z_{i,t}$ is

$$R'(\Delta t) = \frac{\sigma_c^2 + \sigma_\epsilon^2/k}{\Delta t}.$$

Let $(\hat{v}_{i,t}, \Sigma_{i,t})$ denote the posterior mean/variance after processing $z_{i,t}$. The discrete-time Kalman recursion is:

$$\begin{aligned}
\Sigma_{i,t}^- &= \Sigma_{i,t-1} + \sigma_v^2 \Delta t, \\
K_{i,t} &= \frac{\Sigma_{i,t}^-}{\Sigma_{i,t}^- + R'(\Delta t)}, \\
\hat{v}_{i,t} &= \hat{v}_{i,t-1} + \mu_v \Delta t + K_{i,t}\big(z_{i,t} - (\hat{v}_{i,t-1} + \mu_v \Delta t)\big), \\
\Sigma_{i,t} &= (1 - K_{i,t})\Sigma_{i,t}^-.
\end{aligned}$$

Given the mean trading rate $\bar{u}_t$ (with $\bar{u}_t \Delta t = \Delta \bar{x}_t$ under the stock–flow timing), the discrete-time price update (Euler form of (8)) used in the code is

$$\begin{aligned}
p_{t+1} &= p_t + \kappa(v_t - p_t)\Delta t + \lambda \bar{u}_t \Delta t + \phi\sqrt{\Delta t}\,\varepsilon_{t+1}^\eta, \\
\varepsilon_{t+1}^\eta &:= \frac{Z_{t+\Delta t} - Z_t}{\sqrt{\Delta t}} \sim \mathcal{N}(0,1).
\end{aligned}$$

A.5 Price-Augmented Filtering (Robustness Variant)

Because prices are public and informative under (8), a fully consistent informational equilibrium would incorporate p into the observation set and solve a joint filtering/fixed-point problem. As a robustness check aligned with the implemented Euler update above, an *implicit* noisy observation of v_t is constructed from the realized price increment:

$$\tilde{v}_t^{(p)} := p_t + \frac{(p_{t+1} - p_t) - \lambda \bar{u}_t \Delta t}{\kappa \Delta t} = v_t + \frac{\phi}{\kappa\sqrt{\Delta t}}\,\varepsilon_{t+1}^\eta.$$

Conditional on $\mathcal{F}_t$, this yields a Gaussian observation of v_t with measurement variance $R_p = \phi^2/(\kappa^2 \Delta t)$ (scaled by a factor $\sigma_{p,\mathrm{obs}}^2$ in the code to probe robustness). An additional Kalman update is then applied using $\tilde{v}_t^{(p)}$ as a measurement (after processing the private signal), holding the state prediction fixed. Table 7 summarizes the impact of this price-consistent augmentation on the reported k-effects.

References

Brad M. Barber and Terrance Odean. Boys will be boys: Gender, overconfidence, and common stock investment. *The Quarterly Journal of Economics*, 116(1):261–292, 2001. doi: 10.1162/003355301556400.

Pierre Cardaliaguet and Charles-Albert Lehalle. Mean field game of controls and an application to trade crowding. *Mathematics and Financial Economics*, 12(3):335–363, 2018. doi: 10.1007/s11579-018-0206-7.

René Carmona and François Delarue. *Probabilistic Theory of Mean Field Games with Applications I: Mean Field FBSDEs, Control, and Games*, volume 83 of *Probability Theory and Stochastic Modelling*. Springer, Cham, 2018a. doi: 10.1007/978-3-319-58920-6.

René Carmona and François Delarue. *Probabilistic Theory of Mean Field Games with Applications II: Mean Field Games with Common Noise and Master Equations*, volume 84 of *Probability Theory and Stochastic Modelling*. Springer, Cham, 2018b. doi: 10.1007/978-3-319-58973-1.

Rene Carmona, Jean-Pierre Fouque, and Li-Hsien Sun. Mean field games and systemic risk. *Communications in Mathematical Sciences*, 13(4):911–933, 2015. doi: 10.4310/CMS.2015.v13.n4.a4.

Kent Daniel, David Hirshleifer, and Avanidhar Subrahmanyam. Investor psychology and security market under- and overreactions. *The Journal of Finance*, 53(6):1839–1885, 1998. doi: 10.1111/0022-1082.00077.

J. Bradford De Long, Andrei Shleifer, Lawrence H. Summers, and Robert J. Waldmann. Noise trader risk in financial markets. *Journal of Political Economy*, 98(4):703–738, 1990.

Nicolas Fournier and Arnaud Guillin. On the rate of convergence in Wasserstein distance of the empirical measure. *Probability Theory and Related Fields*, 162(3):707–738, 2015. doi: 10.1007/s00440-014-0583-8.

Simon Gervais and Terrance Odean. Learning to be overconfident. *The Review of Financial Studies*, 14(1):1–27, 2001. doi: 10.1093/rfs/14.1.1.

Olivier Guéant, Jean-Michel Lasry, and Pierre-Louis Lions. Mean field games and applications. In *Paris-Princeton Lectures on Mathematical Finance 2010*, volume 2003 of *Lecture Notes in Mathematics*, pages 205–266. Springer, 2010. doi: 10.1007/978-3-642-14660-2_3.

Harrison Hong and Jeremy C. Stein. A unified theory of underreaction, momentum trading, and overreaction in asset markets. *Journal of Finance*, 54(6):2143–2184, 1999. doi: 10.1111/0022-1082.00184.

Minyi Huang, Roland P. Malhamé, and Peter E. Caines. Large population stochastic dynamic games: closed-loop McKean-Vlasov systems and the Nash certainty equivalence principle. *IEEE Transactions on Automatic Control*, 51(11):1730–1755, 2006. doi: 10.1109/TAC.2006.884922.

Aimé Lachapelle, Jean-Michel Lasry, Charles-Albert Lehalle, and Pierre-Louis Lions. Efficiency of the price formation process in presence of high frequency participants: a mean field game analysis. *Mathematics and Financial Economics*, 10(3):223–262, 2016. doi: 10.1007/s11579-016-0161-0.

Daniel Lacker. A general characterization of the mean field limit for stochastic differential games. *Probability Theory and Related Fields*, 165(3–4):581–648, 2016. doi: 10.1007/s00440-015-0641-9.

Daniel Lacker. On the convergence of closed-loop Nash equilibria for the infinite horizon mean-field LQG game. *ESAIM: Control, Optimisation and Calculus of Variations*, 24(2):437–469, 2018. doi: 10.1051/cocv/2017011.

Terrance Odean. Volume, volatility, price, and profit when all traders are above average. *The Journal of Finance*, 53(6):1887–1934, 1998. doi: 10.1111/0022-1082.00078.

Table 2: Model and numerical parameters.

Parameter	Description	Baseline Value	Units
Static Benchmark (Sec. 2.2)			
$\mu_{v,0}$	Prior mean of v	—	value
$\sigma_{v,0}$	Prior sd of v	—	value
$\sigma_{\epsilon,0}$	Signal-noise sd	—	value
Dynamic Model (Sec. 2.3+)			
γ	Risk aversion	1.0	—
α_0	Position-size (risk-budget) scale	1.0	—
χ	Inventory holding cost	0.05	value/(share^2·step)
k	Overconfidence (precision scale)	1.0, 3.0	—
μ_v	Fundamental drift (bull/bear)	$\pm$0.02	value/step
σ_v	Fundamental diffusion vol.	0.10	value/$\sqrt{\text{step}}$
σ_c	Common signal component	0.10	value/$\sqrt{\text{step}}$
σ_ϵ	Idiosyncratic signal loading	0.80	value/$\sqrt{\text{step}}$
κ	Fundamental anchoring	0.005	1/step
λ	Impact strength	0.20	value/share
ϕ	Price/noise-trading volatility	0.50	value/$\sqrt{\text{step}}$
Numerical Parameters			
N	Number of agents	200	—
T	Horizon (steps)	400	step
M	Random seeds (replications)	50	—
p_0	Initial price	0.0	value
v_0	Initial fundamental	0.0	value

Scenario	$\mathbb{E}[\lvert p - v\rvert]$	$\mathbb{E}[\sigma_i(\hat{v}_i)]$	$\mathbb{E}[\sigma_i(x_i)]$	$\mathbb{E}[\Sigma]$	$\mathbb{E}[\rho_t]$
Bull $k = 1$	1.916 ± 0.142	0.202 ± 0.000	0.004 ± 0.000	0.078 ± 0.000	0.000 ± 0.000
Bull $k = 3$	1.911 ± 0.142	0.262 ± 0.000	0.005 ± 0.000	0.043 ± 0.000	0.000 ± 0.000
Bear $k = 1$	1.870 ± 0.125	0.202 ± 0.000	0.004 ± 0.000	0.078 ± 0.000	0.000 ± 0.000
Bear $k = 3$	1.867 ± 0.125	0.262 ± 0.000	0.005 ± 0.000	0.043 ± 0.000	0.000 ± 0.000
Δ Bull $(k = 3 - 1)$	-0.004 ± 0.002	0.059 ± 0.000	0.001 ± 0.000	-0.035 ± 0.000	-0.000 ± 0.000
Δ Bear $(k = 3 - 1)$	-0.003 ± 0.002	0.059 ± 0.000	0.001 ± 0.000	-0.035 ± 0.000	-0.000 ± 0.000

Table 3: Belief and market moments by scenario (mean $\pm$ 95% CI across random seeds). Mispricing uses $\mathbb{E}[|p_t - v_t|]$ (simulated v_t); disagreement uses $\sigma_i(\hat{v}_{i,t})$ (cross-sectional standard deviation across agents).

Scenario	$\mathbb{E}[\lvert p-v\rvert]$	$q_{0.95}(\lvert p-v\rvert)$	$q_{0.99}(\lvert p-v\rvert)$	$\rho_1(\lvert p-v\rvert)$	$\rho_1(p-v)$
Bull $k=1$	1.916 ± 0.142	4.561 ± 0.311	5.434 ± 0.344	0.927 ± 0.009	0.962 ± 0.004
Bull $k=3$	1.911 ± 0.142	4.554 ± 0.309	5.423 ± 0.342	0.926 ± 0.009	0.962 ± 0.004
Bear $k=1$	1.870 ± 0.125	4.403 ± 0.281	5.310 ± 0.321	0.921 ± 0.010	0.963 ± 0.004
Bear $k=3$	1.867 ± 0.125	4.399 ± 0.280	5.305 ± 0.320	0.921 ± 0.010	0.962 ± 0.004
Δ Bull $(k=3-1)$	-0.004 ± 0.002	-0.007 ± 0.006	-0.011 ± 0.007	-0.000 ± 0.000	-0.000 ± 0.000
Δ Bear $(k=3-1)$	-0.003 ± 0.002	-0.004 ± 0.006	-0.005 ± 0.006	-0.000 ± 0.000	-0.000 ± 0.000

Table 4: Mispricing tails and persistence diagnostics by scenario (mean ± 95% CI across random seeds), for mispricing $|p_t - v_t|$ computed using the simulated fundamental v_t.

N	$\Delta\mathbb{E}[\lvert p-v\rvert]$	$\Delta\mathbb{E}[\sigma_i(\hat{v}_i)]$	$\Delta\mathbb{E}[\sigma_i(x_i)]$	$\Delta\mathbb{E}[\bar{\Sigma}]$
200	0.001 ± 0.001	0.000 ± 0.001	0.000 ± 0.000	0.000 ± 0.000
500	-0.000 ± 0.000	0.000 ± 0.001	0.000 ± 0.000	0.000 ± 0.000
2000	0.000 ± 0.000	0.000 ± 0.000	0.000 ± 0.000	0.000 ± 0.000

Table 5: Particle convergence check in N (Bull $k = 1$; mean ± 95% CI across paired seeds; reported as differences relative to the largest N).

λ	$\Delta\mathbb{E}[\lvert p-v\rvert]$	$\Delta\mathbb{E}[\sigma_i(\hat{v}_i)]$	$\Delta\mathbb{E}[\sigma_i(x_i)]$	$\Delta\mathbb{E}[\bar{\Sigma}]$
0.10	0.000 ± 0.002	0.059 ± 0.000	0.001 ± 0.000	-0.035 ± 0.000
0.20	-0.001 ± 0.004	0.059 ± 0.000	0.001 ± 0.000	-0.035 ± 0.000
0.24	-0.007 ± 0.004	0.059 ± 0.000	0.001 ± 0.000	-0.035 ± 0.000

Table 6: Sensitivity of the k-effect to impact strength λ (Bull regime; Δ denotes $k = 3$ minus $k = 1$; mean ± 95% CI across paired seeds).

Filter	$\Delta\mathbb{E}[\lvert p-v\rvert]$	$\Delta\mathbb{E}[\sigma_i(\hat{v}_i)]$	$\Delta\mathbb{E}[\sigma_i(x_i)]$	$\Delta\mathbb{E}[\bar{\Sigma}]$
Private-only	-0.001 ± 0.005	0.060 ± 0.000	0.001 ± 0.000	-0.035 ± 0.000
Private + price	-0.002 ± 0.005	0.060 ± 0.000	0.001 ± 0.000	-0.035 ± 0.000

Table 7: Robustness to incorporating a noisy price observation in filtering (Bull regime; Δ denotes $k = 3$ minus $k = 1$; mean ± 95% CI across paired seeds).

Δt	$\Delta\mathbb{E}[\lvert p-v\rvert]$	$\Delta\mathbb{E}[\sigma_i(\hat{v}_i)]$	$\Delta\mathbb{E}[\sigma_i(x_i)]$	$\Delta q_{0.99}(\lvert p-v\rvert)$
1.00	-0.004 ± 0.004	0.059 ± 0.000	0.001 ± 0.000	-0.004 ± 0.014
0.50	-0.003 ± 0.004	0.050 ± 0.000	0.001 ± 0.000	0.001 ± 0.006
0.25	-0.002 ± 0.002	0.043 ± 0.000	0.001 ± 0.000	0.001 ± 0.007

Table 8: Time-step sensitivity (Bull regime; Δ denotes $k = 3$ minus $k = 1$; mean ± 95% CI across paired seeds). The sufficient contraction proxy is $\alpha_0\lambda/(\chi + \gamma\phi^2) = 0.67 < 1$ in all runs.

Table 9: SPY moment match and regime classification (daily units).

Quantity	**Estimate**	**Baseline**	**Notes**
Primitive anchoring κ	0.0041	0.005	estimated jointly with λ
Impact λ	0.230	0.20	flow proxy normalized (see text)
Flow feedback θ	0.000	0.000	u response to $(v-p)$
Implied κ_{eff}	0.0041	0.005	$\kappa_{\text{eff}} := -\ln(\rho_\star)$ from M
Half-life h_{emp} (days)	62.7	139	diagnostic from AR(1) on y_t
Half-life h_{model} (days)	168.4	139	diagnostic from $\rho_\star$ / κ_{eff}
Mean price $\bar{P}$	409.22	—	used for $s := 1/\bar{P}$
Scale s	0.002444	—	$\Delta \log P \approx s\,\Delta p$
Return vol σ_r	0.0123	—	daily log-return vol
Price-noise ϕ	4.589	0.50	estimated jointly
Implied $\sigma_{\eta,\text{flow}} = \phi/\lambda$	19.98	2.50	inferred mechanically
Regime	baseline	baseline	high anchoring

Table 10: Variance decomposition of $\text{Var}(\Delta p)$ under the joint estimate (SPY vignette).

Component	Variance	Share (%)
Fundamental pull $\text{Var}(A)$	0.02034	0.1
Endogenous flow $\text{Var}(B)$	0.04733	0.2
Exogenous noise $\text{Var}(C)$ (residual)	21.03	99.3
Cross term $2\text{Cov}(A,B)$	0.003932	0.0
Cross term $2\text{Cov}(A,C)$	0.06043	0.3
Cross term $2\text{Cov}(B,C)$	0.005977	0.0
Total $\text{Var}(\Delta p)$	21.17	100.0
Accounting gap	-3.553e-15	-0.0

ϕ	κ	λ	$\alpha_0\lambda/(\chi+\gamma\phi^2)$	$\Delta\mathbb{E}[\lvert p-v\rvert]$	$\Delta\mathbb{E}[\sigma_i(\hat{v}_i)]$	$\Delta\mathbb{E}[\lvert x_i\rvert]$	$\Delta\,\text{std}(\sum_i x_i)$	$\Delta\,\text{std}(r)$	Flag
0.25	0.001	0.10	0.89	-0.000 ± 0.004	0.059 ± 0.000	0.000 ± 0.000	0.038 ± 0.055	-0.000 ± 0.000	
0.25	0.001	0.20	1.78	-0.004 ± 0.005	0.059 ± 0.000	0.000 ± 0.000	0.049 ± 0.084	-0.000 ± 0.000	
0.25	0.001	0.50	4.44	-0.013 ± 0.004	0.059 ± 0.000	0.001 ± 0.001	0.150 ± 0.125	0.000 ± 0.000	
0.25	0.005	0.10	0.89	-0.006 ± 0.005	0.059 ± 0.000	0.001 ± 0.001	0.230 ± 0.247	-0.000 ± 0.000	
0.25	0.005	0.20	1.78	-0.012 ± 0.004	0.059 ± 0.000	0.002 ± 0.001	0.394 ± 0.297	0.000 ± 0.000	
0.25	0.005	0.50	4.44	-0.019 ± 0.003	0.059 ± 0.000	0.002 ± 0.001	0.507 ± 0.173	0.001 ± 0.000	✓
0.25	0.020	0.10	0.89	-0.012 ± 0.003	0.059 ± 0.000	0.007 ± 0.003	1.209 ± 0.650	0.000 ± 0.000	
0.25	0.020	0.20	1.78	-0.017 ± 0.003	0.059 ± 0.000	0.007 ± 0.002	1.197 ± 0.435	0.000 ± 0.000	
0.25	0.020	0.50	4.44	-0.019 ± 0.003	0.059 ± 0.000	0.004 ± 0.002	0.739 ± 0.373	0.001 ± 0.001	✓
0.50	0.001	0.10	0.33	-0.000 ± 0.001	0.059 ± 0.000	0.000 ± 0.000	0.005 ± 0.009	-0.000 ± 0.000	
0.50	0.001	0.20	0.67	-0.001 ± 0.003	0.059 ± 0.000	0.000 ± 0.000	0.006 ± 0.027	-0.000 ± 0.000	
0.50	0.001	0.50	1.67	-0.002 ± 0.004	0.059 ± 0.000	0.000 ± 0.000	0.002 ± 0.016	-0.000 ± 0.000	
0.50	0.005	0.10	0.33	-0.001 ± 0.002	0.059 ± 0.000	0.000 ± 0.000	0.016 ± 0.051	-0.000 ± 0.000	
0.50	0.005	0.20	0.67	-0.005 ± 0.005	0.059 ± 0.000	0.000 ± 0.001	0.042 ± 0.116	-0.000 ± 0.000	
0.50	0.005	0.50	1.67	-0.007 ± 0.005	0.059 ± 0.000	0.000 ± 0.000	0.027 ± 0.064	-0.000 ± 0.000	
0.50	0.020	0.10	0.33	-0.003 ± 0.002	0.059 ± 0.000	0.001 ± 0.001	0.132 ± 0.181	-0.000 ± 0.000	
0.50	0.020	0.20	0.67	-0.008 ± 0.004	0.059 ± 0.000	0.001 ± 0.001	0.295 ± 0.320	0.000 ± 0.000	
0.50	0.020	0.50	1.67	-0.009 ± 0.004	0.059 ± 0.000	0.001 ± 0.001	0.152 ± 0.154	0.000 ± 0.000	
1.50	0.001	0.10	0.04	-0.000 ± 0.000	0.059 ± 0.000	0.000 ± 0.000	0.000 ± 0.001	-0.000 ± 0.000	
1.50	0.001	0.20	0.09	-0.000 ± 0.000	0.059 ± 0.000	0.000 ± 0.000	0.000 ± 0.001	-0.000 ± 0.000	
1.50	0.001	0.50	0.22	-0.000 ± 0.000	0.059 ± 0.000	0.000 ± 0.000	0.000 ± 0.001	-0.000 ± 0.000	
1.50	0.005	0.10	0.04	-0.000 ± 0.000	0.059 ± 0.000	0.000 ± 0.000	0.000 ± 0.004	-0.000 ± 0.000	
1.50	0.005	0.20	0.09	-0.000 ± 0.000	0.059 ± 0.000	0.000 ± 0.000	0.000 ± 0.004	-0.000 ± 0.000	
1.50	0.005	0.50	0.22	-0.001 ± 0.001	0.059 ± 0.000	0.000 ± 0.000	-0.000 ± 0.004	-0.000 ± 0.000	
1.50	0.020	0.10	0.04	-0.000 ± 0.000	0.059 ± 0.000	0.000 ± 0.000	0.004 ± 0.016	-0.000 ± 0.000	
1.50	0.020	0.20	0.09	-0.001 ± 0.001	0.059 ± 0.000	0.000 ± 0.000	0.004 ± 0.016	-0.000 ± 0.000	
1.50	0.020	0.50	0.22	-0.001 ± 0.001	0.059 ± 0.000	0.000 ± 0.000	0.004 ± 0.017	-0.000 ± 0.000	

Table 11: Joint-grid treatment effects Δ_k across (κ, λ, ϕ) (Bull regime; Δ denotes $k=3$ minus $k=1$; mean $\pm$ 95% CI across paired seeds; "Flag" per thresholds in text). The fourth column reports the sufficient contraction proxy $\alpha_0\lambda/(\chi+\gamma\phi^2)$ (with $\Delta t = 1$), which upper bounds $B_t^{\text{sf}}/\Delta t$; values below 1 imply the per-step map is a contraction (Theorem 4.6). In this grid, the realized $\max_t(B_t^{\text{sf}}/\Delta t)$ differs from the proxy by less than 10^{-3}, and $\min_t |\Delta t - B_t^{\text{sf}}| \approx 0.11$, so the fixed point is always bounded away from the singularity $\Delta t = B_t^{\text{sf}}$.

λ (impact)	λ/κ	$\Delta\mathbb{E}[\lvert p-v\rvert]$	$\Delta q_{0.95}(\lvert p-v\rvert)$	$\Delta q_{0.99}(\lvert p-v\rvert)$	$\Delta\,\mathrm{std}(r)$	$\Delta\,\rho_1(\lvert r\rvert)$	Flag
0.10	20.0	0.000 ± 0.002	-0.002 ± 0.005	-0.004 ± 0.003	-0.000 ± 0.000	-0.000 ± 0.000	
0.20	40.0	-0.000 ± 0.005	-0.012 ± 0.012	-0.009 ± 0.015	-0.000 ± 0.000	-0.000 ± 0.000	
0.30	60.0	0.000 ± 0.005	-0.002 ± 0.012	-0.008 ± 0.010	-0.000 ± 0.000	-0.000 ± 0.000	
0.40	80.0	-0.001 ± 0.005	-0.010 ± 0.014	-0.013 ± 0.013	-0.000 ± 0.000	-0.000 ± 0.000	
0.50	100.0	-0.001 ± 0.006	-0.009 ± 0.012	-0.013 ± 0.018	-0.000 ± 0.000	-0.000 ± 0.000	
0.75	150.0	-0.004 ± 0.006	-0.023 ± 0.018	-0.032 ± 0.018	-0.000 ± 0.000	0.000 ± 0.001	
1.00	200.0	-0.006 ± 0.005	-0.040 ± 0.024	-0.029 ± 0.022	0.000 ± 0.000	0.000 ± 0.001	

Table 12: Impact-to-anchoring sweep (Bull regime). Δ denotes $k = 3$ minus $k = 1$; "Flag" marks economically meaningful regions (see text for thresholds).

σ_ϵ	σ_v/σ_ϵ	$\Delta\mathbb{E}[\lvert p-v\rvert]$	$\Delta q_{0.95}(\lvert p-v\rvert)$	$\Delta q_{0.99}(\lvert p-v\rvert)$	$\Delta\,\mathrm{std}(r)$	$\Delta\,\rho_1(\lvert r\rvert)$	$\Delta\mathbb{E}[\sigma_i(\hat{v}_i)]$	$\Delta\mathbb{E}[\sigma_i(x_i)]$	Flag
0.40	0.250	-0.002 ± 0.003	-0.005 ± 0.007	-0.007 ± 0.007	-0.000 ± 0.000	-0.000 ± 0.000	0.037 ± 0.000	0.001 ± 0.000	
0.50	0.200	-0.003 ± 0.003	-0.008 ± 0.009	-0.007 ± 0.007	-0.000 ± 0.000	0.000 ± 0.000	0.044 ± 0.000	0.001 ± 0.000	
0.60	0.167	-0.003 ± 0.004	-0.009 ± 0.011	-0.007 ± 0.009	-0.000 ± 0.000	0.000 ± 0.000	0.050 ± 0.000	0.001 ± 0.000	
0.80	0.125	-0.004 ± 0.006	-0.009 ± 0.013	-0.007 ± 0.012	-0.000 ± 0.000	0.000 ± 0.000	0.060 ± 0.000	0.001 ± 0.000	
1.00	0.100	-0.005 ± 0.007	-0.009 ± 0.013	-0.009 ± 0.014	-0.000 ± 0.000	0.000 ± 0.000	0.068 ± 0.000	0.001 ± 0.000	
1.20	0.083	-0.005 ± 0.008	-0.007 ± 0.015	-0.010 ± 0.016	-0.000 ± 0.000	0.000 ± 0.000	0.075 ± 0.000	0.002 ± 0.000	
2.00	0.050	-0.007 ± 0.012	-0.021 ± 0.022	-0.021 ± 0.017	-0.000 ± 0.000	0.000 ± 0.000	0.100 ± 0.000	0.002 ± 0.000	

Table 13: Signal-to-noise sweep (Bull regime): varying σ_ϵ while holding σ_v fixed. "Flag" marks economically meaningful regions (see text).

κ	λ/κ	$\Delta\mathbb{E}[\lvert p-v\rvert]$	$\Delta q_{0.95}(\lvert p-v\rvert)$	$\Delta q_{0.99}(\lvert p-v\rvert)$	$\Delta\,\mathrm{std}(r)$	$\Delta\,\rho_1(\lvert r\rvert)$	Flag
0.001	200.0	0.001 ± 0.003	-0.003 ± 0.005	-0.002 ± 0.006	0.000 ± 0.000	0.000 ± 0.000	
0.002	100.0	0.000 ± 0.004	-0.000 ± 0.007	-0.004 ± 0.007	0.000 ± 0.000	0.000 ± 0.000	
0.003	66.7	-0.000 ± 0.005	-0.009 ± 0.005	-0.009 ± 0.010	0.000 ± 0.000	0.000 ± 0.000	
0.005	40.0	-0.002 ± 0.004	-0.010 ± 0.011	-0.015 ± 0.010	0.000 ± 0.000	0.000 ± 0.000	
0.010	20.0	-0.004 ± 0.003	-0.007 ± 0.013	-0.010 ± 0.024	0.000 ± 0.000	0.000 ± 0.000	
0.020	10.0	-0.004 ± 0.003	-0.011 ± 0.014	-0.017 ± 0.025	0.000 ± 0.000	-0.000 ± 0.000	

Table 14: Anchoring sweep (Bull regime): varying κ at fixed (λ, ϕ). "Flag" marks economically meaningful regions (see text).

Regime	μ_v	$\Delta\mathbb{E}[\lvert p-v\rvert]$	$\Delta q_{0.95}(\lvert p-v\rvert)$	$\Delta q_{0.99}(\lvert p-v\rvert)$	$\Delta\,\mathrm{std}(r)$	$\Delta\,\rho_1(\lvert r\rvert)$	Flag
Bull	0.010	-0.009 ± 0.004	-0.012 ± 0.018	-0.024 ± 0.018	-0.000 ± 0.000	-0.000 ± 0.000	
Bull	0.020	-0.009 ± 0.005	-0.011 ± 0.015	-0.020 ± 0.021	-0.000 ± 0.000	-0.000 ± 0.000	
Bull	0.030	-0.009 ± 0.005	-0.016 ± 0.019	-0.020 ± 0.021	-0.000 ± 0.000	-0.000 ± 0.000	
Bull	0.050	-0.008 ± 0.007	-0.011 ± 0.015	-0.013 ± 0.021	-0.000 ± 0.000	-0.000 ± 0.000	
Bear	-0.010	-0.009 ± 0.004	-0.028 ± 0.015	-0.031 ± 0.017	-0.000 ± 0.000	-0.000 ± 0.000	
Bear	-0.020	-0.009 ± 0.004	-0.023 ± 0.014	-0.021 ± 0.019	-0.000 ± 0.000	-0.000 ± 0.000	
Bear	-0.030	-0.008 ± 0.005	-0.019 ± 0.021	-0.018 ± 0.020	-0.000 ± 0.000	-0.000 ± 0.000	
Bear	-0.050	-0.007 ± 0.007	-0.009 ± 0.025	-0.018 ± 0.025	-0.000 ± 0.000	-0.000 ± 0.000	

Table 15: Regime-strength sweep: varying $|\mu_v|$ in bull/bear regimes. "Flag" marks economically meaningful regions (see text).

Scenario	κ	ϕ	$\mathbb{E}[\lvert p-v\rvert]$		$q_{0.95}(\lvert p-v\rvert)$		$\mathrm{std}(r)$	
			$k=1$	$k=3$	$k=1$	$k=3$	$k=1$	$k=3$
Baseline	0.005	0.50	1.774 ± 0.273	1.767 ± 0.276	4.164 ± 0.634	4.155 ± 0.633	0.491 ± 0.008	0.491 ± 0.008
Weak anchoring	0.001	0.50	3.972 ± 1.318	3.969 ± 1.320	8.118 ± 2.108	8.113 ± 2.112	0.488 ± 0.008	0.488 ± 0.008
High noise	0.005	1.00	6.113 ± 1.909	6.112 ± 1.910	13.461 ± 3.392	13.460 ± 3.393	0.977 ± 0.015	0.977 ± 0.015
Weak+high	0.001	1.00	9.258 ± 3.875	9.258 ± 3.875	18.993 ± 5.852	18.993 ± 5.851	0.976 ± 0.015	0.976 ± 0.015
Mid-high noise	0.005	0.75	4.377 ± 1.290	4.376 ± 1.291	9.706 ± 2.366	9.704 ± 2.367	0.733 ± 0.012	0.733 ± 0.012
Very high noise	0.005	1.50	9.308 ± 2.886	9.307 ± 2.886	20.516 ± 5.137	20.516 ± 5.137	1.465 ± 0.023	1.465 ± 0.023
Extreme noise	0.005	2.00	12.452 ± 3.763	12.452 ± 3.763	27.326 ± 6.779	27.326 ± 6.779	1.954 ± 0.031	1.954 ± 0.031
Very weak anchoring	0.001	0.50	4.999 ± 1.827	4.997 ± 1.828	9.910 ± 2.868	9.907 ± 2.870	0.488 ± 0.008	0.488 ± 0.008

Table 16: Stress diagnostics: weakening anchoring (κ) and/or increasing noise trading (ϕ) can generate large mispricing and volatility *levels*. Within each stress case, outcomes are nearly unchanged between $k = 1$ and $k = 3$, indicating that level amplification is primarily driven by (κ, ϕ) rather than the overconfidence treatment.

Case	$\mathbb{E}[\lvert p-v\rvert]$	$q_{0.95}(\lvert p-v\rvert)$	$q_{0.99}(\lvert p-v\rvert)$	$\mathrm{std}(r)$	$\mathrm{std}_{\mathrm{xs}}(k_i)$
Fixed k=2.0	1.910 ± 0.234	4.475 ± 0.546	5.380 ± 0.685	0.504 ± 0.011	0.000 ± 0.000
Uniform[1,3] (mean 2)	1.658 ± 0.183	4.027 ± 0.416	5.007 ± 0.549	0.499 ± 0.012	0.563 ± 0.009
Normal(2,0.5) clipped[1,3]	1.658 ± 0.183	4.027 ± 0.417	5.007 ± 0.549	0.499 ± 0.012	0.469 ± 0.015

Table 17: Heterogeneous k at fixed mean $\mathbb{E}[k] = 2$: comparing dispersion in confidence under the same market regime. Column $\mathrm{std}_{\mathrm{xs}}(k_i)$ is the cross-sectional standard deviation of k_i across agents, time-averaged.

Policy	k	$\mathbb{E}[\lvert p-v\rvert]$	$q_{0.95}(\lvert p-v\rvert)$	$\mathrm{std}(r)$
Myopic	1	1.633 ± 0.246	3.622 ± 0.583	0.493 ± 0.015
Myopic	3	1.632 ± 0.246	3.624 ± 0.579	0.493 ± 0.016
Intertemporal	1	1.284 ± 0.132	2.868 ± 0.313	0.496 ± 0.016
Intertemporal	3	1.290 ± 0.134	2.878 ± 0.311	0.496 ± 0.016
Δ Myopic $(k = 3 - 1)$	—	-0.001 ± 0.002	0.002 ± 0.011	0.000 ± 0.000
Δ Intertemporal $(k = 3 - 1)$	—	0.006 ± 0.004	0.010 ± 0.012	-0.000 ± 0.000

Table 18: Myopic vs. intertemporal policy: $\mathbb{E}[\lvert p-v\rvert]$, $q_{0.95}(\lvert p-v\rvert)$, and $\mathrm{std}(r)$ by policy and k.

α	$\mathbb{E}[\lvert p-v\rvert]$ $(k = 1)$	$\Delta\mathbb{E}[\lvert p-v\rvert]$	$\Delta q_{0.5}$	$\Delta q_{0.95}$	Flag
0.00	1.655	-0.003 ± 0.005	-0.000	-0.011	✓
0.05	1.682	-0.003 ± 0.005	-0.002	-0.013	✓
0.10	1.707	-0.003 ± 0.005	-0.003	-0.010	✓
0.20	1.746	-0.004 ± 0.005	0.006	-0.010	✓

Table 19: Impaired-arbitrage extension: $\Delta\mathbb{E}[\lvert p-v\rvert]$ $(k = 3{-}1)$ vs. α (kappa decay rate). "Flag" per thresholds in text.

Sample	Correlation	SE	t-stat
Full	-0.018	0.023	-0.766
Stress (top decile realized vol)	-0.053	0.073	-0.727
Non-stress	-0.025	0.024	-1.009

Table 20: Unconditional volume–volatility correlation (log volume vs realized return volatility): full sample, stress, and non-stress (Newey–West t-stats). Estimates are economically small and not statistically distinguishable from zero in this SPY sample.